
Regulation of MeCP2 induced heterochromatin remodeling

Annette Becker



München 2010

Regulation of MeCP2 induced heterochromatin remodeling

Annette Becker

Dissertation
an der Fakultät für Biologie
der Ludwig-Maximilians-Universität
München

vorgelegt von
Diplom-Biochemikerin Annette Becker
aus Köln

München, den 20. Juli 2010

Erstgutachter: Prof. Dr. Heinrich Leonhardt

Zweitgutachter: Prof. Dr. Ruth Brack-Werner

Tag der mündlichen Prüfung: 21.10.2010

1	SUMMARY	3
1.1	Zusammenfassung	3
1.2	Summary	5
2	INTRODUCTION	7
2.1	DNA methylation	7
2.2	Recognition of methylated DNA by methyl-CpG binding domain proteins	8
2.2.1	Methyl-CpG binding domain protein 1 (MBD1)	8
2.2.2	Methyl-CpG binding domain protein 2 (MBD2)	10
2.2.3	Methyl-CpG binding domain protein 3 (MBD3)	12
2.2.4	Methyl-CpG binding domain protein 4 (MBD4)	12
2.2.5	MeCP2	14
2.3	Biological functions of MeCP2	19
2.3.1	Binding of MeCP2 to DNA <i>in vitro</i>	19
2.3.2	Binding of MeCP2 to chromatin <i>in vitro</i>	20
2.3.3	MeCP2 DNA binding and effect on chromatin architecture <i>in vivo</i>	20
2.3.4	Interacting partners of MeCP2	22
2.3.5	Post-translational modifications of MeCP2 modulate its functions	24
2.3.6	Poly(ADP-ribose)polymerase-1	25
3	QUESTIONS AND AIMS OF THIS WORK	27
4	METHODS AND MATERIALS	28
4.1	Molecular biology methods	28
4.1.1	Construction of expression plasmids	28
4.2	Cell biology methods	29
4.2.1	Cell culture and transfection	29
4.2.2	ImmunoFISH	30
4.2.3	Microscopy, image analysis and statistical evaluation	31
4.3	Biochemical methods	32
4.3.1	<i>In vivo</i> protein interaction assays	32
4.3.2	<i>In vitro</i> protein interaction assays	33
4.3.3	Western blot analysis	34
4.3.4	<i>In vitro</i> poly(ADP-ribosyl)ation assay	34
4.3.5	<i>In vitro</i> poly(ADP-ribose) binding analysis	34
5	RESULTS	36
5.1	MeCP2 RTT mutations affect chromatin organization and inhibition of MeCP2 poly(ADP-ribosyl)ation rescues this defect	36
5.1.1	RTT mutations affect MeCP2 binding and clustering of pericentric heterochromatin	36
5.1.2	Heterochromatin binding and clustering properties map to distinct structures of MeCP2 MBD	40
5.1.3	MeCP2 directly interacts with the nuclear enzyme PARP-1	43
5.1.4	MeCP2 is poly(ADP-ribosyl)ated <i>in vivo</i>	44
5.1.5	Poly(ADP-ribosyl)ation of MeCP2 reduces clustering of pericentric heterochromatin	47
5.1.6	Decrease of poly(ADP-ribosyl)ation rescues chromocenter clustering of RTT mutant MeCP2	50
5.2	Direct interactions of MeCP2 and MBD2 involve poly(ADP-ribosyl)ated domains, that also recognize poly(ADP-ribose)	51
5.2.1	MeCP2 and MBD2 – but not MBD1, MBD3 and MBD4 - get poly(ADP-ribosyl)ated <i>in vivo</i>	51

5.2.2	MeCP2 and MBD2 poly(ADP-ribosyl)ated domains also recognize poly(ADP-ribose) in a noncovalent manner	53
5.2.3	Direct homo- and hetero-interactions between MeCP2 and MBD2 are partially mediated through their poly(ADP-ribosyl)ated and poly(ADP-ribose) recognizing domains	54
6	<u>DISCUSSION</u>	57
6.1	Regulation of MeCP2 induced heterochromatin remodeling	57
6.1.1	Poly(ADP-ribosyl)ation, poly(ADP-ribose) recognition and interactions among MBDs	59
6.1.2	Interaction of MeCP2 with HP1 and heterochromatin association	61
6.1.3	Poly(ADP-ribosyl)ation of MeCP2 has a regulatory effect on MeCP2 mediated large-scale heterochromatin reorganization	61
6.2	MeCP2 poly(ADP-ribosyl)ation as a therapeutic target	64
6.3	Outlook	66
7	<u>APPENDIX</u>	69
7.1	References	69
7.2	Abbreviations	84
7.3	Declaration	86
7.4	Publications	87
7.5	Acknowledgements	100
8	<u>CURRICULUM VITAE</u>	102

1 Summary

1.1 Zusammenfassung

Die epigenetische Information, codiert durch das Methylierungs-Muster der genomischen DNA, wird durch Methyl-Cytosin-Bindende Proteine (z.B. MeCP2) erkannt und in höhere Ebenen der Chromatinstruktur und spezielle Gen-Silencing Muster übersetzt.

Mutationen innerhalb des MECP2-Gens sind die Hauptursache der neurologischen Erkrankung des "Rett Syndroms (RTT)". Wir hatten gezeigt, dass der MeCP2-Spiegel während der Differenzierung ansteigt und ein erhöhtes Zusammenlagern perizentromerischen Heterochromatins in vivo zur Folge hat.

Ziel dieser Studie war es nun, weitere Einblicke in Mechanismus und Regulation der MeCP2-induzierten Reorganisation von Heterochromatin zu gewinnen.

Hierzu wurden anfänglich 21 RTT-induzierende Mutationen, die innerhalb der Methyl-Cytosin-bindenden Domäne (MBD) von MeCP2 liegen, charakterisiert. Wir konnten zeigen, dass einige dieser Mutationen entweder die Fähigkeit von MeCP2 zur Chromatin-Bindung oder die Chromatin-Clusterbildung beeinflussen. Interessanterweise korrelieren diese zwei Phänotypen mit der jeweils entsprechenden Aminosäuren-Position in der Kristallstruktur der MBD-Domäne von MeCP2 und definieren hiermit zwei verschiedene funktionale Strukturen innerhalb dieser Domäne. Mutationen die die Chromatin-Clusterbildung von MeCP2 beeinträchtigen, sind distal der Methyl-Cytosin-bindenden Sites angesiedelt und könnten demnach Protein-Interaktionen, die bei der Aggregation von Heterochromatin beteiligt sind, beeinflussen. Aus diesem Grunde suchten wir weitere Bindungspartner von MeCP2 und identifizierten mittels eines proteomischen Screens das nukleäre Enzym PARP-1 (Poly(ADP-ribose)polymerase-1) als Bindungspartner von MeCP2. Wir konnten eine direkte Interaktion zwischen MeCP2 und PARP-1 sowie poly-ADP-Ribosylierung von MeCP2 feststellen, die bevorzugt innerhalb der TRD (transcriptional repression domain) und dem Bereich zwischen MBD-Domäne und TRD erfolgt. Ferner beobachteten wir, dass diese post-translationale Modifikation der MeCP2-induzierten Chromatin-Clusterbildung entgegenwirkt. Sowohl Deletionen modifizierter Domänen wie auch die chemische Inhibierung der poly-ADP-Ribosylierung erhöhen die Fähigkeit von MeCP2, Heterochromatin zu aggregieren. Auch zeigte sich hierbei, dass die chemische Inhibierung der poly-ADP-Ribosylierung das beeinträchtigte Chromatin-Aggregations Potential einiger MeCP2 RTT Mutanten signifikant erhöht.

Vor kurzem wurden Interaktionen zwischen MeCP2 und Nukleosomen als ein zusätzlicher Faktor vorgeschlagen, der zum MeCP2-induzierten Zusammenlagern perizentrischen Heterochromatins beiträgt. Hierbei könnte MeCP2 bei der Verlinkung von

Chromatin-Fasern entweder als Monomer oder mittels Interaktionen mit sich selbst beteiligt sein; doch wurde eine solche Oligomerisierung von MeCP2 aufgrund hydrodynamischer Analysen in Frage gestellt.

Daher untersuchten wir potentielle direkte Interaktionen zwischen den MBD Proteinen und konnten sowohl Homo- und Hetero-Dimerisierung von MeCP2 und MBD2 aufzeigen. Bei der Interaktion von MeCP2 mit sich selbst und mit MBD2 sind zwei unabhängige Domänen beteiligt, von denen eine bei der Aggregation von Nukleosomen-Arrays *in vitro* eine zentrale Rolle spielt. Auch fanden wir, dass MeCP2 und MBD2 die einzigen MBD-Proteine sind, die poly-ADP-ribosyliert werden. Die modifizierten Domänen dieser beiden Proteine erkennen ihrerseits nicht-kovalente poly-ADP-Ribose und sind an den Homo- und Hetero-Interaktionen von MeCP2 und MBD2 *in vitro* beteiligt.

Somit können wir im Hinblick auf die MeCP2-induzierte Reorganisation von Heterochromatin folgende neue Aspekte vorschlagen:

- 1) Poly-ADP-Ribosylierung von MeCP2 ist ein regulierendes Element beim MeCP2-vermittelten Zusammenlagern perizentrischen Heterochromatins
und
- 2) Direkte Interaktionen von MeCP2 mit sich selbst und anderen MBD-Proteinen stellen potentiell verstärkende Elemente bei der Etablierung höherer Ebenen der Chromatinstruktur dar.

1.2 Summary

The epigenetic information encoded in the genomic DNA methylation pattern is read by methyl-cytosine binding proteins, e.g., MeCP2 and translated into chromatin structure and gene silencing states. Mutations within the *MECP2* gene have been linked to Rett syndrome (RTT), a human neurological disorder. We have previously shown that expression of MeCP2 is upregulated during differentiation and causes large scale chromatin reorganization, in particular clustering of pericentric heterochromatin.

The goal of this study was to gain further insight into the mechanism and regulation of MeCP2 mediated large-scale heterochromatin reorganization.

I first addressed this question by characterizing 21 RTT-inducing missense mutations within MeCP2 methyl cytosine binding domain (MBD) and found that they primarily affect either MeCP2 binding or clustering of chromatin. Interestingly, the phenotypes correlate well with their amino acid positions in the crystal structure and define two distinct functional structures within MeCP2 MBD domain. Mutations impairing chromocenter clustering were located distally from the methylated cytosine binding sites likely affecting protein interactions involved in heterochromatin aggregation. Thus, I subsequently investigated novel MeCP2 binding partners and identified in a proteomic screen the nuclear enzyme poly(ADP-ribose)polymerase-1 (PARP-1). I could show that MeCP2 directly interacts with PARP-1 and is poly(ADP-ribosyl)ated *in vitro* as well as *in vivo* at five major residues within a region in its transcriptional repression domain (TRD) and in the region between the MBD and the TRD (termed interdomain, ID). I further observed, that this modification counteracted MeCP2 capacity to establish higher order chromatin structures as deletion of the modified domains as well as chemical inhibition of poly(ADP-ribosyl)ation increased MeCP2 induced heterochromatin clustering. Importantly, PARP inhibitors rescued the chromatin aggregation function of MeCP2 RTT syndrome mutants. As an additional factor contributing to MeCP2 induced heterochromatin aggregation, multiple interactions between MeCP2 and nucleosomes have previously been proposed with MeCP2 cross-linking heterochromatin fibers either as a monomer or through interactions with itself. However, oligomerization of MeCP2 has been challenged by hydrodynamic studies. I consequently examined interactions among MBD proteins. I found that MeCP2 and MBD2 homo- and hetero-dimerize. MeCP2 interaction to itself and MBD2 involved two independent domains, one reported to mediate aggregation of nucleosomal arrays *in vitro*. Additionally I found that MeCP2 and MBD2 are the only MBDs poly(ADP-ribosyl)ated. Their modified domains further recognize noncovalent poly(ADP-ribose) and are involved in MeCP2 and MBD2 homo- and hetero-interactions *in vitro*.

Based on these data one can propose both, MeCP2 poly(ADP-ribosyl)ation as regulating element in MeCP2 mediated heterochromatin aggregation as well as direct interactions of MeCP2 with itself and other MBD proteins as potentially reinforcing elements contributing to the establishment of higher order chromatin structures *in vivo*.

These findings lay the ground for targeted manipulation of chromatin architecture and thus contribute to our general understanding of its role in development and disease.

2 Introduction

2.1 DNA methylation

DNA methylation is a major epigenetic modification in the genomes of higher eukaryotes. In vertebrates the covalent addition of a methyl group occurs almost exclusively on the C5 position of cytosines (5mC) within CpG dinucleotides. Approximately 60-90% of these dinucleotides are methylated (Bird, 1986), with the exception of CpG-enriched sequences, referred to as CpG islands. The latter occur mostly within or close to promoter regions and are generally unmethylated.

The methylation mark is usually associated with a repressed chromatin state resulting in inhibition of gene expression (Bird and Wolffe, 1999). DNA methylation is important for normal development and is associated with transcriptional silencing in various processes such as X chromosome inactivation, imprinting and carcinogenesis (Bird, 2002).

Methylation of DNA is a postreplicative modification that is catalyzed in vertebrates by the DNA methyltransferase enzymes (Dnmts) Dnmt1, Dnmt3A and Dnmt3B. Dnmt3A and Dnmt3B, also referred to as *de novo* methyltransferases, have been mainly described to introduce cytosine methylation at unmethylated CpG sites and are essential for the establishment of DNA methylation patterns during development (Kaneda et al., 2004; Okano et al., 1999). The maintenance DNA methyltransferase Dnmt1 works on hemimethylated DNA and copies pre-existing methylation patterns onto the daughter DNA strand generated during replication (Chuang et al., 1997; Leonhardt et al., 1992).

Methylated CpGs (mCpGs) could mediate transcriptional silencing by altering the binding sequences of transcription factors and directly prevent transcriptional activation (Campanero et al., 2000; Iguchi-Arigo and Schaffner, 1989). Alternatively, they could be recognized by methyl-CpG binding proteins (MBPs). The latter could, on the one hand, sterically hinder transcription factor binding to gene regulatory sequences (Leonhardt and Cardoso, 2000). On the other hand, MBPs could recruit chromatin remodeling co-repressor complexes to establish a repressive chromatin architecture (Fuks et al., 2003; Jones et al., 1998; Nan et al., 1998; Wade et al., 1999; Zhang et al., 1999). At least three different families of MBPs, methyl-CpG binding domain proteins (MBDs), Kaiso proteins and SRA domain containing proteins, recognize and translate the methylation mark and therefore constitute a link between DNA methylation and chromatin modification state.

2.2 Recognition of methylated DNA by methyl-CpG binding domain proteins

The MBD protein family comprises five members MBD1, MBD2, MBD3, MBD4 and MeCP2 (Figure 1). They all share a conserved methyl-CpG binding domain (MBD), which mediates their binding to methylated DNA. In agreement with the silencing effect of DNA methylation MBD1, MBD2, and MeCP2 have been extensively described as transcriptional repressors (Wade, 2001).

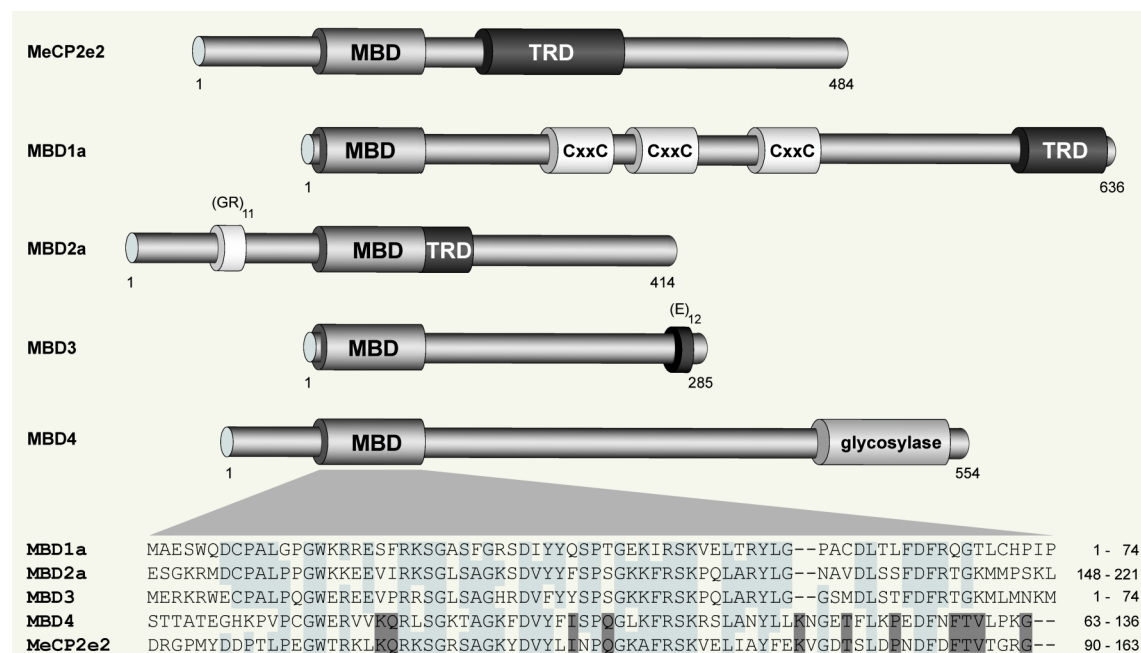


Figure 1. Schematic representation of the MBD protein family and sequence comparison of the MBD domain of murine MeCP2e2, MBD1a, MBD2a, MBD3 and MBD4

The conserved methyl-CpG binding domain (MBD) enables the MBD family members to bind to methylated DNA with the exception of MBD3 due to two amino acid changes within its MBD. MeCP2, MBD1 and MBD2 further contain a transcriptional repression domain (TRD). Depending on its isoform, MBD1 comprises 2 or 3 cysteine-rich (CxxC) domains. The third CxxC motif mediates MBD1 binding to unmethylated DNA. The Gly-Arg repeat of MBD2 and the Glu repeat of MBD3 are represented by (GR)₁₁ and (E)₁₂. MBD4 carries a glycosylase domain involved in the removal of a thymine or uracil from a mismatched CpG site. The numbers represent aa coordinates.

According to the similarity of the alignment of their MBD sequence, the MBD family members can be subdivided into one group comprising MBD1, MBD2 and MBD3 and another subgroup consisting of MeCP2 and MBD4 respectively. Aa identity of the MBD domain among i) all MBD proteins is 23%, ii) the subgroup comprising MBD1, 2 and 3 is 47% and iii) the subgroup of MeCP2 and MBD4 is 49%.

Identical residues regarding all MBDs are marked in light grey. Additional identical residues within MeCP2 and MBD4 are highlighted in dark grey.

2.2.1 Methyl-CpG binding domain protein 1 (MBD1)

MBD1 either contains two or three CxxC zinc finger motifs consisting of eight conserved cysteines (Fujita et al., 1999; Jorgensen et al., 2004). The region of the CxxC domains and the C-terminus of MBD1 are alternatively spliced in humans and mice. Four splicing isoforms have been described in humans (MBD1v1,2,3 and 4; Fujita et al., 1999) and three in mouse (MBD1a,b and d; Jorgensen et al., 2004) with the major difference being

the presence of a third CxxC-domain, the CxxC-3 domain. MBD1 is the only member of the MBD family with two DNA-binding domains that independently mediate MBD1 binding to methylated and unmethylated DNA *in vivo* and *in vitro* (Jorgensen et al., 2004).

In wild type mouse cells, localization of MBD1 to condensed and mCpGs enriched pericentric heterochromatic regions (Hendrich and Bird, 1998; Nan et al., 1996) depends on the MBD domain and is unaffected by deletion of the CxxC-3 domain (Jorgensen et al., 2004). In methylation deficient cells, the CxxC-3 domain mediates localization of MBD1 to heterochromatic foci even in the absence of the MBD (Jorgensen et al., 2004). The two other zinc finger motifs of MBD1, CXXC-1 and CXXC-2, are by themselves unable to mediate DNA binding (Jorgensen et al., 2004). MBD1 was shown to repress transcription from both CpG-rich methylated and unmethylated promoters in reporter gene assays (Fujita et al., 1999; Jorgensen et al., 2004). A transcriptional repression domain (TRD) at the C-terminus of MBD1 has been identified and shown to actively repress transcription even at a distance (Ng et al., 2000). Repression of nonmethylated reporter genes depends on an intact CXXC-3 domain and is not influenced by the presence of a functional MBD (Jorgensen et al., 2004). Methylation dependent silencing by MBD1 *in vivo* depends on both its TRD and MBD and seems to be partially sensitive to the deacetylase inhibitor trichostatin A (TSA) (Ng et al., 2000). Nonetheless, MBD1 has not been found directly associated with any histone deacetylase activity (Ng et al., 2000). Several interaction partners of MBD1 have been recently identified and impact on MBD1 mediated methylation-based transcriptional repression. These include the histone H3 lysine 9 (H3K9) methyltransferase Suv39h1 (Fujita et al., 2003b) and SETDB1 (Sarraf and Stancheva, 2004) and the MBD1-containing chromatin-associated factor (MCAF), also named mAM (Fujita et al., 2003a). MCAF/mAM, a cofactor for the histone methyltransferase ESET/SETDB1 that facilitates the conversion of H3-K9 dimethyl to trimethyl (Wang et al., 2003), enhances MBD1 transcriptional repression in a histone deacetylation independent manner (Fujita et al., 2003a).

MBD1 association to SETDB1 mediates transcriptional repression throughout the cell cycle (Sarraf and Stancheva, 2004). During DNA replication, a S-phase specific transient complex of MBD1/SETDB1 and the p150 subunit of the chromatin assembly factor CAF-1 is formed. This complex is associated with the DNA replication machinery via PCNA (Sarraf and Stancheva, 2004). The CAF-1/MBD1/SETDB1 complex facilitates H3K9 methylation of the H3/H4 dimers associated with CAF-1 during replication coupled chromatin assembly (Sarraf and Stancheva, 2004). This process enables the post-replicative maintenance of the repressive H3K9 modification on methylated daughter DNA strands. Simultaneously, DNA methylation is restored by Dnmt1 (Chuang et al., 1997; Leonhardt et al., 1992). Both MBD1 promoted transcriptional repression and

maintenance of H3K9 methylation are negatively regulated through the addition of the small ubiquitin-like modifier 1 (SUMO1), mediated by the E3 ligases Protein Inhibitors of activated STAT1 (PIAS1 and PIAS3) in human cells (Lyst et al., 2006). Conjugation of SUMO1 to MBD1 does not interfere with MBD1 binding to its endogenous sites but disturbs both MBD1 association to SETDB1 and MBD1 mediated transcriptional repression (Lyst et al., 2006). In addition, MBD1 has been described to be modified by SUMO2/3 (Uchimura et al., 2006). In contrast to the findings by Lyst et al, SUMO2/3 conjugated MBD1 recruits MCAF/SETDB1, resulting in stabilization of heterochromatic regions (Uchimura et al., 2006). Whether conjugation of SUMO1 and SUMO2/3 exert differing effects on MBD1 recruited repressors requires further investigation.

Although MBD1 minus mice do not have developmental defects and appear healthy, they show decreased hippocampal neurogenesis and impaired spatial learning. Furthermore, MBD1 minus neural stem cells exhibit increased genomic instability and elevated expression level of the endogenous virus intracisternal A particle (IAP) (Zhao et al., 2003; Table 1).

Table 1: Phenotype of methyl-CpG binding protein null mouse models

Mouse model	Phenotype	Reference
MBD1 null	no overt phenotypes minor neural defects (decreased hippocampal neurogenesis, impaired spatial learning) increased genomic instability	Zhao et al., 2003
MBD2 null	normal development, viable, fertile maternal nurturing defect altered cytokine production during T-helper cell differentiation due to impaired gene regulation reduced intestinal tumorigenesis	Hendrich et al., 2001 Hutchins et al., 2002 Sansom et al., 2003
MBD3 null	Early embryonic lethality	Hendrich et al., 2001
MBD4 null	Viable, fertile, no overt phenotype 3,3-fold increased C:G to T:A transitions at CpG sites increased colorectal tumor formation with C:G to T:A transitions in the APC gene (upon crossing MBD4 minus mice with mice bearing germline mutation in Apc gene)	Millar et al, 2002.; Wong et al., 2002

2.2.2 Methyl-CpG binding domain protein 2 (MBD2)

MBD2 and MBD3 are the only MBD family members with significant sequence similarity beyond the MBD domain (Hendrich and Bird, 1998; Figure 2). MBD3 lacks a NH₂-terminal extension of MBD2 and has, contrary to MBD2, at its extreme COOH-terminus an acidic Glu repeat (Hendrich and Bird, 1998).

reduced weight of the pups (Hendrich et al., 2001; Table 1). In mouse liver nuclear extracts, MeCP1 consists of two forms, with the major one containing MBD2 (Hendrich et al., 2001; Meehan et al., 1989). This form of MeCP1 is absent in MBD2 minus cells (Hendrich et al., 2001). In addition, MBD2 minus cells exhibit a defect in their repression of methylated reporter constructs that is rescued by reintroducing MBD2 but not MBD3 (Hendrich et al., 2001).

Further, MBD2 minus cells are strikingly affected in their cytokine production of, e.g., interleukin-4 (IL-4) during the differentiation of T-helper cells (Hutchins et al., 2002). During differentiation under normal conditions, expression of IL-4 requires induction by the activator GATA-3 strongly expressed in stimulated naïve helper T cells (Mullen et al., 2001). In MBD2 minus mice however, MBD2 mediated silencing of the IL-4 gene is lost which renders GATA-3 dispensable for IL-4 induction and results in ectopic expression of IL-4 in unstimulated helper T cells (Hutchins et al., 2002).

2.2.3 Methyl-CpG binding domain protein 3 (MBD3)

The occurrence of two aa substitutions within the MBD of mammalian MBD3, but not of *Xenopus* MBD3, causes its inability to bind to methylated DNA *in vitro* and *in vivo* (Hendrich and Bird, 1998; Saito and Ishikawa, 2002; Wade et al., 1999).

MBD3 is a core component of the NuRD repression complex (Zhang et al., 1999). This complex consists, together with MBD3, of seven subunits, including the histone deacetylase core HDAC1 and HDAC2, the histone binding proteins RbAp46/RbAp48, the SWI2/SNF2 helicase/ATPase domain containing Mi-2 (Tong et al., 1998; Xue et al., 1998; Zhang et al., 1998) and the metastasis-associated protein MTA2 (Zhang et al., 1999). MTA2 modulates the activity of the core HDAC1/2 complex (Zhang et al., 1999), with MBD3 being important for MTA2 association with this core unit (Zhang et al., 1999). Deletion of MBD3 leads to early embryonic lethality (Hendrich et al., 2001; Table 1). This drastic effect on murine development most probably reflects MBD3 indispensable role as an important core component of the NuRD complex. It additionally indicates that transcriptional repression, mediated through an active NuRD complex, is required for embryonic development. The much more milder phenotype of MBD2 minus mice gives rise to the assumption that MBD2 role to tether the NuRD repressor to methylated DNA can be accomplished by other mCpG binding proteins as well.

2.2.4 Methyl-CpG binding domain protein 4 (MBD4)

Methylated cytosines are a hotspot for mutations. The primary product of spontaneous hydrolytic deamination of 5mCs, occurring at a very high frequency in the genome, is thymine. The resulting 5mCpG:TpG mismatch requires for its correction a thymine DNA

glycosylase, an activity described for thymine DNA glycosylase (TDG) (Neddermann et al., 1996; Wiebauer and Jiricny, 1989), as well as MBD4 (Hendrich et al., 1999).

MBD4, also named methyl-CpG binding endonuclease 1 (MED1) (Bellacosa et al., 1999) has been mostly characterized for its role in DNA damage repair (Hendrich et al., 1999; Millar et al., 2002; Wong et al., 2002).

It contains a NH₂-terminal MBD and a COOH-terminal catalytic domain that shares high homology to bacterial DNA damage specific endonucleases exhibiting glycosylase/lyase activity during base excision repair (BER) (Michaels et al., 1990). In a yeast two hybrid screen MBD4 was identified to interact with the human mismatch repair (MMR) protein MLH1, the homologue of MutL in *E.coli* (Bellacosa et al., 1999).

MBD4 has been described as a mismatch specific T/U DNA glycosylase, capable of removing a thymine or uracil from a mismatched CpG site through glycosidic bond cleavage *in vitro*. The methylation status of the cytosine in the CpG:TpG or CpG:UpG mismatch however seems to be important in that process (Hendrich et al., 1999; Petronzelli et al., 2000).

MBD4 binds to densely methylated DNA *in vitro* and is localized at strongly methylated heterochromatic foci in mouse nuclei *in vivo* (Hendrich and Bird, 1998). Its MBD preferentially binds to 5mCpG:TpG mismatches and weakly recognizes 5mCpG: 5mCpG or non-methylated CpG:TpG mismatches *in vitro* (Hendrich et al., 1999). In contrast, the C-terminal glycosylase domain binds to the abasic site that arises during the reaction (Hendrich et al., 1999).

Mutations within polyadenine repeats within the MBD4 gene have been found in human colorectal carcinomas with microsatellite instability (MSI) and are in many cases the cause for the synthesis of MBD4 protein lacking its C-terminal catalytic domain (Bader et al., 2000; Riccio et al., 1999). MSI manifests itself as an accumulation of mutations at simple repetitive sequences throughout the genome and is the indicator of an impaired MMR system (Modrich and Lahue, 1996). MBD4 minus mice are viable, fertile and appear to be healthy without any major physical abnormalities (Millar et al., 2002; Wong et al., 2002; Table 1). They, though, exhibit a 3.3-fold higher number of C:G to T:A transitions at CpG sites in comparison to wild type mice (Millar et al., 2002). Crossing of MBD4 minus mice with mice having a germline mutation in the adenomatous polyposis coli (APC) gene results in increased colorectal tumor formation with CpG to TpG mutations in the APC gene (Millar et al., 2002). These *in vivo* studies clearly implicate an important role of MBD4 in the repair of 5mC deamination at mCpGs. The relatively mild phenotype however suggests, that other thymine glycosylases, TDG for instance, might contribute to reduce the mCpG-TpG mutation rate.

Besides its function as a tumor suppressor, MBD4 has been reported to repress transcription in a HDAC dependent manner *in vitro* and directly interacts with Sin3A and HDAC1 (Kondo et al., 2005). Whether the role of MBD4 in transcriptional repression is of physiological relevance still has to be shown. Intriguingly, *in vivo* studies in zebrafish embryos revealed an important role of MBD4 in active demethylation of 5mC (Rai et al., 2008). A two-step coupled mechanism was proposed with the first step being deamination of 5mC by the 5mC deaminase Activated Induced Deaminase (AID) (Morgan et al., 2004), which generates a thymine leading to a G:T mismatch (Rai et al., 2008). This is immediately followed by the removal of the thymine base through MBD4 (Rai et al., 2008).

2.2.5 MeCP2

MeCP2, the prototype of the MBD protein family, was, shortly after characterization of MeCP1 (Meehan et al., 1992; Meehan et al., 1989), the second MBD protein analyzed and the first MBD protein to be cloned (Lewis et al., 1992; Figure 3).

H. sapiens	MVAGMLGLREEKSEDDQLQGLKDKPLKFKKVKKDKKKEEGKHEPVQPSAHHSAEPAEAGKAETSESGSAPAVPEASASPKQRRSIIH	DRGPMYDDPTL	100	
M. fascicularis	MVAGMLGLREEKSEDDQLQGLKDKPLKFKKVKKDKKKEEGKHEPVQPSAHHSAEPAEAGKAETSESGSAPAVPEASASPKQRRSIIH	DRGPMYDDPTL	100	
R. norvegicus	MVAGMLGLREEKSEDDQLQGLKDKPLKFKKVKKDKKKEEGKHEPLQPSAHHSAEPAEAGKAETSESGSAPAVPEASASPKQRRSIIH	DRGPMYDDPTL	100	
M. musculus	MVAGMLGLREEKSEDDQLQGLRDKPLKFKKAKKDKKKEEGKHEPLQPSAHHSAEPAEAGKAETSESGSAPAVPEASASPKQRRSIIH	DRGPMYDDPTL	100	
H. sapiens	PEGWTRKLRKQKRSGRSAGKYDVYLINPQKAFRSKVELIAYFEKVGDTSLDPNDFDFTVTGRG	SPSRREQPKPKPKSPKAPGTGRGRGRPKGSGTTRPK	200	
M. fascicularis	PEGWTRKLRKQKRSGRSAGKYDVYLINPQKAFRSKVELIAYFEKVGDTSLDPNDFDFTVTGRG	SPSRREQPKPKPKSPKAPGTGRGRGRPKGSGTTRPK	200	
R. norvegicus	PEGWTRKLRKQKRSGRSAGKYDVYLINPQKAFRSKVELIAYFEKVGDTSLDPNDFDFTVTGRG	SPSRREQPKPKPKSPKAPGTGRGRGRPKGSGTTRPK	200	
M. musculus	PEGWTRKLRKQKRSGRSAGKYDVYLINPQKAFRSKVELIAYFEKVGDTSLDPNDFDFTVTGRG	SPSRREQPKPKPKSPKAPGTGRGRGRPKGSGTTRPK	200	
H. sapiens	AATSEGVQVQKRVLEKSPGKLLVKMPFQTSPGGKAEGGGATTSTQVMVIKRPRGRKKAEDPQAI	PKRGRKPGSVVAAAAAEAKKAVKESSIRSVQETV	300	
M. fascicularis	AATSEGVQVQKRVLEKSPGKLLVKMPFQTSPGGKAEGGGATTSTQVMVIKRPRGRKKAEDPQAI	PKRGRKPGSVVAAAAAEAKKAVKESSIRSVQETV	300	
R. norvegicus	AAASEGVQVQKRVLEKSPGKLLVKMPFQASPGGKGEAGGATTSAQVMVIKRPRGRKKAEDPQAI	PKRGRKPGSVVAAAAAEAKKAVKESSIRSVQETV	300	
M. musculus	AAASEGVQVQKRVLEKSPGKLLVKMPFQASPGGKGEAGGATTSAQVMVIKRPRGRKKAEDPQAI	PKRGRKPGSVVAAAAAEAKKAVKESSIRSVHETV	300	
H. sapiens	LPVKKRTRRETVSIEVKEVVKPLLVSTLGEKSGKGLTKCKSPGRKSKESSPKGRSSAS	SPPKKEHHHHHHHSES	PKAPVPLLPPLPPPPPEPESSEDP	400
M. fascicularis	LPVKKRTRRETVSIEVKEVVKPLLVSTLGEKSGKGLTKCKSPGRKSKESSPKGRSSAS	SPPKKEHHHHHHHSES	PKAPVPLLPPLPPPPPEPESSEDP	400
R. norvegicus	LPVKKRTRRETVSIEVKEVVKPLLVSTLGEKSGKGLTKCKSPGRKSKESSPKGRSSAS	SPPKKEHHHHHHHSES	PKAPMPLLP--PPPPPEPESSEDP	398
M. musculus	LPVKKRTRRETVSIEVKEVVKPLLVSTLGEKSGKGLTKCKSPGRKSKESSPKGRSSAS	SPPKKEHHHHHHHSES	TKAPMPLLP--PPPPPEPESSEDP	398
H. sapiens	SPPEPQDLSSSVCKEEKMPRGSLES	SDGCPKEPAKTQPAVA-----TAATAAEKYKHRGEGGERKDIVSSM	PRNREEPVD	487
M. fascicularis	SPPEPQDLSSSVCKEEKMPRGSLES	SDGCPKEPAKTQPAVA-----TAATAAEKYKHRGEGGERKDIVSSM	PRNREEPVD	487
R. norvegicus	SPPEPQDLSSSVCKEEKMPRGSLES	SDGCPKEPAKTQPMVAATAATTTTTTTTVAEYKHRGEGGERKDIVSSM	PRNREEPVD	493
M. musculus	SPPEPQDLSSSVCKEEKMPRGSLES	SDGCPKEPAKTQPMVA-----TTTVAEYKHRGEGGERKDIVSSM	PRNREEPVD	485

Figure 3. Alignment of the amino acid sequence of human, macaque, rat, mouse and xenopus MeCP2 Methyl-CpG binding domain and transcriptional repression domain are boxed. Identical residues are highlighted in grey colour. Numbers represent aa. The maximal % identity among all MeCP2s excluding the gaps is 94%.

A minimal NH₂-terminal MBD of MeCP2 was identified that specifically binds to DNA with even just one symmetrically mCpG pair (Nan et al., 1993).

Subsequently, a solution structure of the MBD of rat MeCP2 has been solved by nuclear magnetic resonance (NMR) spectroscopy and shown to form a wedge-shaped structure (Wakefield et al., 1999). One face of the wedge consists of a NH₂-terminal four-stranded antiparallel β -sheet, while the other side is formed by a COOH-terminal three-turn α -helix (Wakefield et al., 1999). The predominantly positively charged β -sheet face and the thin end of the wedge-shaped domain constitute an interface with methylated DNA (Wakefield

et al., 1999). A conserved hydrophobic pocket including the side chains of Tyr123 and Ile125 on the positively charged β -sheet face was proposed to interact through van der Waals` contacts with the methyl group in the major groove of the DNA (Wakefield et al., 1999). This proposal was questioned by a recent analysis of a high resolution X-ray crystal structure of the human MBD bound to DNA (Ho et al., 2008), revealing that the methyl groups bind to a hydrophilic surface including structurally conserved water molecules (Ho et al., 2008). The three residues Asp121, Arg111 and Arg133 perform direct contacts with DNA bases, whereas indirect DNA binding of Tyr123 is mediated via hydrogen bonds from its hydroxyl group to structured water molecules (Ho et al., 2008).

In interphase mouse nuclei, MeCP2 is prominently localized at heterochromatic foci (Lewis et al., 1992). In metaphase chromosomes, MeCP2 presence at the euchromatic arms is rather weak in comparison to its strong localization at pericentromeric heterochromatin (Lewis et al., 1992), highly enriched in heavily methylated major satellite repeats (Jones, 1970; Pardue and Gall, 1970). The overlap of MeCP2 localization with that of 5mC gave rise to the assumption, that it might mediate the biological effects of DNA methylation on chromatin structure and transcription. Accordingly, MeCP2 has been further described to function as a transcriptional silencer through association with corepressor complexes. This association is mediated by its TRD, which was mapped to a region comprising aa 207 to aa 310 (Jones et al., 1998; Nan et al., 1997; Nan et al., 1998). *In vitro* transcription assays demonstrated that MeCP2 specifically represses transcription from methylated but not from unmethylated reporters in a MBD dependent manner (Nan et al., 1997). A Co-Repressor Interacting Domain (CoRID) comprising aa 163 to aa 278 binds to the transcriptional co-repressor mSin3A as well as to the histone deacetylases HDAC1 and HDAC2 (Jones et al., 1998; Nan et al., 1998). Furthermore, *in vivo* reporter gene assays in *Xenopus* and mouse cells demonstrated that MeCP2 mediated transcriptional silencing is partially relieved by inhibition of histone deacetylase activities (Jones et al., 1998; Nan et al., 1998) and might therefore be accomplished to some extent through recruitment of HDACs containing complexes. This partial relief alludes to other repressive mechanisms reinforced by MeCP2 apart from deacetylation (2.3). Intriguingly, besides causing repressive chromatin architecture through promoting modifications of the histone tails, *in vitro* studies demonstrated that MeCP2 alone coordinates chromatin architecture (Georgel et al., 2003). In agreement with these findings, increased expression of MeCP2 in mouse cells induces clustering of pericentric heterochromatin in a dose dependent manner with the MBD being indispensable for MeCP2 aggregation ability (Brero et al., 2005).

In comparison to the MBD and TRD, little is known about the COOH-terminus of MeCP2. Recently a WW domain binding region (WDR), encompassing aa 325 to aa 486 of

MeCP2 including a proline rich region, has been defined according to its ability to associate to the Group II WW domain of several splicing factors (Bedford et al., 1997; Buschdorf and Stratling, 2004).

Human MeCP2 e2 has been described as an intrinsically disordered protein consisting of at least six distinct domains including the MBD, TRD and two COOH-terminal domains (CTD)- α (aa 310 – aa 354) and CTD- β (aa 355 – aa 486) (Adams et al., 2007). Circular dichroism (CD) spectroscopy of recombinant human MeCP2 full length protein revealed that its tertiary structure consists of about 5% α -helix and 35% β -strand/turn and is approximately 60% unstructured (Adams et al., 2007). The MBD contains 10% α -helix, 51% β -strand/turn and 38% unstructured regions while 85% of the TRD (aa 198 – aa 305) are unstructured (Adams et al., 2007). MeCP2 exhibits an unusual low sedimentation coefficient, resulting in a high frictional coefficient ratio, which together with the CD data give rise to the assumption, that MeCP2 tertiary structure is coil-like and similar to that of a partially denatured protein (Adams et al., 2007). Using the FoldIndex program (Prilusky et al., 2005) to predict the location of order and disorder within MeCP2, MeCP2 was shown to have short regions of order, spread between long stretches of internal disorder (Adams et al., 2007). Hydrodynamic analyses of MeCP2 using either analytical ultracentrifugation or sucrose gradient centrifugation experiments further described MeCP2 as a monomer (Adams et al., 2007; Klose and Bird, 2004).

MeCP2 consists of four exons coding for two different isoforms due to alternative splicing. The two isoforms differ only in some aa at their extreme NH₂-terminus (Kriaucionis and Bird, 2004). The different part of the NH₂-terminus of human MeCP2 e1 comprises 21 aa encoded by exon 1 and lacks the 9 aa encoded by exon 2, whereas the initiator Met for MeCP2 e2 is in exon 2 (Kriaucionis and Bird, 2004; Mntzakanian et al., 2004). On the mRNA level, MeCP2 e1 is more abundant in mouse tissues and human brain in comparison to the previously described MeCP2 e2 isoform (Kriaucionis and Bird, 2004). Additionally, MeCP2 e1 protein is much more present in mouse brain extracts than MeCP2 e2 (Kriaucionis and Bird, 2004). That both isoforms show the same cellular localization in mouse cells (Kriaucionis and Bird, 2004; Kumar et al., 2008) and that neither the sequence of the MBD nor TRD are affected by alternative splicing indicate that the functions of these two isoforms might overlap to great extent.

Table 2: MeCP2 mouse models

Mouse model	MeCP2 mutation	Phenotype (of male mice)	Reference
MeCP2 null	Δ of ex 3 Δ of ex 3 & 4 Δ of ex 3 and part of ex 4	after 5 weeks: tremor, motor dysfunction, breathing abnormalities, ataxia, hindlimb clasping, hypoactivity, reduced brain weight & neuronal cell size Age of death: 10 weeks	Chen et al., 2001 Guy et al., 2001 Pelka et al., 2006
MeCP2 conditional null	Nestin-Cre transgene mediated CNS specific MeCP2 deletion	same as MeCP2 null	Chen et al., 2001 Guy et al., 2001
	CamK-Cre93 transgene mediated MeCP2 deletion in post-mitotic neurons	after 3 months: gain of body weight, ataxia, reduced nocturnal activity, reduced brain weight & neuronal cell size Normal life span	Chen et al., 2001
MeCP2 truncation	Truncation at aa 308	After 6 weeks: tremor, motor dysfunction, stereotypic forepaw movements, hypoactivity, seizures, learning & memory deficits. Hyperactelyation of H3 in brain & spleen Age of death: 15 months	Shahbazian et al., 2002
MeCP2 knock-in	Point mutation resulting in R168X stop mutation	By 7 weeks: breathing dysfunction, hindlimb clasping and atrophy, hypoactivity Decreased life span of ~12 weeks	Lawson-Yuen et al., 2007
	Point mutation resulting in A140V missense mutation	Cellular abnormalities in brain: increased cell packing density, abnormal dendritic branching of neurons Life span: > 14 months	Jentarra et al., 2010
(PTM mutations)	Point mutation resulting in S80A missense mutation	Overweight, reduced locomotor activity similar to MeCP2 null mice Normal life span	Tao et al., 2009
	Point mutation resulting in S421A; S424A mutation	Increased locomotor activity Normal life span	Tao et al., 2009
MeCP2 conditional rescue	Silencing of endogenous mouse MeCP2 gene through insertion of a lox-Stop cassette into intron 2 Crossing of MeCP2 ^{lox-Stop} allele with TM-inducible Cre-ER transgene	at 6 weeks: RTT symptoms comparable to MeCP2 null model of Guy et al., 2001 Age of death: 11 weeks - daily TM injections at 4 weeks of age: either rapid death or complete rescue of phenotypes - weekly TM injections of RTT symptomatic mice: complete phenotype rescue	Guy et al., 2007
	MeCP2 transgene, controlled by CAGGS promotor, with MeCP2 e2 cDNA downstream of Stop cassette flanked by LoxP Crossing of MeCP2 transgenic mice with MeCP2 ^{+/-} mice to obtain MeCP2 null mice with CAGGS MeCP2 transgene Brain specific activation of MeCP2 transgene through: Nestin-Cre; Tau-Cre; CamK-Cre 93; CamK-Cre 159	Compared to MeCP2 null mice (Chen et al., 2001), rescued mice exhibit: a) extended life span by: - 8 months with Nestin-Cre and Tau-Cre induced MeCP2 activation - 4 weeks with CamKinaseII induced MeCP2 activation b) delayed motor dysfunction and lethargy c) normal body and brain weight and no decreased neuron size	Giacometti et al., 2007
MeCP2 transgene	Transgenic expression of human MeCP2 under endogenous human promoter	2-fold overexpression: enhanced motor & contextual learning, forepaw clasping at 10-12 weeks hypoactivity, aggressiveness, seizures, motor abnormalities, enhanced synaptic plasticity at 20 weeks Age of death: ~ 1 year	Collins et al., 2004
	MeCP2 expression under neuron-specific promoter of Tau Fusion protein of 31 aa of Tau & MeCP2.	WT mice homozygous for transgene: small size at weaning, don't mate. After 9 months: motor dysfunction, ataxia, tremors Normal lifespan	Luikenhuis et al., 2004

Abbreviations: Δ, deletion; ex, exon; CamK, Calmodulin-kinase II; CNS, central nervous system; aa, amino acid; TM, tamoxifen; Cre-ER, fusion of Cre recombinase and modified estrogen receptor

Rett Syndrome (RTT, MIM 312750) is a postnatal progressive neurodevelopmental disorder predominantly affecting females with an incidence of 1 in 10,000 to 15,000 female births (Amir et al., 1999; Hagberg, 1985; Hagberg et al., 1983). The disorder is accompanied by a wide spectrum of phenotypes. Affected girls seem to develop normally until six to 18 months, at which time they enter a developmental arrest that is followed by strongly impaired motor skills, stereotypic hand movements, loss of speech, seizures, abnormal breathing, microcephaly, ataxia and other symptoms. Besides classic RTT, deviating forms have additionally been described displaying some features of the classic syndrome but exhibiting differences in severity and disease onset. Though RTT was initially reported by Andreas Rett in 1966, it took over 40 years until the discovery, that mutations within the MECP2 gene located in Xq28 cause classic RTT (Amir et al., 1999; Amir and Zoghbi, 2000). Most of these mutations occur *de novo* in the paternal germline. Due to X chromosome inactivation (XCI), a female bearing a mutation within the MeCP2 gene is normally mosaic, with half of her cells expressing the wild-type MeCP2 allele and the other half expressing the mutant MeCP2 allele (Chahrour and Zoghbi, 2007). RTT mutations comprise frequently missense, nonsense and frameshift mutations, although deletions encompassing whole exons have also been described. Eight hot-spot missense and nonsense mutations account for 70% of all mutations, whereas deletions within the COOH-terminus constitute 10%. Although little is known about the COOH-terminus of MeCP2, the high frequency of RTT - causing mutations within this domain together with the finding that a mouse model with a truncating mutation of MeCP2 at aa 308 displays RTT similar phenotypes (Shahbazian et al., 2002; Table 2) underline the importance of this domain. MeCP2^{308/Y} mice, expressing MeCP2 without the COOH-terminal part after the TRD exhibit normal behavior until six weeks of age. After that, they start to develop progressive neurological phenotypes that are milder in the case of heterozygous females (Shahbazian et al., 2002). Although truncated MeCP2 seems to be localized normally at pericentric heterochromatin, hyperacetylation of histone H3 in brain and spleen indicate altered chromatin architecture (Shahbazian et al., 2002).

MeCP2 null mice were generated either lacking exon 3 (Chen et al., 2001) or both exons 3 and 4 (Guy et al., 2001) as well as conditional mutant mice that are deficient of MeCP2 exclusively in the brain (Chen et al., 2001; Guy et al., 2001; Table 2). These mice are viable and fertile but start to develop neurological symptoms such as nervousness and body trembling at five weeks of age leading to death at approximately ten weeks (Chen et al., 2001; Guy et al., 2001). Although null mice and conditional mutants do not exhibit severe abnormalities in the brain architecture, they show reduced brain size and brain weight together with smaller and more densely packed neuronal cell bodies and nuclei (Chen et al., 2001; Guy et al., 2001). The phenotypes in mice, especially smaller brain-

and neuronal cell size, are very similar to the condition of RTT patients. The identical phenotypes of a brain specific MeCP2 deletion and a MeCP2 null mouse suggest that the phenotype is mostly due to deficiency of MeCP2 in the brain rather than in peripheral tissues. Further, deletion of MeCP2 in postnatal neurons results in similar but less severe phenotypes at a later age of the mice, suggesting the importance of MeCP2 in mature neurons (Chen et al., 2001). Besides MeCP2 loss of function, also gain in MeCP2 dosage are the cause for similar neurological phenotypes as observed on transgenic mice expressing MeCP2 at increased levels compared to the wild type (Collins et al., 2004; Luikenhuis et al., 2004; Table 2). Interestingly, MeCP2 null mice crossed with MeCP2 transgenic mice are fertile, do not display RTT like behavior and are indistinguishable from wild type (wt) mice. These observations demonstrate that restoring normal MeCP2 protein level rescues the severe phenotype of both MeCP2 null animals and transgenic mice (Collins et al., 2004; Luikenhuis et al., 2004).

2.3 Biological functions of MeCP2

2.3.1 Binding of MeCP2 to DNA *in vitro*

As already mentioned, MeCP2 has been initially described to specifically bind one symmetrically methylated CpG pair via its MBD (Lewis et al., 1992). MeCP2 further requires four or more adenine/ thymine (A/T) base pairs adjacent to the methylated CpG for strong binding *in vitro* (Klose et al., 2005). A/T runs have also been detected at MeCP2 target sequences *in vivo* (Klose et al., 2005). Strikingly, an AT hook domain, normally leading to binding of a protein to the minor groove of A/T rich DNA (Lewis et al., 1992; Nan et al., 1993), resides within MeCP2 (aa 168 - aa 205) but seems to be dispensable for MeCP2 specificity for A/T runs (Klose et al., 2005). In contrast, selective binding to mCpGs followed by an A/T run relies on MeCP2 MBD (Klose et al., 2005).

In addition, recombinant MeCP2 has been shown to be capable of binding both unmethylated and methylated DNA (Adams et al., 2007; Georgel et al., 2003; Ishibashi et al., 2008; Nikitina et al., 2007b) with a 3-fold higher preference for its methylated substrate (Fraga et al., 2003). MeCP2 MBD as well as TRD have been each described as independent binding domains for unmethylated DNA *in vitro* (Adams et al., 2007). Under low ionic strength, MeCP2 binds to long, linear unmethylated DNA (Georgel et al., 2003), while in the presence of an unmethylated competitor, MeCP2 induced methylation specific binding is promoted (Ishibashi et al., 2008; Nikitina et al., 2007b). It is striking that under the same conditions, the RTT mutant R106W neither binds methylated nor unmethylated DNA (Nikitina et al., 2007b). In contrast, the COOH-terminal truncation mutants R294X and H370X behave similar to the wt protein, demonstrating that the

missing COOH-terminal regions are not necessary for binding to DNA (Nikitina et al., 2007b). Visualization of the MeCP2-DNA complexes of wt and truncation mutants by electron microscopy (EM) reveal that MeCP2 is able to cross-link both unmethylated as well as methylated DNA fibres into complex structures, including loops and juxtapositions of DNA (Georgel et al., 2003; Nikitina et al., 2007b).

2.3.2 Binding of MeCP2 to chromatin *in vitro*

Besides DNA, recombinant MeCP2 binds both unmethylated and methylated DNA packed into chromatin with slightly enhanced binding in the case of methylated polynucleosomes (Nikitina et al., 2007b). Depending on the molar ratio between MeCP2 and nucleosome, MeCP2 induces the formation of distinct structural changes of 12-mer polynucleosome arrays under low salt as well as physiological ionic conditions (Georgel et al., 2003; Nikitina et al., 2007b). At molar ratios of < 1 MeCP2 per nucleosome, binding of MeCP2 within one extended 12-mer chromatin fibre results in local compaction of several nucleosomes. At a ratio around 1, the whole array gets transformed into a highly compacted, ellipsoidal structure that sediments as a 60S particle during analytical ultracentrifugation. At a ratio of > 1 , binding of MeCP2 causes assembly of independent 60S particles into oligomeric suprastructures, interpreted as a novel protein induced chromatin tertiary structure (Georgel et al., 2003). Compared to MeCP2, linker histones do not exhibit such a strong compaction ability, as they cause under the same low salt conditions more or less decondensed open zigzag conformations of nucleosomes and linker DNA (Bednar et al., 1998). Of note, MeCP2 chromatin compacting domain is described to be distinct from the MBD *in vitro*, as the truncation mutant R168X lacking the domains behind the MBD is impaired in forming higher order chromatin structures (Georgel et al., 2003). Recombinant MeCP2 was illustrated to bind to methylated nucleosomes close to the linker DNA entry-exit site (Ishibashi et al., 2008; Nikitina et al., 2007a) and the interaction between MeCP2 and chromatin results in the protection from micrococcal nuclease (Mnase) digestion of a 11bp linker DNA segment (Nikitina et al., 2007a). Whereas MeCP2 protects one linker, H1 leads to a protection of around 20 bp of DNA covering two linker DNA segments in a symmetrical manner (Nikitina et al., 2007a).

2.3.3 MeCP2 DNA binding and effect on chromatin architecture *in vivo*

The observation that MeCP2 shows also affinity for unmethylated DNA *in vitro* (2.3.1 and 2.3.2) raises the question which role methylation of DNA plays concerning MeCP2 DNA recognition *in vivo*. As already described, MeCP2 is predominantly localized at pericentric heterochromatic regions in mouse cells, that are highly enriched in strongly methylated major satellite repeats and tend to form clusters known as chromocenters (Hsu et al.,

1971). MeCP2 localization to heterochromatin *in vivo* requires a functional MBD (Nan et al., 1996) and is impaired in mutant cells exhibiting nearly no level of genomic mCpGs (Jorgensen et al., 2004; Nan et al., 2007; Nan et al., 1996). High throughput DNA sequencing of total MeCP2 bound chromatin of mature mouse brain further demonstrated MeCP2 global distribution and its nearly precise tracking of mCpG density genome wide (Skene et al., 2010). Of note, MeCP2 significant enrichment across chromatin mirroring mCpG density seems to result from its high abundance in mature mouse brain (16×10^6 molecules per neuronal nucleus), as MeCP2 binding profile in wt mouse liver with much lower level of MeCP2 (0.5×10^6 molecules per liver nucleus) resembles the one of MeCP2 null brain (Skene et al., 2010).

During myogenic differentiation of mouse myoblasts a severe increase in chromatin clustering has been observed, resulting in decreased number of heterochromatic foci (Brero et al., 2005). In parallel, an increase in methylated CpGs as well as augmented expression of MeCP2 and MBD2 takes place, suggesting a direct role of these proteins in heterochromatin reorganization (Brero et al., 2005). In the absence of differentiation, overexpression of MeCP2 in mouse cells induces aggregation of pericentric heterochromatin in a dose dependent manner with the clustering ability mostly based on the MBD (Brero et al., 2005). Neither HDAC containing complexes recruited via MeCP2 CoRID nor the H3K9 methylation pathway seem to be essential for MeCP2 mediated reorganization of heterochromatin (Brero et al., 2005). Of note, a MeCP2 mutant, lacking the NH₂-terminus and the MBD, still accumulates at heterochromatin albeit at lower level in comparison to a construct including the MBD, indicating other modes of MeCP2 heterochromatin association (Brero et al., 2005). MeCP2 impact on chromatin architecture *in vivo* is supported by the findings that isolated neurons from MeCP2 null mouse brain as well as nuclear extracts from the cortex of MeCP2^{308/Y} RTT mutant mice display increased level of histone H3 acetylation (H3Ac) compared to the wt (Shahbazian et al., 2002; Skene et al., 2010). In neurons of mature wt mouse brain, the amount of MeCP2 has been estimated to be half of the one of nucleosomes (Skene et al., 2010). Whereas in most cell types H1 is present at one molecule per nucleosome, H1 occupancy in wt neurons resembles the one of MeCP2 with one molecule every two nucleosomes (Allan et al., 1984; Woodcock et al., 2006). Intriguingly, an approximately two-fold upregulation of H1 is found in MeCP2 null neurons, indicating a potential competition for binding to methylated chromatin between MeCP2 and the linker histone in the wt state (Ishibashi et al., 2008; Skene et al., 2010).

2.3.4 Interacting partners of MeCP2

MeCP2 binding to methylated DNA and chromatin suggests roles in transcriptional repression as well as modulation of chromatin architecture. In addition to binding methylated DNA and chromatin, four major classes of MeCP2 interacting partners involved in transcriptional regulation, RNA splicing, DNA methylation and post-translational modifications (PTM) have been described (Figure 4).

Besides the deacetylase activity containing Sin3A complex, MeCP2 has been found associated to the co-repressors c-Ski, N-CoR (Kokura et al., 2001) and CoREST (You et al., 2001; Lunyak et al., 2002), to a histone methyltransferase activity specific for H3K9 (Fuks et al., 2003; Lunyak et al., 2002) and to the ATPase dependent chromatin remodelling proteins Brahma (Brm) and ATRX (Harikrishnan et al., 2005; Kernohan et al., 2010; Nan et al., 2007). These interactions reinforce MeCP2 mediated transcription silencing.

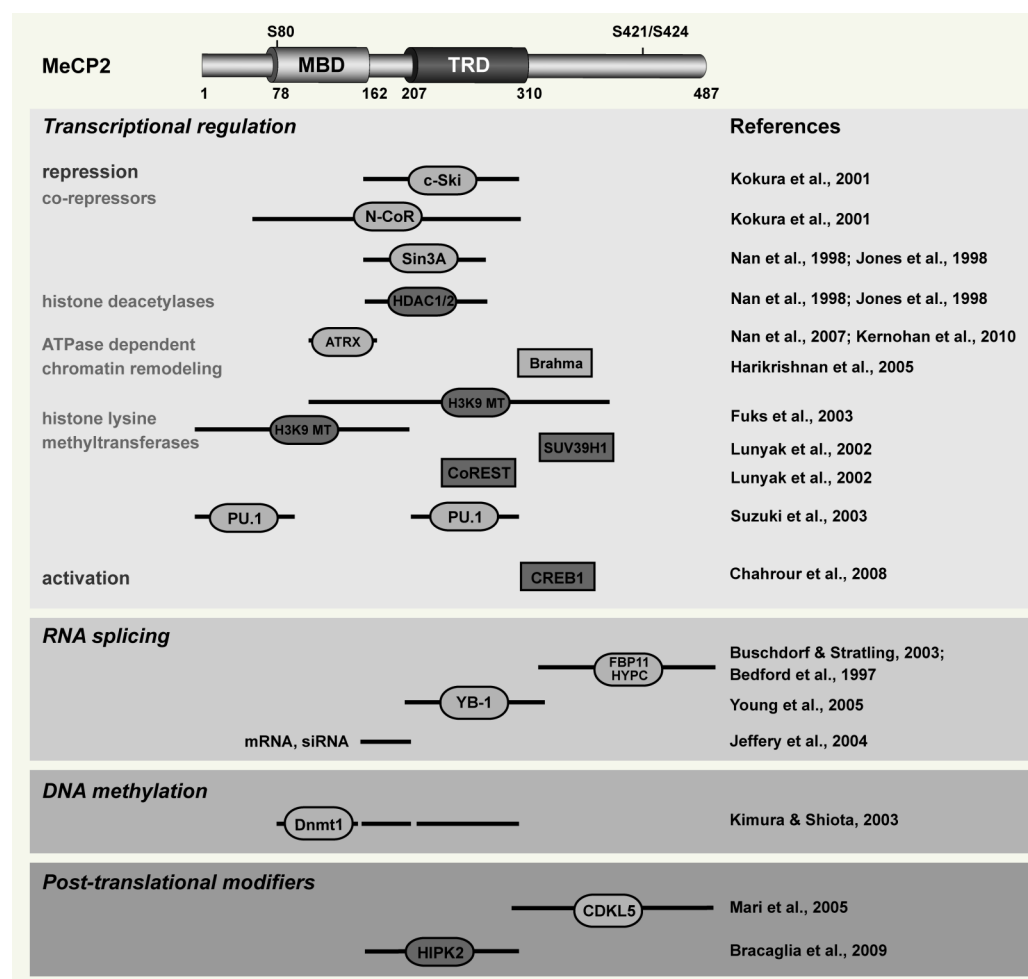


Figure 4. Summary of MeCP2 interacting partners

MeCP2 interacting partners and their mapped interacting domains are illustrated. Boxes in light grey indicate direct protein-protein interactions, boxes in dark grey implicate physical associations. Phosphorylation of the sites Ser80, Ser421 and Ser424 has been indicated in the regulation of MeCP2 chromatin association. Numbers represent aa coordinates; MT stands for methyltransferase.

A recent study revealed the transcriptional activator CREB1 as a new interaction partner of MeCP2 (Chahrour et al., 2008). Sequential ChIP experiments demonstrated further that MeCP2 and CREB1 are simultaneously associated with a promoter of an activated target gene, whereas CREB1 was bound in the case of a repressed target (Chahrour et al., 2008). This contradictory link of MeCP2 to gene activation is supported by the finding that the majority of promoters occupied by MeCP2 (63%) are transcriptionally active and that most of the highly methylated promoters are not bound by MeCP2 (Yasui et al., 2007).

In addition, MeCP2 has been linked to RNA splicing. MeCP2 binds to the Group II domains of the splicing factors FBP11 (Bedford et al., 1997; Buschdorf and Stratling, 2004) and HYPK (Buschdorf and Stratling, 2004). Y box binding protein 1 (YB-1), a component of messenger ribonucleoprotein particles (mRNPs), associates with MeCP2 in a RNA depending manner (Young et al., 2005). MeCP2 has been further shown to be involved in alternative splicing of reporter minigenes (Young et al., 2005). Microarray analysis of cerebral cortex mRNA isolated from wt and RTT mutant mice MeCP2^{308/Y} (Moretti et al., 2005; Shahbazian et al., 2002; 2.2.6) revealed abnormal alternative splicing patterns in the mutant mouse brain (Young et al., 2005). These findings together with the observation that MeCP2 forms complexes with mRNA as well as siRNA (Jeffery and Nakielny, 2004) underline its potential role in RNA splicing.

MeCP2 was shown to form an association with Dnmt1 that excludes HDAC1 and does not seem to be repressive (Kimura and Shiota, 2003). On the contrary, MeCP2 binds hemimethylated DNA and constitutes together with Dnmt1 a complex with methyltransferase activity to hemimethylated DNA (Kimura and Shiota, 2003). These data suggest a role of MeCP2 in Dnmt1 mediated maintenance methylation.

MeCP2 has been recently described to associate to cyclin-dependent kinase-like 5 (CDKL5), a putative Ser/Thr kinase, capable to phosphorylate itself as well as MeCP2 *in vitro* (Mari et al., 2005). These findings together with the observation, that mutations within the CDKL5 gene have been associated with a RTT like phenotype (Mari et al., 2005; Scala et al., 2005) suggest that CDKL5 and MeCP2 may be involved in the same molecular pathway. Of note, the capability of CDKL5 to modify MeCP2 *in vitro* has been questioned (Lin et al., 2005).

In addition, MeCP2 directly associates with homeodomain-interacting protein kinase 2 (HIPK2), involved in regulation of cell growth and apoptosis (Calzado et al., 2007; Rinaldo et al., 2007). MeCP2 further gets specifically phosphorylated by HIPK2 at Ser80 *in vivo* and *in vitro* (Bracaglia et al., 2009) and has been reported to promote HIPK2 mediated apoptosis. For this, a functional MBD as well as phosphorylation of Ser80 of MeCP2 seem to be necessary (Bracaglia et al., 2009).

2.3.5 Post-translational modifications of MeCP2 modulate its functions

Recently post-translational modifications have been described for MeCP2 that seem to exert balancing effects in the modulation of its function and might embody a key mechanism by which MeCP2 regulates gene expression.

Depolarization of cultured neurons (with KCl) results in reduced association of MeCP2 to the promoter of the Brain derived neurotrophic factor (Bdnf) with increased transcription of Bdnf as a consequence (Chen et al., 2003; Martinowich et al., 2003). Activity-dependent phosphorylation of Ser421 has been proposed as the driving force for MeCP2 disassociation from the Bdnf promoter (Zhou et al., 2006), with the calcium/calmodulin-dependent protein kinase IV (CaMK IV) being important to mediate Ser421 phosphorylation *in vivo* (Tao et al., 2009). Phosphorylation of Ser421 was additionally shown to have impact on MeCP2 regulated neuronal spine maturation and dendritic growth (Zhou et al., 2006). In contrast to Ser421, Ser80 of MeCP2 has been observed to be phosphorylated in resting neurons and dephosphorylated upon neuronal activity (Tao et al., 2009). ChIP experiments revealed that phosphorylation of Ser80 is critical for maintaining MeCP2 association to chromatin (Tao et al., 2009). This opposing regulation of phosphorylation of Ser80 and Ser421 upon neuronal activity suggests that phosphorylation of Ser80 might be important for MeCP2 function in resting neurons, whereas phosphorylation of Ser421 seems to be indispensable for MeCP2 in depolarized neurons. Intriguingly, MeCP2^{S80A} knock-in mice with a Ser to Ala mutation show decreased locomotor activity, similar to the locomotor activity of MeCP2 minus mice, whereas MeCP2^{S421A/S424A} mice had increased locomotor activity relative to the wt (Tao et al., 2009).

Phosphorylation of MeCP2 was further shown to serve as a nuclear export signal for the intracellular localization of MeCP2 during neuronal cell differentiation (Miyake and Nagai, 2007). While MeCP2 is transferred from the cytosol into the nucleus during neuronal maturation, its phosphorylated form is exclusively present in the cytosolic fraction (Miyake and Nagai, 2007).

2.3.6 Poly(ADP-ribose)polymerase-1

Poly(ADP-ribose)polymerase-1 (PARP-1) is the founder of the superfamily of PARP proteins encompassing up to 17 members. PARP-1 comprises three major domains, the NH₂-terminal DNA binding domain (DBD), the automodification domain and the COOH-terminal catalytic domain. The DBD has been proposed to mediate the stimulation of PARP catalytic activity in response to DNA breaks via two zinc fingers (Cys-Cys-His-Cys motifs) (Ikejima et al., 1990) and recruits PARP to DNA through two helix-turn-helix motifs (Buki and Kun, 1988; Sastry et al., 1989). The automodification domain contains the BRCA1 C-terminus (BRCT) domain, a protein-protein interacting motif constituting PARP-1 major protein interface with numerous nuclear partners and itself (Ame et al., 2004). This domain also contains many of the acceptor residues of ADP-ribose chains involved in PARP-1 automodification (Duriez et al., 1997), which results from the stimulation of its catalytic activity upon binding to DNA strand breaks. The catalytic domain carries the ADP-ribose transferase activity catalyzing initiation, elongation and branching of ADP-ribose polymers (Simonin et al., 1993). It also contains those amino acids known as the 'PARP signature', which are the most conserved residues within the PARP family (de Murcia and Menissier de Murcia, 1994; Ruf et al., 1996) and form a β - α -loop- β - α structure responsible for NAD⁺ binding (Ruf et al., 1998). PARP-1 uses NAD⁺ to catalyze the covalent attachment of ADP-ribose units to Glu and Asp of a target protein and in the case of automodification to itself. This post-translational modification, termed poly(ADP-ribosyl)ation, leads to an attached polymer consisting of a linear or multibranched polyanion, that can also be bound in a noncovalent manner by proteins bearing a poly(ADP-ribose) (PAR) binding motif (Pleschke et al., 2000). Nuclear proteins, mostly involved in establishing and mediating chromatin architecture such as histones, high mobility group proteins, topoisomerases and chromatin remodelling complexes are the predominant targets for the covalent addition of poly(ADP-ribose), with histone H1, H2A and H2B as the major poly(ADP-ribosyl)ated chromatin proteins (Rouleau et al., 2004). The restoration of poly(ADP-ribosyl)ated proteins to their native unmodified state is mediated by the poly(ADP-ribose)glycohydrolase PARG (Alvarez-Gonzalez and Althaus, 1989).

PARP-1 role in DNA damage recognition, signalling and regulation of the chromatin structure upon damage either through physical interaction or poly(ADP-ribosyl)ation of proteins has been extensively studied. Relaxation of chromatin at DNA breaks induced by poly(ADP-ribosyl)ation of histone tails or their non-covalent binding to automodified PARP-1 has been proposed to facilitate the access of the repair machinery to lesions (Ogata et al., 1980a; Ogata et al., 1980b; Poirier et al., 1982). PARP-1 knockout models

as well as inhibition assays of PARP catalytic activity revealed its importance as a survival factor involved in the surveillance and maintenance of genome integrity (de Murcia et al., 1997; Masutani et al., 1999; Wang et al., 1997). Further, they indicated PARP-1 involvement in various inflammation processes (Shall and de Murcia, 2000).

Recently, PARP1 has been implicated in the regulation of chromatin structure and gene expression under physiological conditions (Kraus and Lis, 2003; Quenet et al., 2009; Tulin et al., 2002). It has been described as a structural component of chromatin inducing the formation of NAD⁺ reversible compact chromatin structures, which are transcriptionally repressed but distinct from H1 higher condensation states *in vivo* (Kim et al., 2004; Wacker et al., 2007). Biochemical studies combined with atomic force microscopy identified both the DBD and the catalytic domain of PARP-1 as cooperating to promote chromatin compaction and transcriptional repression (Wacker et al., 2007).

3 Questions and aims of this work

Based on recent findings of our group regarding MeCP2 role in heterochromatin organization *in vivo*, this work addresses the regulation of this process and its misregulation in disease.

The following questions were raised:

- i) Is MeCP2 mediated heterochromatin clustering affected in Rett syndrome (Chapter 5.1)?
- ii) Is MeCP2 induced heterochromatin remodeling regulated by post-translational modifications and do other methyl-CpG binding domain (MBD) family members get post-translationally modified (Chapter 5.1 and 5.2)?
- iii) Are interactions of MeCP2 with other proteins as well as homo- and hetero-associations among the MBD family involved in chromatin organization (Chapter 5.1, 5.2 and Appendix)?

4 Methods and Materials

4.1 Molecular biology methods

4.1.1 Construction of expression plasmids

All plasmids constructs generated for this study were made employing standard cloning procedures and transformation of *Escherichia coli* (*E. coli*) (Sambrook and Russel, 2001). Using the alkaline lysis method (Birnboim and Doly, 1979), plasmid DNA was isolated from transformed *E. coli* and verified by sequencing or restriction enzyme analysis.

Mammalian expression constructs coding for GFP- or YFP-tagged rat MeCP2 full length (MeCP2G) and deletions (MeCP2Y.3) were previously described (Brero et al., 2005). The mammalian expression constructs MeCP2G.9 and MeCP2G.8 were generated from the above plasmids by PCR amplification using the primers listed in Table 3. Deletion constructs MeCP2G.11 - 15 designed with flanking XhoI and BamHI sites according to the sequence of MeCP2G were custom synthesized into pPCR Script (Sloning Bio Technology) and subcloned into the XhoI and BamHI sites of MeCP2G.6 (Agarwal et al., 2007).

MeCP2G.16 - 18 as well as point mutations within MeCP2G.11 and MeCP2G.14 were generated using site directed mutagenesis (Table 3) as described in detail before (Makarova et al., 2000; Wang and Malcolm, 1999). Expression vectors encoding GFP-tagged fusions of human wt or mutant MeCP2 cDNA cloned into the pEGFP-C1 vector as well as the expression constructs encoding GFP-fused mouse MBD proteins were described before (Kudo et al., 2003; Hendrich and Bird, 1998).

For expression in Sf9 insect cells the Bac-to-Bac Baculovirus Expression System (Invitrogen) was used and the above mentioned rat MeCP2 constructs were cloned into pFastBac1 either by direct restriction enzyme digestion and ligation subcloning or using first PCR amplification (Table 3). Sf9 expression constructs encoding mouse GFP-fused MBDs were generated from the above plasmids performing PCR amplification employing the primers listed in Table 3. To express PARP-1 with a NH₂-terminal strep-tag, a sequence encoding the strep-tactin target peptide strep tag III was synthesized into pPCR-Script-Amp (Entelechon) flanked by BamHI and NotI sites and subcloned into pFastBac1 using the same sites. Human PARP-1 fl and deletion constructs were generated by PCR amplification using primers with NotI and XhoI sites (Table 3) and subcloned in frame with the strep-tag in the pFastBac1 vector.

Table 3: Oligonucleotides used for generation of MBD and PARP-1 constructs

Plasmid	Oligonucleotide sequence	Expression in
pFB-st-PARP-1	ss ataagaatgctggccgagccatggcggaggtcttcggataa as ccgctcgagttaccacaggaggtcttaaaattgaatt	Sf9 cells
pFB-st-PARP-1-ABC	ss ataagaatgctggccgagccatggcggaggtcttcggataa as ccgctcgagtttaggagggcggagggctggccgccac	
pFB-st-PARP-1-D	ss ataagaatgctggccgagccatgacagcctcctgctcctgtgtg as ccgctcgagttatctcattctcttttcagatttggt	
pFB-st-PARP-1-EF	ss ataagaatgctggccgagccatgttaactcttaaggaggagca as ccgctcgagttaccacaggaggtcttaaaattg	
pFB-eGFP	ss ataagaatgctggccgagccatggtgagcaaggcgca as ctagtctagattacttgtagcagctcgtccatgcccga	
pFB-MeCP2G.9	ss cgcggatccgccatggggagcccttcaggagagaacag as ataagaatgctggccgctccgggtcttgctctcttgat	
pFB-MeCP2G.8	ss ggaagatctgccatggaaaaccgtcagcattgaggtcaag as ataagaatgctggccgcttacttgtagcagctcgtccatgcc	
pFB-mMBD1aG	ss acgctcgagcagccatggctgagtcctggcaggact as atagtttagcggccgcacaaaactctcttctcaa	
pFB-mMBD2aG	ss acgctcgagcagccatgctgctgagccagggggag as atagtttagcggccgcagcctcatctccactgtc	
pFB-mMBD3G	ss acgctcgagcagccatggagcggagaggtgggagt as atagtttagcggccgcacactcgtctggctccgg	
pFB-mMBD4G	ss acgctcgagcagccatggagagcccaaccttgggg as atagtttagcggccgcaagatagacttaattttc	
pFB-mMBD2aG.1	ss acgctcgagcagccatgctgctgagccagggggga as atagtttagcggccgacactctctccgctctccgt	
pFB-mMBD2aG.2	ss acgctcgagcagccatggactgcccggccctcccc as atagtttagcggccgcagcctcatctccatctc	
pMeCP2G.9	ss ccgctcgagccatggggagcccttcaggagagaaca as cgcggatccttccgggtcttgctctcttgatggggagcac	
pMeCP2G.8	ss ggaagatctgccatggaaaaccgtcagcattgaggtcaag as ataagaatgctggccgcttacttgtagcagctcgtccatgcc	
pMeCP2G.16	ss gattttgacttcaactgtaactgggagagttcaagtgaaaagg as cttctccaggacccttttcaacttgaactctcccagttacagt	
pMeCP2G.17	ss gagggaggtgggctaccaatctgctggtggcagctgctgct as ttggcctctgagcagcagctgcccaccgagatggtgtagc	
pMeCP2G.11_E205A	ss agaccaaaggcagcagcattcagcaggttaaggatccaccggtcgcc as ggcgaecgggtggatccttacttctgctgagctgctgcttgggtct	
pMeCP2G.11_E169A	ss atggggagcccttcaggagagcctcagaaaccctagaagccc aa gggctctttaggtggtttctgagctctcctggaaggctccccat	
pMeCP2G.11_K175A_K177A_K180A	ss ggagagaacagaacacactaaagcgcctctcccagcagctccaggaactggc as gccagttcctggagctgctgggagatgctggcgccttaggtggtttctgtctctcc	
pMeCP2G.11_K175A	ss gagaaacagaacacactaaagcgcctcccaaaatctccaaagctcc as ggagccttgggagatttggcgccttaggtggtttctgttctc	
pMeCP2G.11_K177A	ss ccacctaagaagccccgactctcccaagctccaggaactgg as ccagttcctggagccttgggagatgctggctctttaggtgg	
pMeCP2G.11_K180A	ss cctaagaagcccaaatctcccagcagctccaggaactggc as gccagttcctggagctgctgggagatttggcctcttagg	
pMeCP2G.11_K200A	ss gcactgggagaccagcggcagcagcattcagaagg as ccttctgatgctgctgctgctgctgcttcccagtg	
pMeCP2G.14_E258A_D260A	ss agaaaacgaaaagctgcaagctgccccagggccattctcaagaaa as ttcttaggaatggcctgggggagcagctgcttctctctct	
pMeCP2G.14_D260A	ss agaaaacgaaaagctgcaagctgccccagggccattctcaagaaa as ttcttaggaatggcctgggggagcagctgcttctctctct	
pMeCP2G.14_E258A	ss cctggcagaaaagcgaagctgcaagctgccccagggccattctcaagaaa as aggaatggcctgggggtcagctgcaagcttctctctct	
pMeCP2G.14_K267A_K271A	ss cccaggccattctcaagcagcgggtagagcgcctgggaggtggaaggatcc as ggatccttcacactcccagcgccttaccocgtgcttaggaatggcctggg	
pMeCP2G.14_K254A	ss gatcaaacgccccggcagagcgcgaaagctgaaagctg aa cagcttcagctttctcgcctctgcccagggcgtttgagc	
pMeCP2G.14_K267A	ss ccaggccattctcaagcagcgggtagaaaagcctgg as ccaggcttctaccccgtgcttaggaatggcctgg	
pMeCP2G.14_K271A	ss tctcaagaaacgggtagagcgcctgggaggtggaagg as ccttcacactcccagcgccttaccocgttcttagga	

The letters in bold highlight the amino acids substituted by site directed mutagenesis.

4.2 Cell biology methods

4.2.1 Cell culture and transfection

Pmi28 diploid mouse myoblasts were cultured as described in (Kaufmann et al., 1999). Cells were grown to 70-80 % confluency on 16 mm glass cover slips in 6 well plates and transfected using TransFectin (BioRad). For transfection, 3 µg of plasmid DNA together with 3 µl transfectin were incubated in serum free medium for 20 min at RT and added to

the cells. After incubation at 37°C for four hours, the medium was changed and the culture was incubated at 37°C overnight. For PARP inhibition assays cells were treated with 10 mM 3AB (Alexis) and 400 µM NU1028 (Sigma) immediately after media change for 12-15 hours. Within this time, medium plus inhibitors were refreshed every three hours. Transfected cells were fixed with 3.7 % formaldehyde in 1 x PBS for 10 min. In the PARP inhibition experiment 10 mM 3AB and 400 µM NU1028 were also added to the solutions during the fixation. All washing steps after fixation were performed with 1xPBS plus 0.01 % Tween-20. Nuclear DNA was counterstained using TOPRO-3 (Invitrogen), Hoechst 33258 or DAPI (4',6'-diamidino-2-phenylindol) and samples were mounted in vectashield (Vector Laboratories) or moviol.

HEK 293-EBNA cells (Invitrogen) were cultured and transfected as described (Agarwal et al., 2007).

Mouse embryonic fibroblast (MEF) cells were cultured in Dulbecco's modified Eagle's medium (DMEM; 1 g/l glucose; GIBCO) supplemented with 10 % fetal bovine serum, transfected with TransFectin according to the manufacturer's instructions and fixed with formaldehyde.

The human foreskin fibroblast (Bj-hTERT) cell line (ATCC BJ-5ta) was derived by transfection of human foreskin fibroblasts with the pGRN145 hTERT expression plasmid and selection of stable immortalized cell clones (Bodnar et al., 1998). It is a diploid human cell line with a modal chromosome number of 46 that occurred in 90 % of the cells counted and karyotypically normal X and Y sex chromosomes. Human Bj-hTERT fibroblasts were cultured in DMEM medium containing 10 % FCS, glutamine and gentamicin. Cells were transfected using the Amaxa nucleofactor (Amaxa AG) or TransFectin (BioRad) following the manufacturer's protocols.

Sf9 insect cells were maintained in EX-CELL 420 Insect Serum Free (SAFC) medium supplemented with 10 % fetal bovine serum shaking at 100 rpm and 28°C. Transfection of Sf9 cells to produce recombinant baculovirus, was performed using Cellfectin (Invitrogen) according to the manufacturer's instructions.

4.2.2 ImmunoFISH

For fluorescence *in situ* hybridization, the following DNA probes were used: repetitive specific human DNA probe pUC 1.77 (Cooke and Hindley, 1979) for chromosome 1, alphoid DNA probe pMR9A for the centromeric region 9q12 of chromosome 9 and alphoid DNA probe pHUR-195 for the centromeric region 16q11.2 of chromosome 16. These DNA probes were labeled by standard nick translation with Cy5-dUTP (Amersham). The labeled DNA was further purified by ethanol-precipitation and the pellet resuspended in hybridization solution (70 % formamide, 2 x SSC, 10 % dextran sulfate,

pH 7.0). The probes were denatured at 80 °C for 5 minutes.

For immunoFISH cells were fixed with 4 % paraformaldehyde in PBS for 10 minutes and permeabilized with 0.25 % Triton X-100 in PBS for additional 10 minutes. Primary (rabbit polyclonal anti-MeCP2) and secondary (anti-rabbit IgG Alexa Fluor 568; Molecular probes) antibodies were diluted in PBS with 0.2 % fish skin gelatin and incubated sequentially for one hour each at room temperature. After immunostaining, the cells are post-fixed with 4 % paraformaldehyde for 60 minutes followed by post-permeabilization with 0.5 % Triton X-100 in PBS for 10 minutes, 0.1 M HCl for 10 minutes and 20 % glycerol for 4 minutes. Probes were added to the cells and sealed with rubber cement to decrease evaporation of the probe over night. They were then denatured simultaneously at 75°C for 5 minutes and hybridized over night at 37°C. Non-hybridized probe was washed off using 50 % formamide in SSC at 45°C three times followed by two washes with 2 x SSC. DNA was counterstained with DAPI and the cells were mounted using vectashield (Vector Laboratories).

MeCP2 expressing cells were identified by the positive staining with the anti-MeCP2 antibody and complete Z stacks of images (voxel size: 80 x 80 x 200 nm) of the DAPI (excited at 405 nm) and Cy5 (excited at 633 nm) signals for whole DNA and chromosomes 1, 9 and 16 pericentric heterochromatin regions, respectively, were acquired on a Leica SP5 laser scanning microscope using a 63 x/1.4NA oil objective. FISH signals were counted manually through these stacks.

4.2.3 Microscopy, image analysis and statistical evaluation

Chromocenter counting: Fixed cells were examined on a Zeiss Axiovert 200 epifluorescence microscope. Image stacks (0.5 µm Z interval) were acquired with a 63 x Plan-Apochromatic NA 1.4 or 40 x Plan-Neofluar NA 1.3 oil immersion phase contrast objectives and a PCO Sensicam QE cooled CCD camera. Images were processed with Adobe Photoshop and ImageJ version 1.38x (<http://rsb.info.nih.gov/ij>). 3D rendering of image stacks was performed using AMIRA software.

The acquired image stacks were analyzed using a semi-automated approach. For this we developed a custom application using the priithon platform. Image stacks were treated as three-dimensional volumes and segmented displaying an optical section view and a maximum intensity Z-projection. Nuclei and chromocenters were automatically identified by intensity based thresholding and implementation of the water algorithm (Harmon and Sedat, 2005). Identified nuclei and chromocenters were outlined and numbered and the performance of the algorithm was controlled by visual inspection using optical section views and maximum intensity Z - projections. Parameters were adjusted to account for

different sample brightness and chromocenter density. All intermediate images, parameters and counting results were automatically saved.

Chromocenter binding: Confocal Z stacks (voxel size: 0.05 x 0.05 x 0.3 μm) of 10 cells expressing similar levels of the GFP fusion protein were collected on either Zeiss LSM510Meta or Leica SP5 confocal microscopes, using 63 x/1.4NA oil objective and 405 nm DPSS (for Hoechst 33258, DAPI), 488 nm argon (for GFP) and 633 nm He - Ne (TOPRO-3) laser excitation. Care was taken in selecting the imaging conditions to avoid under and over exposed pixels, while keeping the imaging conditions constant. The heterochromatic foci were identified by staining with TOPRO-3, Hoechst 33258 or DAPI. Image analysis was done using ImageJ. The average mean intensity at the chromocenters versus the nucleoplasm was assessed by selecting four regions of equal size in the two compartments, calculating the mean fluorescent intensity in each compartment and then taking a ratio between both.

In the case of chromocenter counting assays, cumulative frequencies of chromocenter numbers were tested for statistical significance utilizing the Kolmogoroff-Smirnoff test (applied in Figure 6 and 12).

For chromocenter binding assays, statistical significance was checked through t-test (applied in Figure 5C).

For counting of FISH chromosome signals, the t-test was performed for statistical analysis (applied in Figure 7).

4.3 Biochemical methods

4.3.1 *In vivo* protein interaction assays

HEK 293-EBNA or MEF cells, transfected with expression plasmids as indicated, were pelleted after washing with 1 x PBS and lysis was performed for 10 min on ice. For interaction studies (Figure 9A) 300 μl buffer A (20 mM Tris-HCl, pH 7.5; 150 mM NaCl; 0.5 mM EDTA; 2 mM PMSF; 0.5 % NP40) was used. For disruption of protein-DNA associations to obtain high amount of protein (Figure 10A, D and E; Figure 11; Figure 14) buffer B (25 mM Tris-HCl, pH 8.0; 1 M NaCl; 50 mM glucose; 10 mM EDTA; 0.2 % Tween-20; 0.2 % NP40) was used. All buffers were supplemented with protease inhibitors (Complete Mini; Roche).

Mouse brain tissue (6 grams; Figure 10B) was first fractionated to obtain pure nuclei as described in detail before (Prusov and Zatsepina, 2002). The isolated nuclei were incubated in buffer B for 15 min on ice. 500 μl of the extract were diluted 1:4 with buffer C (25 mM Tris-HCl, pH 8.0; 50 mM glucose; 10 mM EDTA; 0.2 % Tween-20; 0.2 % NP40), to obtain a NaCl concentration of 250 mM. After centrifugation (20,000 x g, 15 min, 4 $^{\circ}\text{C}$)

rabbit polyclonal anti-MeCP2 antibody (40 µg) or chromatographically purified rabbit IgG (40 µg; Organon Teknika) were added to the supernatant and incubated for 1.5 hours rotating at 4 °C. To pull down the immunocomplexes, 50 µl protein A agarose beads (Fast Flow; Upstate), equilibrated with the corresponding buffer, were added and incubated for one hour.

For immunoprecipitation using the GFP binder (ChromoTek; Rothbauer et al., 2008), 50 µl protein A agarose beads were incubated with 100 µg GFP binder for one hour, then added to the extract and again incubated for one hour at 4 °C rotating. After a short spin, the supernatant was removed and the beads were washed three times with 500 µl of the same buffer used during cell lysis. The beads were resuspended in 1x SDS-containing sample buffer, boiled for 10 min at 95 °C and analyzed by SDS-PAGE electrophoresis followed by Western blotting.

4.3.2 *In vitro* protein interaction assays

Sf9 insect cells were infected with the recombinant baculovirus (P3 stock) and incubated at 28 °C with shaking for 5 days. The cells were pelleted by centrifugation (200 x g, 5 min, 4 °C) and resuspended in either buffer B (25 mM Tris-HCl, pH 8.0; 1 M NaCl; 50 mM glucose; 10 mM EDTA; 0.2 % Tween-20; 0.2 % NP40) or buffer D (PBS containing 300 mM NaCl and 0.05 % NP40). All buffers were supplemented with protease inhibitors (Complete Mini; Roche). After incubation on ice for 10 min, cells were disrupted with a high-pressure homogenizer (EmulsiFlex-C5, Avestin) followed by centrifugation at 14,000 x g for 30 min.

Strep-tagged recombinant proteins were purified by incubating the supernatant with 500 µl of Strep-Tactin Sepharose (IBA) beads for three hours at 4°C on a rotary shaker. To elute strep-tagged proteins, the beads were incubated with D-Desthiobiotin (0.5 mg/ml; IBA), dissolved in 1x PBS, for 30 min at 4°C. After centrifugation (200 x g, 2 min), beads were separated from the eluate containing the purified proteins.

GFP fusion proteins were immobilized using the GFP-Trap (ChromoTek) as described (Rothbauer et al., 2008).

Purified untagged human MeCP2 (pTYB1) was produced and purified as described (Georgel et al., 2003).

For *in vitro* binding assays, immobilized recombinant GFP- or strep-tagged proteins as indicated were incubated for one hour at 4 °C on a rotary shaker with equal amounts of purified proteins or protein extracts in 500 µl buffer D (Figure 9B, C and D) or PBS (Figure 20A) or PBS either supplemented with 50 mM NaCl or 100 mM NaCl (Figure 20B). After a short spin, the beads were washed three times with the same buffer used

for the incubation step before and dissolved in 50 μ l 1x SDS-containing sample buffer and boiled for 10 min at 95 °C.

4.3.3 Western blot analysis

Western blot analysis was performed as described (Mortusewicz et al., 2006), using PVDF membrane (BioRad) or nitrocellulose membrane (GE Healthcare). Immunoreactive bands were visualized either by ECL plus or ECL advanced Western Blot Detection Kit (Amersham). The following primary antibodies were used for Western blot analysis: rabbit polyclonal anti-MeCP2 (Upstate), mouse monoclonal anti-GFP (Roche), mouse monoclonal anti-PARP-1 (F-2, Santa Cruz), mouse monoclonal anti-PAR (Trevigen). Secondary antibodies used were: horseradish peroxidase conjugated anti-mouse IgG (Amersham), horseradish peroxidase conjugated anti-rabbit IgG (Sigma). In the case of strep-tagged proteins, the membrane was incubated with horseradish peroxidase conjugated StrepTactin (BioRad) for 1.5 hours at room temperature (RT).

4.3.4 *In vitro* poly(ADP-ribosyl)ation assay

In vitro poly(ADP-ribosyl)ation analysis of recombinant GFP or MeCP2G immobilized onto GFP-Trap beads (ChromoTek), were performed as described in (Schreiber et al., 2002) with following modifications: purified st-PARP-1 (50 ng) from Sf9 cells, 20 μ M cold NAD⁺ in addition to [α -³²P]NAD⁺ and 100 ng DNase I activated DNA (Alexis) were used. After the reaction, the proteins were washed three times with buffer B to disrupt binding to st-PARP-1.

4.3.5 *In vitro* poly(ADP-ribose) binding analysis

For autoactivation of hPARP-1, 50 μ L reaction buffer 10 x (500 mM Tris-HCl pH8, 1 M NaCl, 40 mM MgCl₂, 2 mM DTT, 2 mM NAD⁺, 20 μ g/mL DNase I activated calf thymus DNA, 500 μ g/mL BSA, 25 μ Ci ³²P- NAD⁺) were incubated with 25 μ g purified hPARP-1 in a final volume of 500 μ L. The reaction was incubated for 30 min at 25 °C. Degradation of the DNA was achieved through addition of 1 μ g DNase I and 2 mM CaCl₂ and incubation at 37°C for 1 h. Next, a treatment with proteinase K was performed at 37 °C overnight in order to degrade the proteins (0,1 % (v/v) SDS, 50 μ g proteinase K). Finally, the last aa linked to the poly(ADP-ribose) was removed by incubation with 0,1 M NaOH and 20 mM EDTA at 37 °C for 1 h. Neutralization was achieved through addition of 0,1 M HCl. The purification of the free poly(ADP-ribose) was processed by phenol/chloroform extraction

followed by ethanol precipitation. After 2 washes with 80% EtOH, the pellet was solubilized in 200 μ L of distilled water and stored at -20 °C.

To renature the proteins that were separated by SDS-PAGE and blotted on nitrocellulose (GE Healthcare), the membrane was treated with 1 x PBS three times for 30 min. Afterwards, the membrane was incubated with the radioactive polymer diluted in 10 ml 1 x PBS for 1 h at 25 °C on a rotating wheel. Afterwards, the membrane was washed three times with 1 x PBS for 15 min on the wheel and exposed overnight at -80 °C (32p autoradiography film; Amersham).

5 Results

5.1 MeCP2 RTT mutations affect chromatin organization and inhibition of MeCP2 poly(ADP-ribosyl)ation rescues this defect

5.1.1 RTT mutations affect MeCP2 binding and clustering of pericentric heterochromatin

We have recently shown that the MBD of MeCP2 has the ability to reorganize and cluster pericentric heterochromatin. As most RTT missense mutations affect this domain (Figure 5A), we set out to investigate whether they are impaired in binding or clustering of heterochromatin.

We selected Pmi28 mouse myoblasts as our cellular assay system since this cell line was used before to characterize the dose-dependent effect of wt MeCP2 on the spatial organization of chromocenters and it expresses a very low to undetectable level of endogenous wt MeCP2 (Brero et al., 2005). Moreover, it showed a stable and nearly normal karyotype (39, X0; data not shown), which minimized variations of chromocenter number caused by variable numerical chromosome aberrations.

We used mammalian expression constructs containing the mutant human MECP2 e2 isoform cDNAs fused at the COOH-terminus of the enhanced GFP coding sequence (Kudo et al., 2003). All 21 missense mutations within the MBD are highlighted in pink in Figure 5A and the corresponding amino acid exchanges are indicated above the sequence alignment. Intranuclear localization of the fusion proteins and the induction of chromocenter clustering in transfected cells were assessed by fluorescence microscopy using the AT-selective DNA dyes Hoechst 33258, DAPI or TOPRO-3 to independently visualize pericentric heterochromatin.

We first tested these MeCP2 RTT mutants for their accumulation at chromocenters by taking a ratio of average mean intensity of protein bound at chromocenters versus nucleoplasm. The results indicate that all the mutant proteins showed an enrichment at chromocenters (ratio greater than 1), but to very different extents (Figure 5C). R111G mutant protein accumulated to the lowest extent in pericentric heterochromatin and it mislocalized instead to the nucleoli (Figure 5B). This is in agreement with the recent finding that R111G exhibits complete loss of MeCP2 function and no longer represses Sp1-mediated transcriptional activation of methylated and unmethylated promoters (Kudo et al., 2003). Except for P101H, R133H, E137G and A140V, all other MeCP2 mutants analyzed accumulated at chromocenters less than the wt, with more than half of them significantly affected in their accumulation ability (Figure 5C).

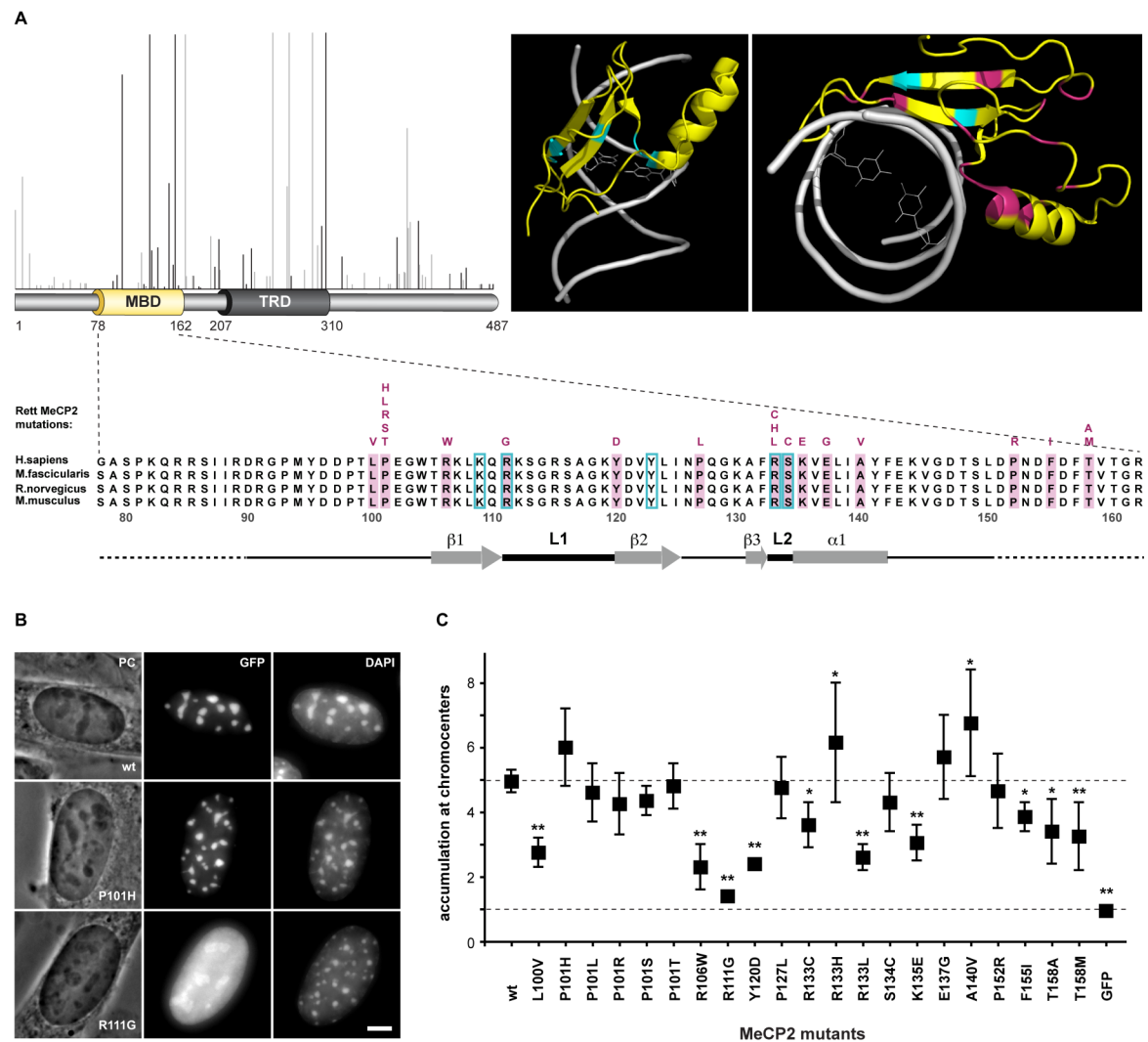


Figure 5. Mutant MeCP2 proteins accumulate at chromocenters *in vivo* to very different extent

(A) Top left panel shows the mutation spectrum in RTT patients (based on IRSA <http://mecp2.chw.edu.au/cgi-bin/mecp2/search/printGraph.cgi>), with missense mutations shown in black and others in light grey color. Location of individual mutations is indicated in a schematic representation of the MeCP2 protein (numbers represent aa coordinates). MBD stands for methyl-CpG binding domain, TRD for transcription repression domain and NLS for nuclear localization signal. Top right panel shows the X-ray structure of the MBD of MeCP2 (displayed in yellow) interacting with its target 5mC within the DNA double helix (shown in white) (PDB accession code 3C2I) (Ho et al., 2008). Structural data were displayed and annotated using PyMOL software (<http://pymol.sourceforge.net/>). The residues that directly interact with the two 5mC are shown in cyan and the RTT mutations included in our study in pink. Bottom panel: the analyzed RTT mutations are listed (in pink) above the corresponding wt aa within the sequence of MeCP2 MBD. **(B)** Representative maximum intensity projections generated from image stacks of mouse myoblasts expressing wt GFP-fused MeCP2 and mutants thereof. DNA was counterstained with DAPI. PC: phase contrast. Scale bar: 5 μ m. **(C)** The plot shows the fold accumulation at chromocenters of the 21 RTT mutants, wt MeCP2 and GFP in mouse myoblasts. Asterisks represent statistically significant difference in regard to the wt: * for $P < 0.05$; ** for $P < 0.001$. All mutants accumulated significantly different ($p \leq 0.05$) with respect to GFP alone (not shown). The experiment was repeated at least two times with 10 cells per mutant evaluated each time.

Since several mutants associated less efficiently with heterochromatin, we further addressed whether they would be impaired in their ability to cluster heterochromatin *in vivo*. To assess the degree of heterochromatin clustering in a quantitative manner, we scored the number of chromocenters in cells expressing either GFP-tagged wt or mutant MeCP2. In Figure 6 the clustering potential of the proteins is displayed as cumulative

frequency curves, which represent the percentage of nuclei with up to a certain number of chromocenters. Cells expressing the RTT mutants P101H, P101R and P152R showed a highly significant increase in chromocenter numbers compared to wt MeCP2 expressing cells (Figure 6). The most dramatic effect had the R111G amino acid exchange, which completely abolished chromocenter clustering (Figure 6C and Figure 6B). Additionally, 10 more mutants exhibited significantly decreased clustering abilities in comparison to wt MeCP2 (Figure 6B). In contrast, the other mutants behaved similarly to the wt. Among them is the A104V exchange that has been reported in association with very mild clinical symptoms (Orrico et al., 2000). Altogether, two thirds of the RTT MeCP2 missense MBD mutants were significantly affected in clustering potential compared to wt MeCP2.

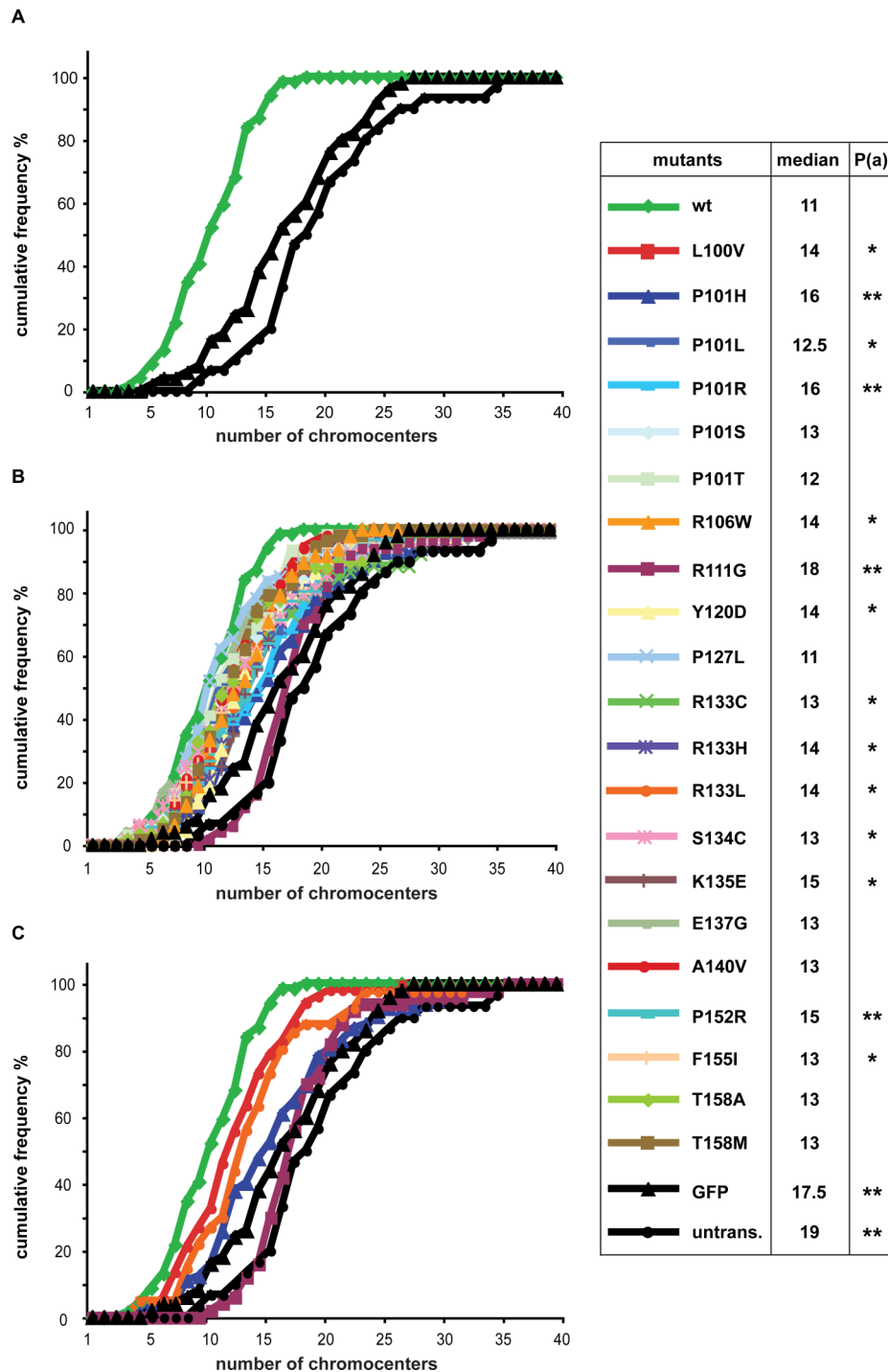


Figure 6. RTT mutant proteins are affected in their ability to cluster chromocenters

Pmi28 mouse myoblasts transfected with an expression vector coding for GFP or GFP-fused MeCP2 construct as indicated. Z-stacks of images were recorded of nuclei with similar expression levels of the GFP-tagged protein and constant image acquisition parameters.

(A) The plot shows the percentage of cumulative frequencies of chromocenter numbers in cells expressing GFP-tagged wt MeCP2 in comparison to untransfected and GFP expressing cells. (B) Cumulative frequencies of chromocenter numbers in cells expressing each of the 21 GFP-tagged MeCP2 mutants. (C) depicts RTT mutants with extreme phenotypes together with the controls (wt MeCP2, GFP and untransfected cells). The table lists the median number of chromocenters for each mutant and depicts the p value with asterisks representing statistically significant difference in regard to the wt: * for $P < 0.05$; ** for $P < 0.001$. The experiment was repeated two times with at least 25 cells evaluated per mutant each time.

We further tested whether the clustering ability of selected mutants was also conserved in human cells. We performed immunostaining in combination with fluorescence in situ hybridization using three DNA probes simultaneously to detect the major pericentric heterochromatin regions present in chromosomes 1, 9 and 16 (Figure 7) of human cells either expressing wt or mutant MeCP2. The outcome of this analysis is shown in Figure 7 and essentially confirms the results obtained in mouse cells.

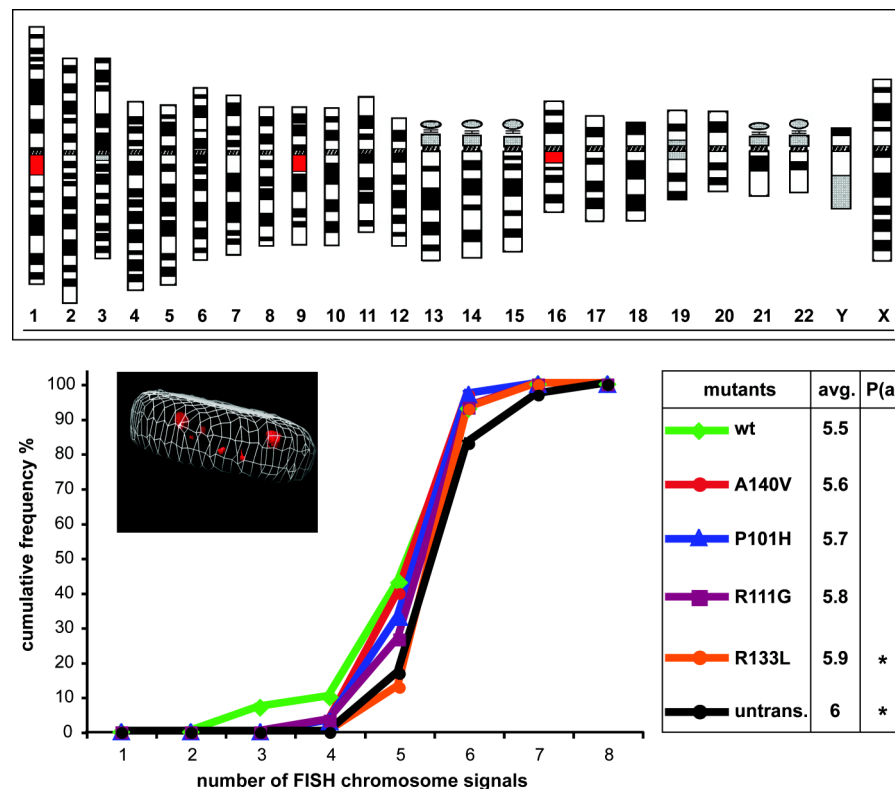


Figure 7. MeCP2 induces heterochromatin clustering in human diploid cells

Top panel: ideogram of G-banded human chromosomes (www.pathology.washington.edu/galleries/cytogallery/main.php?file=human%20karyotypes). Chromosomes 1, 9 and 16 were selected for our analysis as they contain the largest pericentric heterochromatin regions (marked in red). Bottom panel: Cells were transfected with constructs coding for GFP-tagged wt and mutant human MeCP2 and clustering of these heterochromatic regions was analyzed by simultaneous hybridization with three DNA probes from the pericentric heterochromatin DNA of the indicated three chromosomes. Cells expressing the GFP-tagged MeCP2 proteins were identified by immunostaining with anti-MeCP2 antibody and DNA was counterstained with DAPI. Confocal Z stacks of images from the GFP-MeCP2 signal, overall DNA signal and DNA FISH probes were then acquired. The three dimensional rendering of one such cell is shown where the contour of the nucleus is depicted by the white grid and the FISH signals of the three pericentric heterochromatin regions in red. The cumulative frequency of the FISH signals counted is shown by the graph. The table lists the average number of chromosome signals and presents the p value through asterisks representing statistically significant difference in regard to the wild type: * for $P < 0.05$. Experiments were repeated twice with 30 cells evaluated each time per construct.

5.1.2 Heterochromatin binding and clustering properties map to distinct structures of MeCP2 MBP

Next, we tested whether the chromocenter clustering ability of the RTT mutants generally correlated with their degree of accumulation at these regions. We plotted the median of chromocenter number versus the average accumulation at chromocenters (Figure 8A).

Mutants falling onto an interpolated line connecting the negative GFP alone control and the positive wt MeCP2 control show an inverse correlation between binding to chromocenters and corresponding numbers of chromocenters, i.e. lower accumulation at chromocenters is accompanied by less clustering. Interestingly, the majority of mutants deviated from this inverse correlation. Some of the mutants were deficient in heterochromatin binding but only mildly affected in clustering of chromocenters (bad binders) and grouped below the line (Figure 8A, green). The majority of mutants were not deficient in binding to heterochromatin but disproportionately affected in chromocenter clustering (bad clusterers) and grouped above the line (Figure 8A, red). Interestingly, when we applied the same color code to label the corresponding residues within the 3D structure of MeCP2 MBD (Ho et al., 2008), the two subclasses surprisingly segregated into two different regions of this domain (Figure 8B). The latter indicated that, in addition to the residues known to make contact with the 5mCs (Figure 5A and 8B, blue), this domain could now be further functionally divided into a subdomain primarily affecting heterochromatin association (in green) and a second subdomain involved in clustering chromatin (in red). The most drastic examples for clustering deficient mutants involved aa located distally from the 5mC interacting pocket (Figure 8B). This MBD subdomain could be primarily involved in connecting chromatin fibers either through direct interaction with DNA or, more likely, with other chromatin proteins.

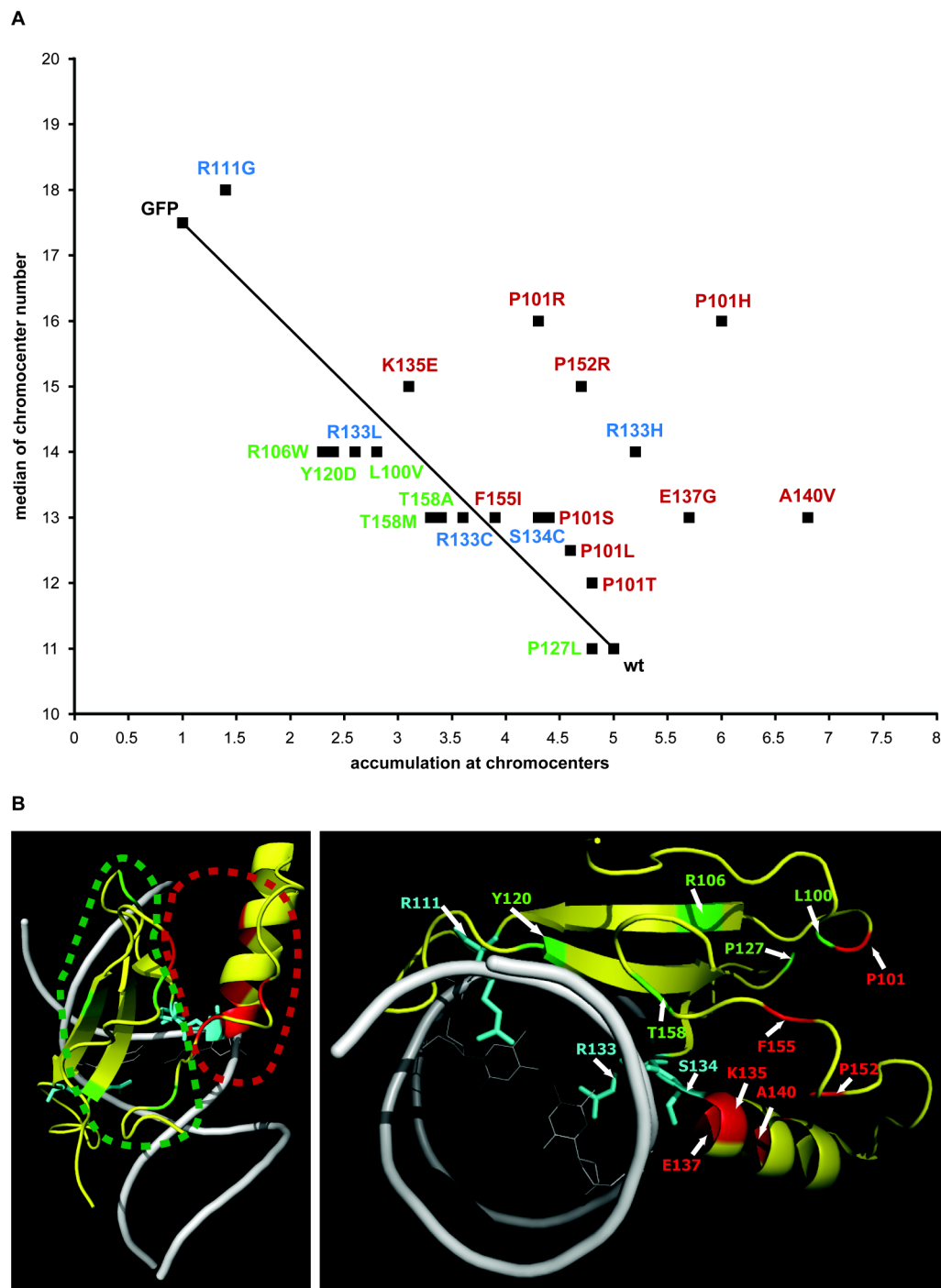


Figure 8. Correlation analysis of chromocenter clustering and accumulation at chromatin

(A) Accumulation at chromocenters (Figure 5) and median of chromocenter number (Figure 6) were plotted on the X and Y-axis, respectively. The scatter plot neither indicates an overall direct nor an inverse correlation. The line connecting the GFP alone and GFP-MeCP2 delineates the inverse relationship between accumulation at chromocenters and chromocenter number (clustering). Mutants grouping above the line are color coded in red and the ones grouping below the line are in green. Mutants in residues directly interacting with 5mC are shown in blue (Figure 5A). **(B)** Structure of the MBD (in yellow) of MeCP2 in complex with DNA (in white) is displayed as in Figure 5A, the residues are color coded as in **(A)**.

5.1.3 MeCP2 directly interacts with the nuclear enzyme PARP-1

To further elucidate the mechanism and regulation of MeCP2 induced chromocenter clustering, we performed a proteomic screen for interaction partners of MeCP2. Lysates of HEK293-EBNA cells transfected with plasmids coding for GFP- and RFP-tagged MeCP2 were subjected to immunoprecipitation with either anti-GFP or anti-RFP antibodies (data not shown). Mass spectrometry analysis of proteins bound to MeCP2 revealed PARP-1 as the most abundant binder enriched by GFP- as well as RFP-fused MeCP2, but not by GFP or RFP alone. PARP-1 is a nuclear enzyme activated by DNA breaks or particular DNA structures and involved in the regulation of chromatin structure and function during DNA repair and transcription (Hassa et al., 2006; Schreiber et al., 2006). Immunoprecipitation assays followed by Western blot analysis for co-precipitated endogenous PARP-1 confirmed this interaction (Figure 9A). Furthermore, direct binding between purified strep-PARP-1 (st-PARP-1) and MeCP2-GFP was observed by pull down assays with recombinant proteins produced in Sf9 insect cells (Figure 9B). To ensure that the interaction is not bridged by DNA, ethidium bromide (EtBr) was added throughout the experiment (Dantzer et al., 2004) and extraction of all GFP-tagged proteins was performed at 1 M NaCl to disrupt potential protein-DNA association. To map the domains involved in the interaction, a series of fluorescently-tagged deletion constructs comprising the major domains of MeCP2 were incubated with st-PARP-1 and vice versa PARP-1 deletions were incubated with MeCP2. The outcome of these pull-down assays indicated that the MBD as well as the domain spanning the region between the MBD and the TRD (termed interdomain, ID) and TRD interacted with the DNA-binding as well as the BRCT-motif bearing automodification domain of PARP-1 (Figure 9C and Figure 9 D).

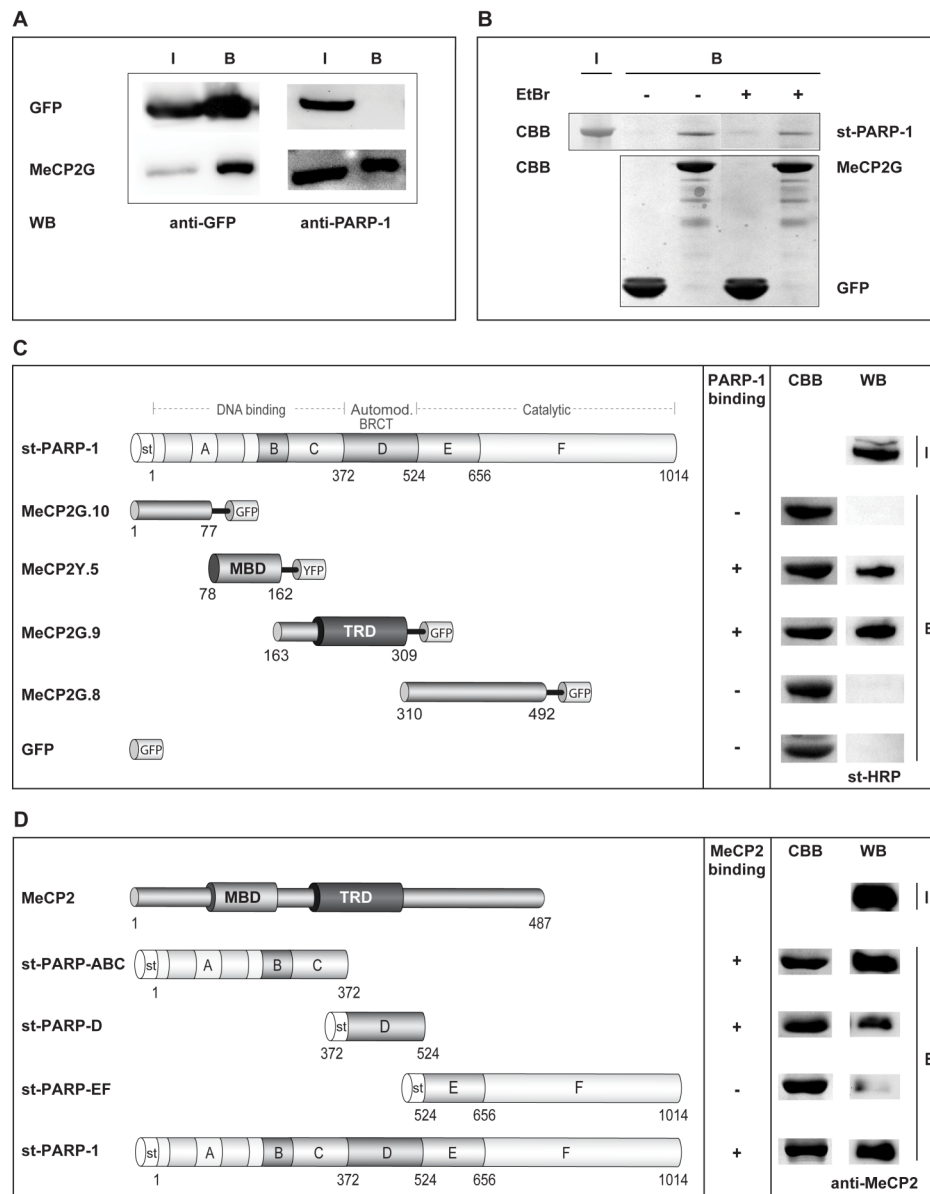


Figure 9. MeCP2 interacts via ID/TRD and MBD domain with the DNA binding and autoactivation domain of PARP-1

(A) GFP or MeCP2-GFP (MeCP2G) proteins were expressed in HEK293-EBNA cells. Cell extracts were analyzed by immunoprecipitation using immobilized GFP binder followed by Western blotting for co-precipitated endogenous PARP-1 with anti-PARP-1 antibody. The blot was reprobed with anti-GFP antibodies to control for precipitated GFP. **(B)** For pull-down analysis, GFP or MeCP2G proteins were immobilized on GFP-Trap beads, incubated for 1 hour with purified strep-PARP-1 (st-PARP-1) at 425 mM NaCl and either treated or not treated with ethidium bromide (EtBr; 10 μ g/ml). After SDS-PAGE, proteins were stained with Coomassie Brilliant Blue (CBB). **(C)** Left panel: schematic representation of fluorescently-tagged MeCP2 deletions and st-PARP-1. Fusion with GFP and YFP and aa coordinates are indicated. Right panel: pull-down experiment with immobilized GFP-tagged MeCP2 deletions and st-PARP-1 at 425 mM NaCl, analyzed by Western blot with strep-HRP (st-HRP) conjugate. **(D)** Left panel: schematic representation of MeCP2 and strep-fused deletion constructs of PARP-1. Right panel: interaction of immobilized strep-fused PARP-1 truncations and purified untagged MeCP2 was assessed by pull-down assay and Western blot with anti MeCP2 antibody. Input cell extract (I) and bound fraction (B). PARP-1 binding results are summarized by + or -.

5.1.4 MeCP2 is poly(ADP-ribose)ated *in vivo*

Prompted by the observed interaction with PARP-1, we tested whether MeCP2 was poly(ADP-ribose)ated. Immunoprecipitation assays of extracts from mouse brain tissue

with either anti-MeCP2 antibody or control rabbit IgG followed by immunoblot analysis with anti-poly(ADP-ribose) antibody showed specific poly(ADP-ribosyl)ation of endogenous MeCP2 (Figure 10B). In addition, we observed poly(ADP-ribosyl)ation of ectopically expressed MeCP2G (Figure 10A) as well as *in vitro* poly(ADP-ribosyl)ation of recombinant MeCP2G in the presence of st-PARP-1 and [α - 32 P]NAD⁺ (Figure 10C). Subsequent mapping identified the ID and TRD to be strongly poly(ADP-ribosyl)ated *in vivo* (Figure 10D) whereas the NH₂-terminus plus MBD as well as the COOH-terminus showed almost no modification. We could further narrow down the modified domain to the ID (aa 163 - aa 206; poly(ADP-ribosyl)ated domain 1) and to less extent to aa 244 to aa 275 (poly(ADP-ribosyl)ated domain 2) (Figure 10D). We subsequently tested deletion constructs lacking the poly(ADP-ribosyl)ated regions (Figure 10E). While deletion of poly(ADP-ribosyl)ated domain 2 (MeCP2G.17; deletion of aa 244 - aa 275) resulted in slightly less poly(ADP-ribosyl)ation than the full length, the construct lacking the poly(ADP-ribosyl)ated domain 1 (MeCP2G.16; deletion of aa 163 - aa 206) showed a strong decrease and the double deletion (MeCP2G.18) had an even stronger effect (Figure 10E).

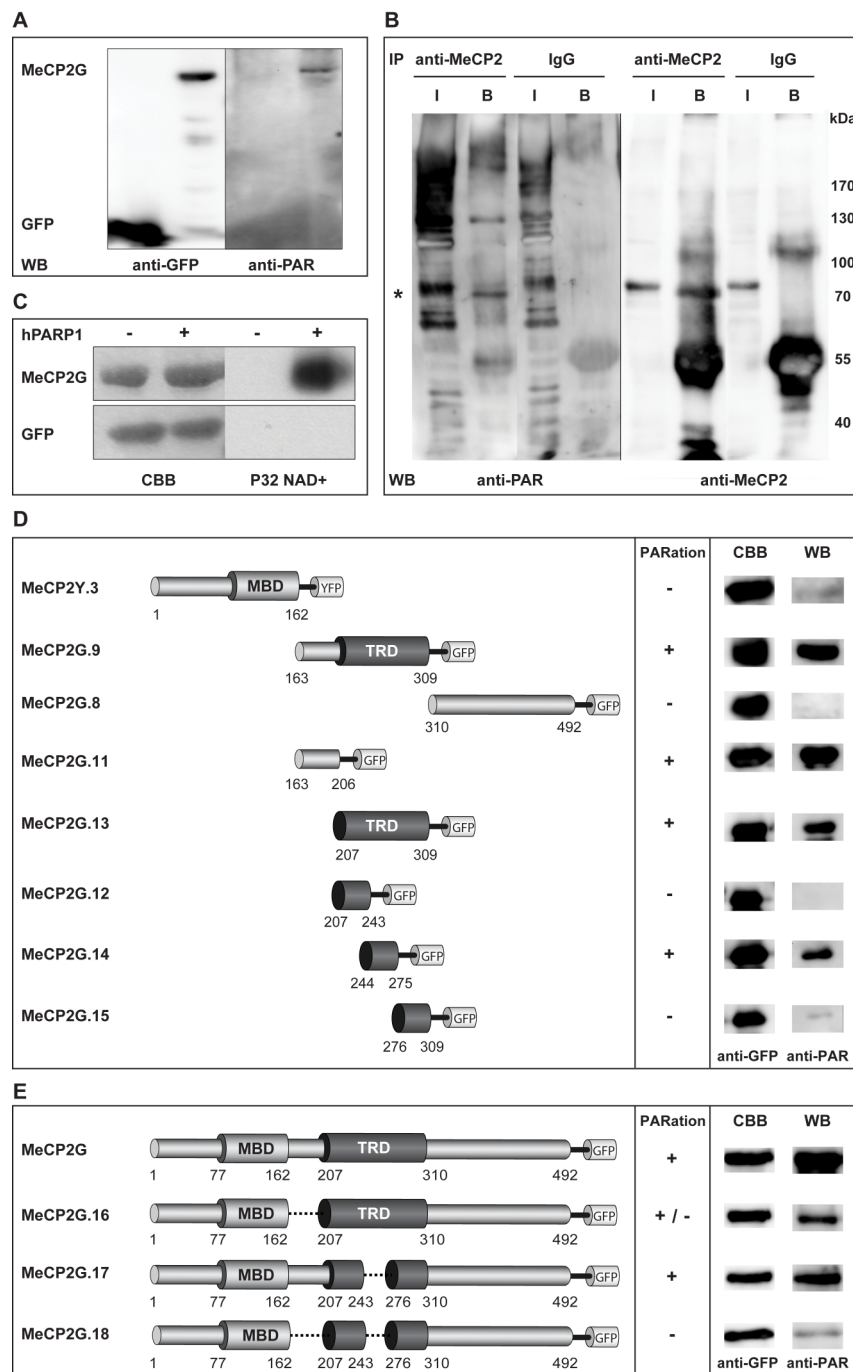


Figure 10. MeCP2 gets poly(ADP-ribosylated) *in vitro* as well as *in vivo* in brain

(A, D and E) GFP, MeCP2G and GFP-fused MeCP2 mutants were expressed in HEK293-EBNA cells (A and D) or mouse embryonic fibroblast (MEF) cells (E). After immunoprecipitation with the GFP-Trap, poly(ADP-ribosylation) of the precipitated proteins was checked by Western blot analysis with anti-poly(ADP-ribose) (anti-PAR) followed by anti-GFP antibodies. (D and E) Left panel: schematic representation of GFP or YFP-tagged MeCP2 constructs with the corresponding aa coordinates. (B) Immunoprecipitations from wt mouse brain extracts were performed with the antibodies indicated and analyzed for poly(ADP-ribosylation) of endogenous MeCP2 by Western blotting with anti-PAR followed by anti-MeCP2 antibodies. The asterisks points out the expected lane position of endogenous MeCP2. (C) Recombinant immobilized GFP and MeCP2G proteins were incubated with $[\alpha\text{-}^{32}\text{P}]\text{NAD}^+$, DNase I-treated calf thymus DNA with or without purified st-hPARP-1. After SDS-PAGE, poly(ADP-ribosylation) was detected by autoradiography (right panel). Precipitated proteins were stained with CBB (left panel). Poly(ADP-ribosylation) (PARation) results are summarized by +, - or +/-.

Poly(ADP-ribosylation) mostly takes place on Glu and Asp residues. To identify the poly(ADP-ribosyl)ated sites of MeCP2, single or double mutations were generated using site directed mutagenesis and resulting mutants were analyzed for poly(ADP-ribosylation). None of the mutations with changes from Glu or Asp to Ala were able to abolish poly(ADP-ribosylation) (Figure 11), indicating that Lys which are very abundant in these regions and were previously identified as poly(ADP-ribosylation) sites (Altmeyer et al., 2009; Cervantes-Laurean et al., 1996), are modified in MeCP2. We therefore mapped for poly(ADP-ribosyl)atable Lys and identified two (K175 and K177) within poly(ADP-ribosyl)ated domain 1 and three (K254, K267, K271) within poly(ADP-ribosyl)ated domain 2.

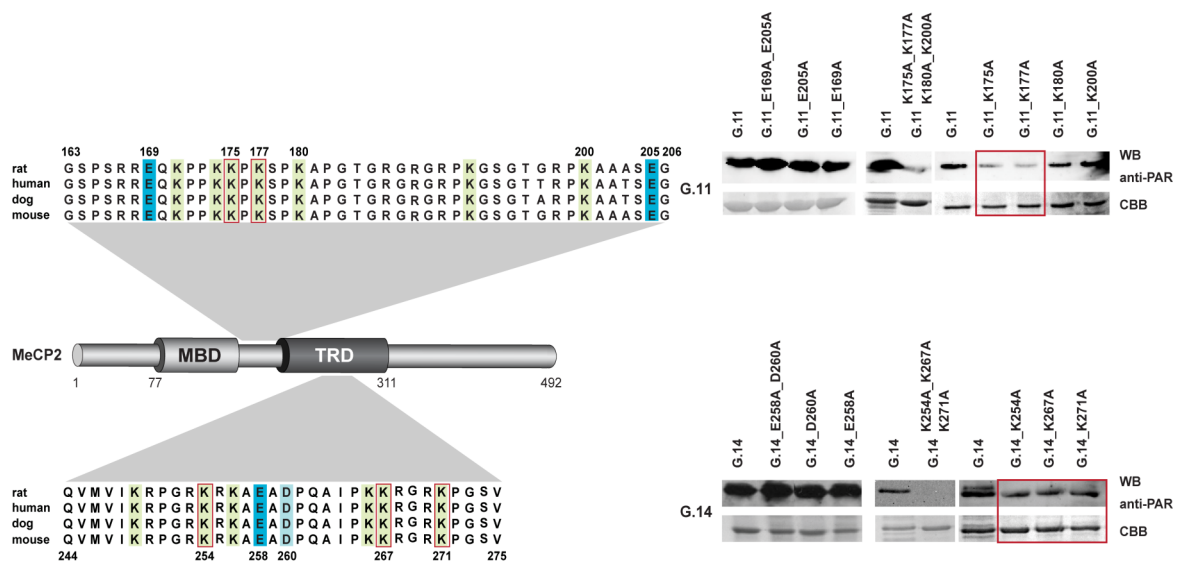


Figure 11. Identification of MeCP2 poly(ADP-ribosylation) sites

Left panel: sequence comparison of aa 163 to aa 206 (poly(ADP-ribosyl)ated domain 1) and aa 244 to aa 275 (poly(ADP-ribosyl)ated domain 2) of rat, human, dog and mouse MeCP2. The mutated poly(ADP-ribosyl)atable sites are marked in blue and in green and by the aa number. Poly(ADP-ribosyl)atable sites, that were not mutated are in green and not marked by the aa number. Right panel: MeCP2G.11 and MeCP2G.14 carrying the indicated mutations were expressed in HEK293-EBNA cells. After immunoprecipitation with the GFP-Trap, poly(ADP-ribosylation) of the precipitated proteins was checked by Western blot analysis with anti-PAR. Immobilized proteins were stained with CBB.

5.1.5 Poly(ADP-ribosylation) of MeCP2 reduces clustering of pericentric heterochromatin

To address the functional consequences of poly(ADP-ribosylation) on MeCP2 ability to bind and aggregate heterochromatin (Brero et al., 2005) we first compared the median numbers of heterochromatic centers in mouse cells expressing either MeCP2G or one of the deletion constructs lacking the poly(ADP-ribosyl)ated regions (Figure 12A).

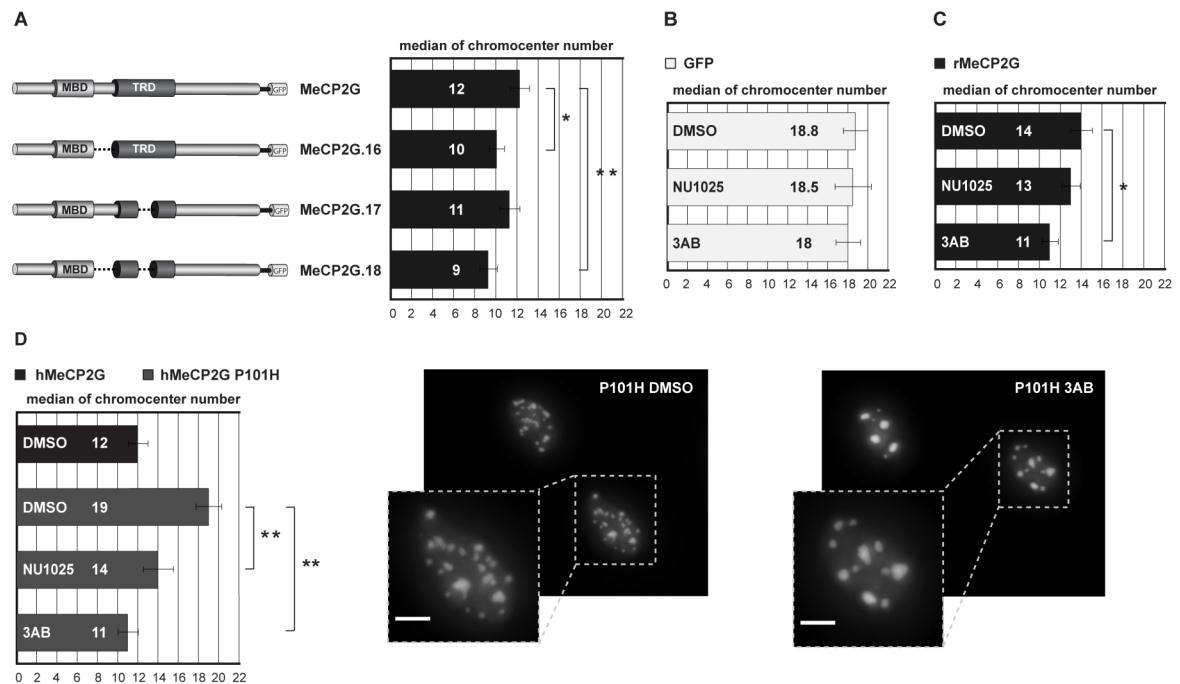


Figure 12. Poly(ADP-ribosylation) counteracts clustering of pericentric heterochromatin

Pmi28 mouse myoblasts were transfected with an expression vector coding for GFP or GFP-fused MeCP2 constructs. Using constant image acquisition parameters, Z-stacks of images were recorded of nuclei with similar expression levels of the GFP-tagged protein. Graphs show mean numbers of chromocenters of cells expressing the indicated proteins. Error bars represent 95 % Confidence Interval (C.I.). Experiments were repeated two times with at least 30 cells per construct each time. Asterisks represent statistically significant difference: * for $P < 0.05$; ** for $P < 0.001$. **(A)** Cells expressing MeCP2G or GFP-fused MeCP2 deletions lacking the poly(ADP-ribosylated) domains (compare also with Figure 10E). **(B, C and D)** Cells were transfected with vectors as indicated and treated with PARP inhibitors NU1025 (400 μ M), 3AB (10 mM) or DMSO control for about 15 hours. **(D)** Right panels: maximum intensity projections generated from image stacks of cells expressing hMeCP2G P101H either treated with DMSO (control) or 3AB. Shown are overview images and representative magnified nuclei. Scale bar: 5 μ m.

As shown before, MeCP2G but not GFP alone induced clustering of chromocenters (Brero et al., 2005) (Figure 6A and 12B). While deletion of poly(ADP-ribosylated) domain 2 (MeCP2G.17) showed no significant change in chromocenter numbers compared to MeCP2G, the amount of chromocenters in cells expressing the poly(ADP-ribosylated) domain 1 deletion (MeCP2G.16) or the double deletion (MeCP2G.18) was significantly reduced (Figure 12A). We could exclude major conformational changes caused by these deletions since the mutant proteins localized at chromocenters as the wt protein (Figure 13). To ensure that the increase of chromocenter clustering was based on reduced poly(ADP-ribosylation) levels and was not simply due to deletion of aa within MeCP2, we treated cells with the PARP inhibitors NU1025 or 3-amino-benzamide (3AB). As the chromocenter numbers of GFP expressing cells treated with NU1025 or 3AB were comparable to DMSO treated cells we concluded that the inhibitors themselves did not have a significant effect on chromocenter aggregation (Figure 12B). In stark contrast, MeCP2G expressing cells incubated with 3AB exhibited significantly increased clustering of pericentric heterochromatin relative to the DMSO control (Figure 12C), whereas

MeCP2G expressing cells treated with NU1025 had decreased numbers of chromocenters but not to a significant degree.

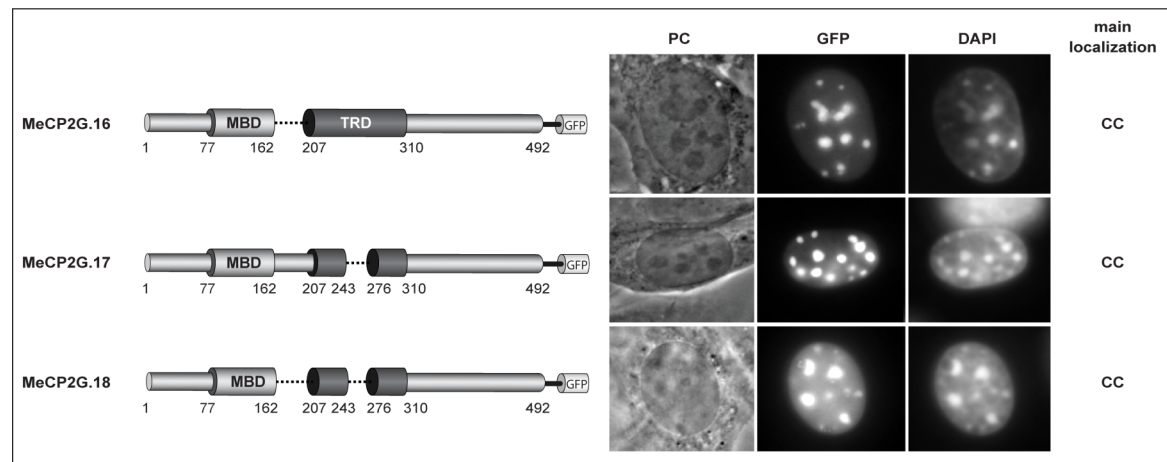


Figure 13. Overview of the subcellular localization of MeCP2 deletions

Pmi cells were transfected with plasmids coding for GFP fusions with the domains of MeCP2 as indicated on the left side. After fixation, DNA was counterstained with DAPI to highlight chromocenters (CC). PC: phase contrast. Scale bar: 5 μ m.

Furthermore, enhanced aggregation of chromocenters was also measured in MeCP2G expressing PARP-1^{-/-} mouse embryonic fibroblast cells (Figure 14B), which exhibited reduced poly(ADP-ribosylation) levels of MeCP2G in comparison to wt cells (Figure 14A).

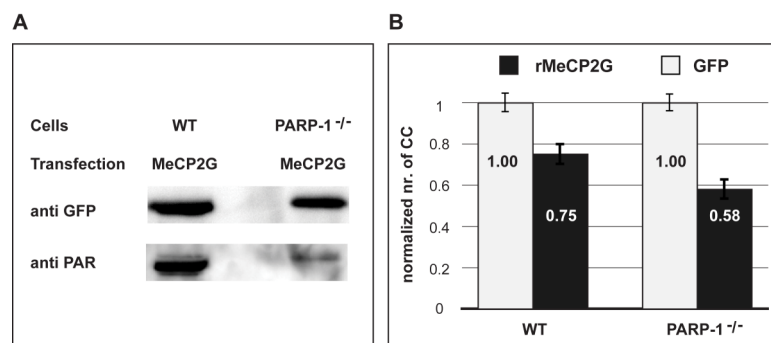


Figure 14. MeCP2 poly(ADP-ribosylation) decreases in PARP-1^{-/-} cells and its chromocenter clustering ability increases

(A) MeCP2 exhibits decreased poly(ADP-ribosylation) in PARP-1^{-/-} mouse embryonic fibroblast (MEF) cells compared to wt cells. GFP-fused MeCP2 was expressed in WT as well as in PARP-1^{-/-} MEF cells. After immunoprecipitation using the GFP-Trap, poly(ADP-ribosylation) of precipitated proteins was checked via Western blotting with anti-PAR followed by anti-GFP antibodies. **(B)** PARP-1^{-/-} MEF cells exhibit enhanced MeCP2 induced chromocenter aggregation in comparison to WT cells. WT or PARP-1^{-/-} MEF cells were transfected with an expression vector coding for GFP or MeCP2G. Z-stacks of images were recorded from nuclei with similar high expression levels of the protein using constant image acquisition parameters. Experiments were repeated two times with at least 30 cells per construct each time and are shown normalized to the control GFP expressing cells.

5.1.6 Decrease of poly(ADP-ribosylation) rescues chromocenter clustering of RTT mutant MeCP2

As decreased levels of poly(ADP-ribosylation) lead to increased clustering ability of MeCP2 (Figure 12A and Figure 12C) and as some RTT mutants were significantly affected in heterochromatin aggregation (Figure 6 and Figure 8), we tested whether modulation of poly(ADP-ribosylation) can rescue these mutants.

We selected RTT mutant P101H that showed highly impaired chromatin clustering (Figure 6 and Figure 8) and treated cells expressing this mutant or wt MeCP2 with the PARP inhibitors 3AB and NU1025. Remarkably, the impaired clustering ability of the mutant hMeCP2 P101H was rescued by treatment with either of the PARP inhibitors to a level comparable to wt hMeCP2G (Figure 12D and Figure 15).

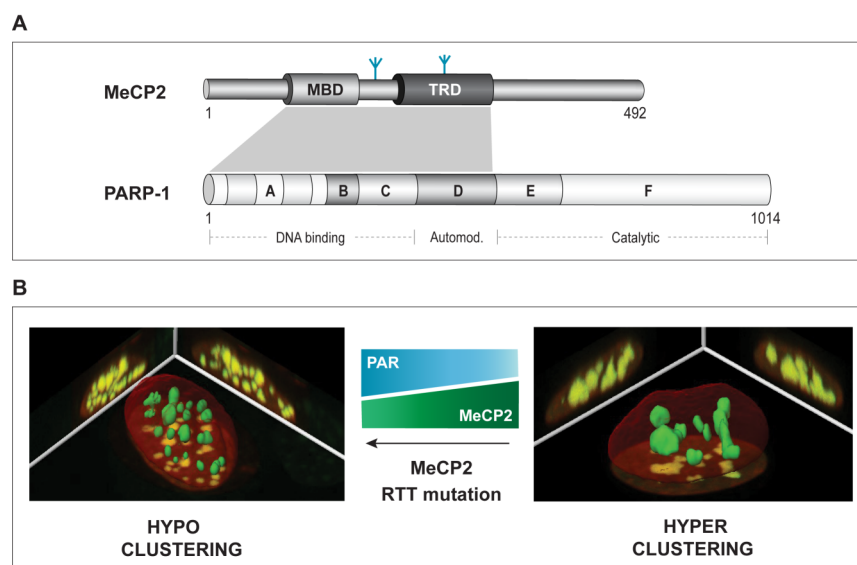


Figure 15. Summary of factors influencing MeCP2 mediated heterochromatin clustering

(A) Schematic representation of MeCP2, its poly(ADP-ribosyl)ated regions (illustrated by the blue branches) and the interacting domains between MeCP2 and PARP-1 (marked in grey). Numbers represent aa coordinates. **(B)** Higher level of MeCP2 and/or inhibition of MeCP2 poly(ADP-ribosylation) by, e.g., 3AB causes increased clustering (hyperclustering). MeCP2 mutation such as the P101H mutation found in RTT syndrome patients decreases chromocenter clustering. The defect however can be rescued by inhibition of poly(ADP-ribosylation) that compensates the clustering deficiency of mutant MeCP2 P101H protein.

In summary, we found that MeCP2 interacts with PARP-1 and is poly(ADP-ribosyl)ated *in vivo* and *in vitro*. This posttranslational modification negatively regulated the formation of higher-order heterochromatin structures and its inhibition counteracted the effect of RTT mutations.

5.2 Direct interactions of MeCP2 and MBD2 involve poly(ADP-ribosyl)ated domains, that also recognize poly(ADP-ribose)

5.2.1 MeCP2 and MBD2 – but not MBD1, MBD3 and MBD4 - get poly(ADP-ribosyl)ated *in vivo*

Prompted by the finding that MeCP2 gets poly(ADP-ribosyl)ated (5.1), we tested whether other members of the MBD protein family are also modified. We performed immunoprecipitation assays using immobilized GFP binder of extracts from cells over-expressing GFP or GFP-fused full length (fl) MBDs followed by Western blot analysis with anti-poly(ADP-ribose) antibody. The results showed that MBD2 is also poly(ADP-ribosyl)ated *in vivo* whereas MBD1a, MBD3 and MBD4 did not exhibit detectable poly(ADP-ribose) signal (Figure 16).

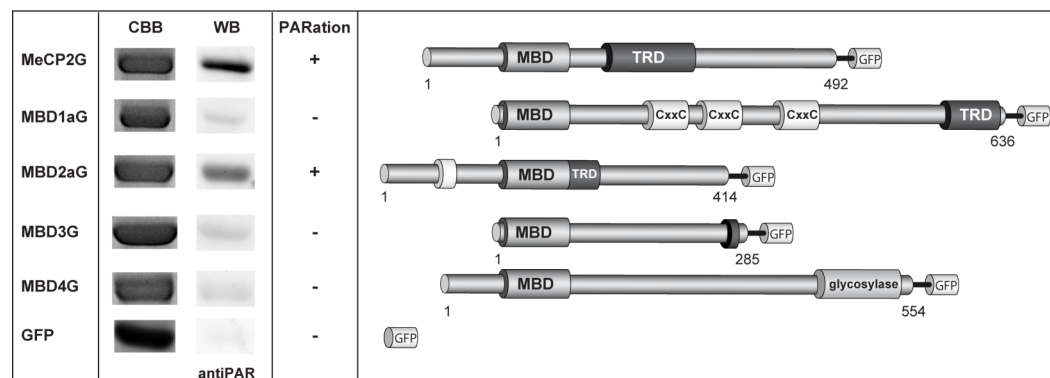


Figure 16. MeCP2 and MBD2 get poly(ADP-ribosyl)ated *in vivo*

GFP-labelled fl methyl-CpG binding (MBD) proteins as indicated were expressed in Sf9 cells. For immunoprecipitation of the proteins, cell extracts were subjected to immobilized GFP binder. To examine poly(ADP-ribosyl)ation of the precipitated proteins, Western blot (WB) analysis was performed with anti-poly(ADP-ribose) (anti PAR). To examine equal loading, the precipitated proteins were in parallel separated by SDS-PAGE and stained with Coomassie Brilliant Blue (CBB). Right panel: schematic representation of the GFP-fused protein constructs with the corresponding aa coordinates.

Concerning MeCP2, we narrowed down this modification to a region comprising the interdomain (ID, aa 163 – aa 206) and the TRD (aa 207 - aa 309). Subsequent mapping of MBD2a poly(ADP-ribosyl)ated domains identified the NH₂-terminus (NTD) (MBD2aG.1) as modified whereas the domain MBD2aG.2, highly identical to MBD3, did not show any modification (Figure 17).

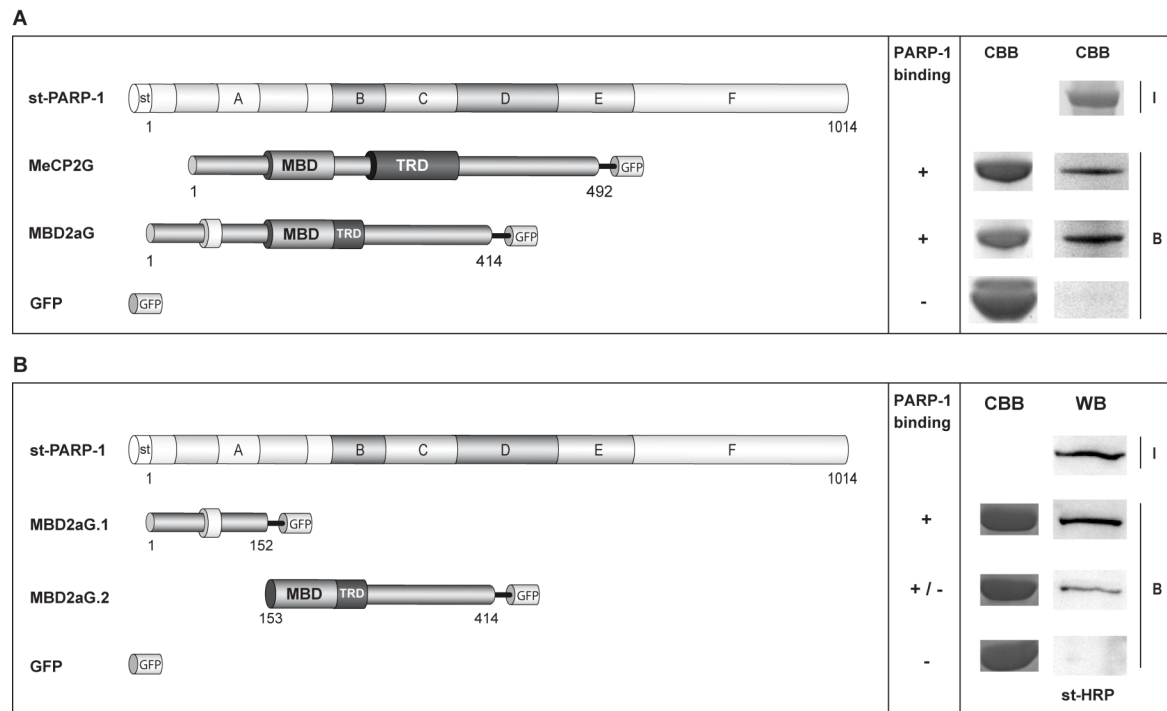


Figure 18. Interaction of MeCP2 and MBD2 with PARP-1

(A and B) Immobilized GFP-fused fl MeCP2 and MBD2 fl and mutant constructs were incubated with purified st-PARP-1 at 200 mM NaCl. After the pull-down experiment, the proteins were separated by SDS-PAGE and (A) stained with CBB or (B) analyzed by Western Blot using st-HRP conjugate.

Left panel: schematic representation of GFP-fused protein constructs with the corresponding aa coordinates.

5.2.2 MeCP2 and MBD2 poly(ADP-ribosyl)ated domains also recognize poly(ADP-ribose) in a noncovalent manner

We further set out to examine whether MeCP2 and MBD2 directly recognize poly(ADP-ribose) (PAR). Equal amounts of purified immobilized GFP and GFP-fused MBD fl proteins were separated by SDS PAGE, blotted onto nitrocellulose and incubated with radioactive labeled PAR. Whereas no radioactive signal was detectable in the case of GFP, MeCP2 and MBD2a showed direct PAR binding (Figure 19).

We subsequently determined which domains are involved in PAR recognition. Incubation of MeCP2 and MBD2 mutant constructs, blotted onto nitrocellulose, with radioactive PAR identified the region spanning MeCP2 ID and TRD as directly binding to PAR, whereas MBD, NTD and CTD did not give any signal (Figure 19A). We could further narrow down MeCP2 PAR recognizing domains to the ID (aa 163 – aa 206; poly(ADP-ribosyl)ated domain 1) and to less extent to aa 244 to aa 275 (poly(ADP-ribosyl)ated domain 2) (Figure 19A), both regions already identified to contain MeCP2 covalently poly(ADP-ribosyl)ated sites (5.1). Examining MBD2 mutant constructs, we could see that the covalently modified MBD2aG.1 strongly recognized PAR, whereas with MBD2aG.2 no radioactive signal was detectable (Figure 19B).

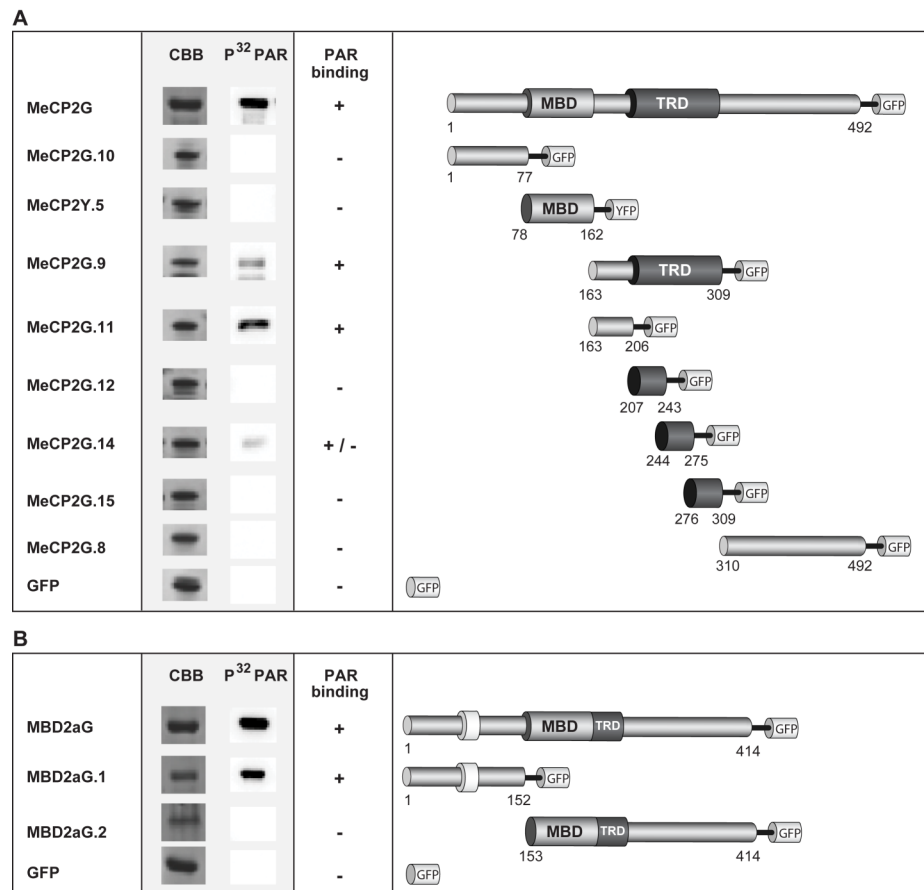


Figure 19. MeCP2 and MBD2 recognize noncovalent poly(ADP-ribose)

GFP and fluorescently labeled fl and mutant MeCP2 and MBD2 were expressed in Sf9 cells. After immunoprecipitation using immobilized GFP binder, the immobilized proteins were separated by SDS-PAGE, blotted onto nitrocellulose and incubated with [α -³²P] poly(ADP-ribose) (PAR) to check for non-covalent binding to PAR. As a loading control, the precipitated proteins were in addition separated by SDS-PAGE and CBB stained. Right panel: schematic representation of GFP- or YFP-fused protein constructs with the corresponding aa coordinates.

5.2.3 Direct homo- and hetero-interactions between MeCP2 and MBD2 are partially mediated through their poly(ADP-ribosyl)ated and poly(ADP-ribose) recognizing domains

We have recently demonstrated, that the expression level of both MeCP2 and MBD2 increase during myogenic differentiation along with increased clustering of heterochromatin (Brero et al., 2005). We further showed that increased ectopic expression of MeCP2 and MBD2 in mouse cells induces aggregation of pericentric heterochromatin in a dose dependent manner (Brero et al., 2005).

As one additional factor contributing to the heterochromatin clustering of MeCP2 and MBD2 *in vivo*, we have recently proposed oligomerization of these chromatin bound proteins (Brero et al., 2005), although hydrodynamic studies demonstrated recombinant MeCP2 as a monomer (Adams et al., 2007; Klose and Bird, 2004). Subsequently, we investigated potential direct interactions of MeCP2 and MBD2. We performed *in vitro* pull down experiments using recombinant fl MBDs extracted from Sf9 cells in 1M NaCl

containing lysis buffer to disrupt potential protein-DNA associations. Whereas GFP alone did not bind to immobilized strep-labelled MeCP2 (stMeCP2) and MBD2a (stMBD2a), GFP-fused fl MeCP2 exhibited strong association to both stMeCP2 and stMBD2 (Figure 20A). Also GFP-tagged fl MBD2a clearly bound to itself as well as to stMeCP2 (Figure 20B). In agreement with these *in vitro* data, we additionally observed physical interactions between fluorescently-labelled MeCP2 and MBD2a performing immunoprecipitation experiments of mammalian cell extracts (data not shown).

Further mapping of MeCP2 domains responsible for MeCP2 homo-association and interaction to MBD2 revealed the region spanning MeCP2 ID and TRD as well as MeCP2 CTD to directly interact with stMeCP2 and stMBD2. The CTD exhibited a slightly weaker association when compared to that of ID and TRD (Figure 20A). Subsequent mapping of MBD2a oligomerizing domains showed, that both NTD as well as CTD of MBD2a interacted to MeCP2 and MBD2 (Figure 20B).

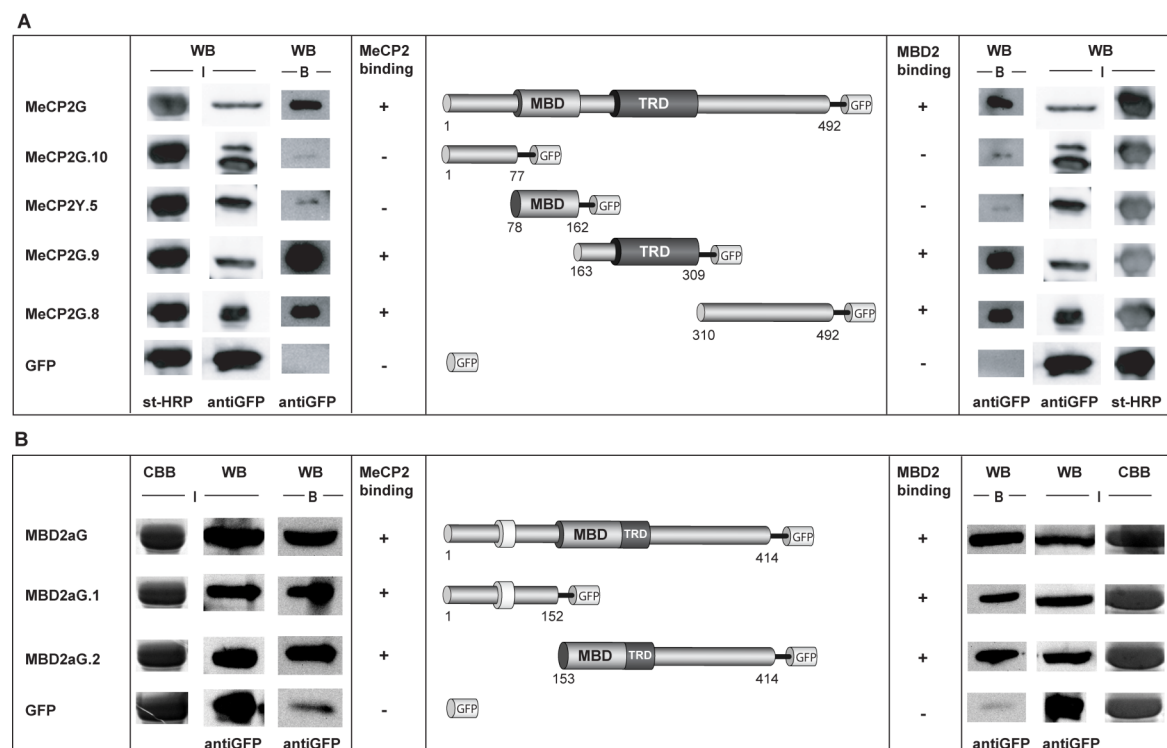


Figure 20. Mapping of domains responsible for MeCP2 and MBD2 homo- and hetero-interactions
 Pull-down experiments with immobilized strep-fused fl MeCP2 or MBD2 and fluorescently-labeled MeCP2 or MBD2 constructs as indicated. **(A)** The interactions were performed in PBS buffer. Interacting GFP-tagged proteins were assessed by Western blot with anti-GFP, followed by st-HRP conjugate. **(B)** Pull-down experiments using immobilized strep MeCP2 were done in PBS supplemented with 100 mM NaCl, the assays with strep MBD2 were incubated in PBS plus 50 mM NaCl. The interacting proteins were analyzed by Western blot with anti GFP and CBB for the strep-fused proteins respectively. Input cell extract (I) and bound fraction (B).

Summarizing we can say that MeCP2 and MBD2 homo- and hetero-interact. MeCP2 binding to itself and MBD2 involves two independent domains, one recently reported to

induce clustering of nucleosomal arrays *in vitro* (Georgel et al., 2003; Ghosh et al., 2010; Nikitina et al., 2007b). In addition I found that MeCP2 and MBD2 are the only MBD proteins poly(ADP-ribosyl)ated. Their modified domains further recognize noncovalent PAR and are involved in MeCP2 and MBD2 direct homo- and hetero-binding.

6 Discussion

The main objective of this study was to elucidate the mechanism underlying MeCP2 mediated large-scale heterochromatin reorganization and its regulation. The MBD and the heterochromatin protein 1 (HP1) families – recognizing either methylation of DNA or of histones - constitute the two major protein classes that are enriched at pericentric heterochromatin. We addressed both the interaction between MeCP2 and HP1 as well as homo- and heterodimerization of MeCP2 and other MBD members to determine whether these associations contribute to the higher order organization of chromatin *in vivo*. We could show the interaction between MeCP2 and HP1 and found an interdependency between HP1 localization to heterochromatin and the presence of MeCP2 (Agarwal et al., 2007; Appendix). In addition, we identified self-association of MeCP2 *in vivo* and *in vitro* and analyzed MeCP2 interactions with other MBD family members (5.2).

We aimed to find further proteins associated with MeCP2, performing an unbiased proteome-wide screen and found the nuclear enzyme PARP-1 as a direct binding partner, capable of poly(ADP-ribosyl)ating MeCP2 *in vitro* (5.1). Examining poly(ADP-ribosyl)ation of endogenous MeCP2, we were able to show that this post-translational modification exerts a regulative effect on MeCP2 mediated large-scale chromatin reorganization *in vivo*. We observed that the deletion of MeCP2 poly(ADP-ribosyl)ated regions, or chemical inhibition of PARP activity, increases MeCP2-mediated heterochromatin clustering. Whilst analyzing RTT-inducing missense mutations within MeCP2 MBD, we identified several mutations that exert a strong effect on the capability of MeCP2 to aggregate heterochromatin. Notably, we could demonstrate that inhibition of poly(ADP-ribosyl)ation rescues the chromatin clustering ability of a MeCP2 RTT mutant strongly impaired to reorganize chromatin (5.1). Prompted by the novel modification of MeCP2 and its effect on large-scale reorganization of heterochromatin, we also examined poly(ADP-ribosyl)ation of other MBDs and found a correlation between oligomerization of the MBD family members, their poly(ADP-ribosyl)ation and poly(ADP-ribose) recognition (5.2).

6.1 Regulation of MeCP2 induced heterochromatin remodeling

MeCP2 was originally described as a transcriptional regulator imposing local repressive chromatin structures through recruitment of histone-modifying enzymatic activities (Fuks et al., 2003; Harikrishnan et al., 2005; Jones et al., 1998; Kokura et al., 2001; Lunyak et al., 2002; Nan et al., 1997; Nan et al., 2007; Nan et al., 1998). Recent reports further implicate the intrinsic capability of MeCP2 to organize global heterochromatin

architecture (Brero et al., 2005; Georgel et al., 2003; Skene et al., 2010). Our lab has shown that MeCP2 induces large-scale chromatin reorganization *in vivo* - in particular clustering of pericentric heterochromatin - in a dose-dependent manner (Brero et al., 2005). The MBD is necessary and sufficient for MeCP2 chromatin aggregation ability, and a MeCP2 deletion construct lacking the NH₂-terminal region and the MBD is not able to induce clustering of chromatin *in vivo* (Brero et al., 2005).

In agreement with these findings, *in vitro* assays demonstrate that MeCP2 can independently compact polynucleosomes into highly condensed suprastructures (Georgel et al., 2003; Nikitina et al., 2007b). Nucleosome interaction studies using human MeCP2 - either truncated at aa 294 or aa 370, as well as *Xenopus* MeCP2 truncated at aa 404 - indicate that mostly residues in the COOH-terminal regions of MeCP2 are involved in chromatin binding (Chandler et al., 1999; Nikitina et al., 2007b). Further, the TRD alone (aa 203 – aa 305) of *Xenopus* MeCP2 has been shown to be incapable of associating with mononucleosomes (Chandler et al., 1999).

Multiple interactions of MeCP2 with DNA and chromatin have been proposed to induce compaction of polynucleosomal arrays *in vitro*. One such interaction involves binding of MeCP2 MBD to the linker DNA entry-exit site. Whereas DNA methylation is required for this step, MeCP2 CTD is dispensable (Ishibashi et al., 2008; Nikitina et al., 2007a). Another mode of interaction of MeCP2 with DNA brings the linker DNA at the nucleosome entry-exit site in close proximity and results in a “stem conformation”, inducing array compaction without nucleosome clustering (Nikitina et al., 2007b). For this step, the MBD is indispensable, whereas DNA methylation and COOH-terminal residues are not required as demonstrated on the RTT mutant R294X (Nikitina et al., 2007b). The predominant interaction results in a high degree of nucleosome clustering and takes place between MeCP2 CTD and the nucleosomes and leads to a “loop conformation”. (Georgel et al., 2003; Ghosh et al., 2010; Nikitina et al., 2007b; Figure 21). Importantly, maximal compaction of nucleosomal arrays involving secondary and tertiary chromatin structures does not take place in the absence of the region COOH-terminal from the MBD (Georgel et al., 2003; 2.3.2).

As a potential mechanism underlying MeCP2 coordination of global chromatin architecture, a sandwich-like formation of MeCP2 with nucleosomes and / or DNA has been proposed, most probably requiring at least two chromatin or DNA binding sites within MeCP2 (Georgel et al., 2003; Nikitina et al., 2007b). In this regard, it is noteworthy that MBD and TRD have each been described as independent binding domains for unmethylated DNA *in vitro* (Adams et al., 2007; Figure 21 orange arrows). Oligomerization of MeCP2, resulting in nucleosome-MeCP2-MeCP2-nucleosome or DNA-MeCP2-MeCP2-DNA complexes, has also been proposed (Brero et al., 2005). The

fact that MeCP2 induces different levels of chromatin structure *in vitro* depending on the ratio of MeCP2 to nucleosomes, together with the *in vivo* findings that increasing doses of MeCP2 result in increased heterochromatin aggregation strengthen this hypothesis (Brero et al., 2005; Georgel et al., 2003 and 2.3). However, hydrodynamic studies describing recombinant MeCP2 as a monomer have challenged oligomerization of MeCP2 (Adams et al., 2007; Klose and Bird, 2004).

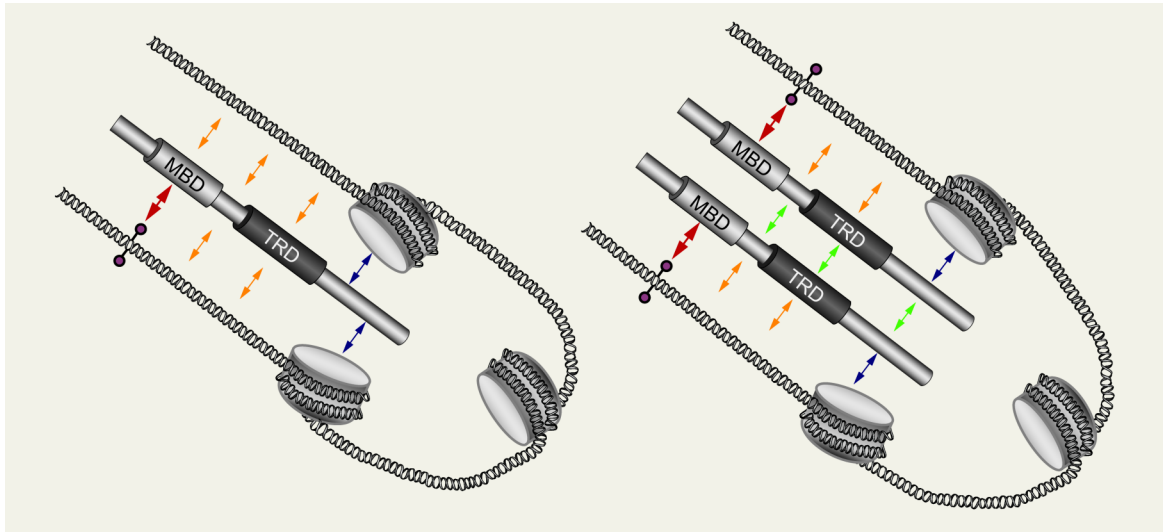


Figure 21: Combinatorial interactions of MeCP2 with DNA and chromatin leading to chromatin compaction

Left side: Nucleosome-MeCP2-nucleosome as well as DNA-MeCP2-DNA interactions as underlying cause for MeCP2 induced chromatin clustering. Right side: Oligomerization of MeCP2 (indicated by the green arrows) involved in MeCP2 mediated cross-linking of nucleosomes.

Interactions between MeCP2 methyl-CpG binding domain (MBD) and methylated DNA (illustrated by the lollipop) are indicated by a red arrow (Lewis et al., 1992). Orange arrows implicate unspecific DNA binding of MeCP2 interdomain and transcriptional repression domain (TRD) (Adams et al., 2007; Ghosh et al., 2010). The blue arrows stand for associations to nucleosomes mediated through MeCP2 COOH-terminal domain (Georgel et al., 2003; Ghosh et al., 2010; Nikitina et al., 2007b).

6.1.1 Poly(ADP-ribosylation), poly(ADP-ribose) recognition and interactions among MBDs

In this study, we were able to demonstrate that MeCP2 indeed has the capability to form direct homo-associations via two domains independently, one comprising the ID and TRD (aa 164 to aa 310) and the other spanning the residues COOH-terminal from the TRD (5.2). Whereas both domains exhibit strong binding to fl MeCP2, ID plus TRD exhibits a slightly stronger association when compared to that of the CTD. To ensure that the interaction is direct and not bridged by DNA, extraction of all proteins was performed at 1 M NaCl to disrupt potential protein-DNA association. Besides confirming MeCP2 dimerization *in vivo* using RFP- and GFP-fused fl constructs, we also show that the MBD independently, as well as the residues COOH-terminal from the MBD can associate with fl MeCP2 under physiological conditions (data not shown). The binding between MBD

and full-length MeCP2 *in vivo* is most probably bridged by DNA as demonstrated by its gradual loss when proteins are extracted in increasing salt concentrations *in vitro*.

Our data favour a mechanism for the MeCP2-induced interconnection of nucleosomes involving MeCP2 homo-associations, mostly through the ID plus TRD (aa 164 - aa 310) and to a lesser extent via the CTD. The latter establishes in addition parallel contacts to nucleosomes (Georgel et al., 2003; Ghosh et al., 2010; Nikitina et al., 2007b; Figure 21). Furthermore, hetero-association of MeCP2 with other chromatin-bound MBD proteins could cause and stabilize MeCP2-mediated heterochromatin aggregation as can be seen from the association between MeCP2 and MBD2 *in vitro*. We show both, MeCP2 direct binding to MBD2 and vice versa, as well as the independent interaction of the ID plus TRD and the CTD of MeCP2 with full-length MBD2. We also observed strong direct binding of MBD2 with itself.

Furthermore, multiple homo- and hetero-interactions among the whole MBD protein family members, excluding MBD3, were identified *in vitro* (data not shown, Valentina Casa). This further suggests that a multitude of homo- and hetero-associations between the MBD proteins could coordinate heterochromatin reorganization *in vivo*.

Our hypothesis is supported by the fact that, except for MBD3, all MBD proteins are localized at pericentric heterochromatin and are capable of inducing dose-dependent chromatin aggregation. Functional redundancy between the MBD proteins has been suggested based on the finding that clustering of pericentric heterochromatin is maintained in MeCP2-deficient mice (Brero et al., 2005). Moreover, our findings could suggest overlapping functions as a result of cross-interactions which in all probability mediate and stabilize chromatin aggregation.

Besides homo- and hetero-dimerization among MBD proteins, additional binding sites between MeCP2 and MBD2 are brought about by their mutual recognition of PAR (Figure 22). Whether and to which extent poly(ADP-ribosyl)ation and PAR binding affects homo- and hetero-interactions of MeCP2 and MBD2 *per se*, needs further investigation.

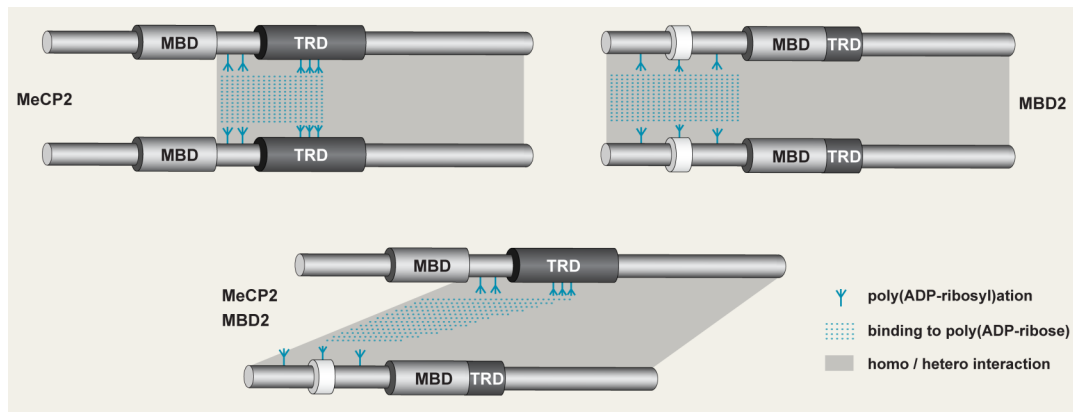


Figure 22. Homo- and hetero-interactions of MeCP2 and MBD2 involve poly(ADP-ribosyl)ated and poly(ADP-ribose) recognizing domains

Covalent poly(ADP-ribosylation) is indicated by blue branches. Noncovalent binding to poly(ADP-ribose) is illustrated by a blue box. Direct protein-protein-interactions are indicated in dark grey. MBD stands for methyl-CPG binding domain, TRD for transcriptional repression domain.

6.1.2 Interaction of MeCP2 with HP1 and heterochromatin association

Whereas MBDs are able to induce rearrangement of heterochromatin *in vivo* (Brero et al., 2005), we observed that HP1 proteins are not (Agarwal et al., 2007; Appendix). HP1 α is mainly localized at pericentric heterochromatin and HP1 γ only exhibits weak heterochromatin binding in myoblasts, which express a very low level of MBDs. In differentiated myotubes, however, accelerated heterochromatin accumulation of the two HP1 isoforms takes place correlated with increased level of MeCP2 and other MBDs (Agarwal et al., 2007). This, together with the observed interaction between MeCP2 and HP1s (Agarwal et al., 2007), suggests a potential cross-talk between both factors with their transcription silencing pathways probably contributing to the propagation and maintenance of higher order chromatin structures. Our assumption is further supported by the association of MeCP2 with the histone H3 methyltransferase SUV39H1 (Lunyak et al., 2002) along with the finding that tri-methylation of histone H3 at lysine 9 generates binding sites for HP1 (Bannister et al., 2001; Lachner et al., 2001). In the light of MeCP2 poly(ADP-ribosylation) and poly(ADP-ribose) recognition, it is noteworthy that poly(ADP-ribosylation) and poly(ADP-ribose) binding has recently been described specifically for HP1 α and proposed to regulate HP1 α protein associations at pericentric heterochromatin (Quenet et al., 2008).

6.1.3 Poly(ADP-ribosylation) of MeCP2 has a regulatory effect on MeCP2 mediated large-scale heterochromatin reorganization

In addition to oligomerization of MBDs as an additional layer mediating and stabilizing higher order heterochromatin reorganization, we further propose poly(ADP-ribosylation) of MeCP2 as a regulatory element in that process. Post-translational modifications of

MeCP2, such as phosphorylation, have recently been described to exert balancing effects in the modulation of MeCP2 chromatin association (Chen et al., 2003; Tao et al., 2009). Here we could show that poly(ADP-ribosylation) of MeCP2, residing within the ID (K175 and K177) and TRD (K254, K267 and K271) exerts a negative effect on MeCP2 mediated chromatin clustering *in vivo*. Both, deletion of the poly(ADP-ribosyl)ated domains and chemical inhibition of the PARP activity leads to stronger aggregation of pericentric heterochromatin (5.1 and Figure 23). Importantly, decreasing the poly(ADP-ribosylation) level of an aggregation-deficient RTT mutant bearing a missense mutation within its MBD, rescues its chromatin aggregation function to a level comparable with wt MeCP2. Our data argue for a complex interplay between MeCP2 MBD as well as poly(ADP-ribosylation) within ID and TRD resulting in MeCP2-mediated higher order chromatin organization.

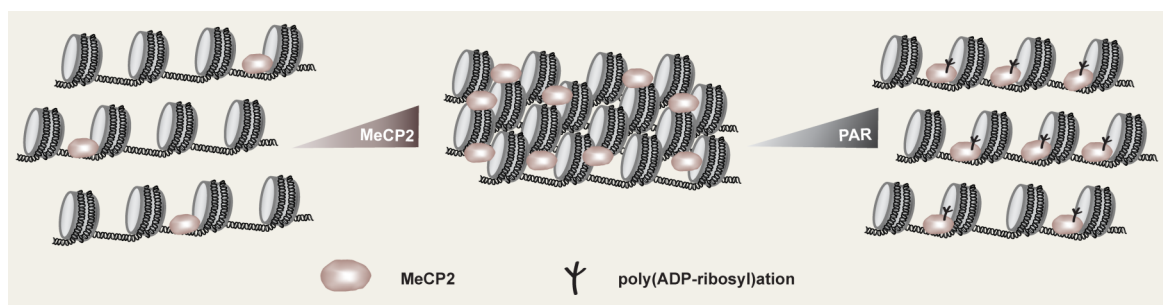


Figure 23: Poly(ADP-ribosylation) of MeCP2 counteracts its dose-dependent chromatin clustering

Although the MBD has been demonstrated to be necessary and sufficient for heterochromatin aggregation *in vivo*, it has previously been shown that an NH₂-terminal deletion lacking the MBD still exhibits preferred binding to pericentric heterochromatin but does not mediate chromatin clustering (Brero et al., 2005). Fluorescence recovery after photobleaching (FRAP) studies demonstrate that in addition to the MBD, the ID and TRD strengthen MeCP2 chromatin binding *in vivo* (Kumar et al., 2008; Marchi et al., 2007). Whereas the MBD is sufficient to induce compaction of polynucleosomes through interactions with DNA *in vitro*, the region COOH-terminal from the MBD establishes associations with chromatin. The latter is in addition indispensable for maximal nucleosomal array compaction involving secondary and tertiary chromatin structures (Georgel et al., 2003; Nikitina et al., 2007b; 2.3.2). Furthermore, the region spanning ID and TRD has been shown to be responsible for the recruitment of enzymes involved in chromatin condensation (Jones et al., 1998; Kokura et al., 2001; Nan et al., 1998). Altogether, these reports clearly suggest the MBD in mediating large-scale chromatin reorganization *in vivo* and underscore our hypothesis that modifications within ID and TRD regulate this process.

We propose that varying degrees of poly(ADP-ribosyl)ation within MeCP2 could establish (different) anionic phosphate-containing islands, gradually offsetting the positive charge of the predominantly cationic MeCP2 protein. This could modulate MeCP2 affinity to negatively charged DNA, RNA or chromatin as well as to chromatin-modifying proteins such as the deacetylases containing mSIN3A complex (Jeffery and Nakielny, 2004; Jones et al., 1998; Lewis et al., 1992; Nan et al., 1998; Nikitina et al., 2007b).

It is striking that all poly(ADP-ribosyl)ated sites of MeCP2 (K175; K177; K254; K267; K271) reside within highly disordered regions of the protein, namely aa 160 to aa 200 and aa 247 to aa 272 (Adams et al., 2007). Many intrinsically disordered protein domains acquire a well-defined conformation upon interaction with their target such as RNA, DNA or proteins, and in the case of different associating partners, might adopt varying structures resulting in numerous binding domains (Hansen et al., 2006). Both poly(ADP-ribosyl)ation sites bearing disordered regions of MeCP2 have been demonstrated to be involved in multiple interactions with different proteins including MeCP2 itself and MBD2, as reported in this study (Figure 4 and 5.2). They also constitute autonomous binding domains to unmethylated DNA (aa 164 – aa 210; aa 245 – aa 270) (Ghosh et al., 2010). Interestingly, ID and TRD have recently been described as establishing a significant increase in their secondary structure content upon binding to DNA (Ghosh et al., 2010). Furthermore, it has been demonstrated (using fluorescence anisotropy and CD) that both ID and TRD are enabled to bind to MBD in solution and that these trans-interactions induce changes in secondary structure (Ghosh et al., 2010). Post-translational modifications within the disordered NH₂-terminal domain of core histones have been proposed to facilitate the formation of secondary structures coupled with target binding as in the case of HP1 and H3K9 methylation (Hansen et al., 2006). It is tempting to speculate that the level of poly(ADP-ribosyl)ation within the unstructured regions of MeCP2 might regulate the ability of these domains to undergo binding-induced structural changes *in vivo* and further stabilize certain MeCP2 conformations.

The fact that a decreased poly(ADP-ribosyl)ation level within the highly disordered ID and TRD compensates the heterochromatin clustering defect of the P101H MBD RTT mutant, reveals a complex interplay between MeCP2 domains, their regulation by poly(ADP-ribosyl)ation and the functional consequences for MeCP2-mediated higher order chromatin organization. We propose that residues within the MBD domain of MeCP2 as well as poly(ADP-ribosyl)ation within ID and TRD, work in concert to mediate and regulate MeCP2 function in modulating global chromatin architecture.

It has recently been proposed that MeCP2 is organized into a NH₂-terminal moiety consisting of the MBD and its flanking regions (aa 1 – aa 75; ID: aa 164 – aa 210) that exert modulating and stabilizing effects on MBD DNA binding *in vitro* (Ghosh et al.,

2010). The second unit is shown to be formed by TRD and the CTD that can independently induce chromatin compaction and intra-associations of nucleosomal arrays (Ghosh et al., 2010). As a higher ratio of TRD-CTD is required to induce chromatin clustering comparable with full MeCP2 *in vitro*, synergy between both units has been suggested to underlay full MeCP2 function regarding DNA binding and chromatin clustering (Ghosh et al., 2010). Based on our findings, we can add both homo-interactions of MeCP2 involving ID, TRD and CTD as potential additional factors for MeCP2-induced chromatin compaction (Figure 21 and 22), as well as poly(ADP-ribosylation) within ID and TRD, regulating and affecting MeCP2 large-scale heterochromatin reorganization (Figure 23).

6.2 MeCP2 poly(ADP-ribosylation) as a therapeutic target

Prompted by the finding that RTT patients show abnormal neuronal morphology but no neuronal death (Armstrong et al., 1995), it was assumed that re-expression of MeCP2 in deficient neurons could restore their functionality. Indeed, it could be demonstrated that activation of MeCP2 expression in MeCP2 hemizygous and heterozygous mice exhibiting advanced RTT-like symptoms results in a clear reversal of nearly all phenotypes (Giacometti et al., 2007; Guy et al., 2007; Table 2).

Based on earlier observations indicating a role of MeCP2 as gene-specific transcriptional repressor, it has been hypothesized that in the absence of functional MeCP2, silencing of its target genes may be impaired with neuronal dysfunction as a consequence. The expression of *Bdnf* in cultured neurons has been found to be repressed by MeCP2 in the resting neuronal state. Upon neuronal activity however, MeCP2 dissociates from the promoter allowing expression of *Bdnf* (Chen et al., 2003; Martinowich et al., 2003; Tao et al., 2009). In apparent contradiction, the level of *Bdnf* in MeCP2 mutant mouse brain is surprisingly decreased (Chang et al., 2006). In fact, increasing *Bdnf* expression in a MeCP2-mutant brain with a conditional *Bdnf* transgene was found to result in a partial rescue of phenotype, suggesting therapeutic opportunities via regulation of the *Bdnf* level (Chang et al., 2006; Ricceri et al., 2008).

MeCP2 recent localization at 5mC throughout the genome as well as an accelerated H3 acetylation level and upregulation of H1 in MeCP2 null neurons, strongly argue for a global function of MeCP2 in regulating chromatin structure (Skene et al., 2010). Besides mechanistic relevance (6.1.3), our data suggest novel pharmacological approaches regarding RTT syndrome through restoration of MeCP2 global role as architectural protein.

We identified several RTT-inducing MBD missense mutations affecting MeCP2 large-scale heterochromatin reorganization. We observed that MeCP2 MBD is separated into two subdomains, one responsible for heterochromatin binding, the other involved in chromatin aggregation. Residues that mostly affect chromatin clustering are located distally from the 5mC interacting pocket suggesting that their role in connecting chromatin fibres is probably through interactions with other proteins. Using PARP inhibitors, we could show that reducing the poly(ADP-ribosylation) level within two disordered regions of MeCP2 (ID and TRD) rescues the phenotype of a MBD RTT mutant severely impaired in heterochromatin aggregation. It has been demonstrated that some RTT-inducing mutations within the MBD alter its secondary structure and influence the interdomain associations between MBD and other domains (Ghosh et al., 2008). Our results give rise to the possibility that “strengthening” the stability of the structure within non RTT-affected regions through modulation of their poly(ADP-ribosylation) using pharmacological inhibition could improve or even restore the function of a RTT-mutated domain. The recent finding, that crosstalk and additive functions between MeCP2-defined regions and disordered residue stretches are important for MeCP2 stability and folding, support our hypothesis (Ghosh et al., 2010). Our observation that endogenous MeCP2 from mouse brain tissue exhibits poly(ADP-ribosylation) makes this modification a potentially important therapeutic target. It is thus noteworthy that PARP inhibitors have already been shown to exert a protective effect on other neurological disorders (Chiarugi and Moskowitz, 2003; Kauppinen and Swanson, 2007). They have further entered clinical trials as chemotherapy sensitizing agents as well as agents for the treatment of acute cardiac ischemia (<http://www.clinicaltrial.gov/>).

The poly(ADP-ribosylated) residues K175 and K177 within MeCP2 ID have been reported to be altered in RTT syndrome patients to nonsense mutations leading to truncated MeCP2 shortly after its MBD. K177 has also been listed as a frameshift mutation (<http://mecp2.chw.edu.au/mecp2/>). In addition, the modified residues within the TRD K254, K267 and K271 have been observed in RTT patients either as nonsense (K254 and K267) or frameshift (K271) mutations (<http://mecp2.chw.edu.au/mecp2/>).

Most nonsense and frameshift mutations described in RTT syndrome truncate MeCP2 after the MBD. In particular, nonsense mutations R168X and R255X are amongst the most frequent RTT mutations (<http://mecp2.chw.edu.au/mecp2/>) and create a short protein without MeCP2 poly(ADP-ribosylated) sites. RTT-similar phenotypes and the reduced lifespan of male MeCP2^{R168X} mice with a truncating mutation of MeCP2 at aa 168 (Lawson-Yuen et al., 2007) clearly underline the importance of the COOH-terminal residues from aa 168 on for proper functioning of MeCP2 (Table 2). That MeCP2 poly(ADP-ribosylated) sites have been shown mutated in RTT, strongly suggests that

aberrant MeCP2 poly(ADP-ribosyl)ation could also contribute to protein dysfunction in RTT syndrome as it has been recently proposed for phosphorylation of MeCP2 (Tao et al., 2009; Zhou et al., 2006). Although we have observed that poly(ADP-ribosyl)ation within MeCP2 ID and TRD counteract MeCP2 clustering of heterochromatin, it is likely that the lack of MeCP2 poly(ADP-ribosyl)atable sites *per se*, resulting in abolished modulation of MeCP2 chromatin reorganization through poly(ADP-ribosyl)ation, could impact on the proper performance of MeCP2 in neurons. Whether, and to which extent MeCP2 knock-in mice with lysine to alanine mutations of MeCP2 poly(ADP-ribosyl)ated sites would display RTT phenotypes, is a tempting question to address the impact of MeCP2 poly(ADP-ribosyl)ation on the pathogenesis of RTT disease.

6.3 Outlook

i) The generation of a poly(ADP-ribosyl)ation-deficient MeCP2 fl construct, bearing point mutations of the five major poly(ADP-ribosyl)ated residues examined in this study, will be a feasible and useful tool to analyze the exact effect of poly(ADP-ribosyl)ation on MeCP2 function.

In that regard, future studies should address MeCP2 chromatin remodelling and binding *in vivo* as well as *in vitro*. The fl mutant should allow to distinguish whether the increased global heterochromatin clustering upon PARP inhibition *in vivo* exclusively depends on a decreased poly(ADP-ribosyl)ation level within MeCP2 or if it may also be the result of a reduced poly(ADP-ribosyl)ation level, *per se*, or within PARP (Kim et al., 2004; Wacker et al., 2007).

Regarding *in vitro* studies, compaction of polynucleosomes as well as DNA- and 5mC binding should be dissected employing the poly(ADP-ribosyl)ation-deficient MeCP2 fl construct.

FRAP experiments comparing modified and unmodified MeCP2 to reveal the effect of poly(ADP-ribosyl)ation on MeCP2 chromatin binding kinetics *in vivo* as well as extraction experiments to check whether modified MeCP2 is mostly chromatin-bound or soluble, will complement the study. In line with the finding that MeCP2 tracks 5mC throughout the genome (Skene et al., 2010), chromatin immunoprecipitation (ChIP) experiments in combination with bisulfite sequencing should determine the binding pattern of poly(ADP-ribosyl)ation-deficient fl MeCP2 relative to the wt. ChIP analysis to obtain the histone modification pattern of cells, either expressing wt or poly(ADP-ribosyl)ation-impaired MeCP2, will further reveal the effect of MeCP2 modification on chromatin architecture.

ii) High resolution nanoscopy (Schermelleh et al., 2008) should allow a structural comparison of pericentric heterochromatin, bound by wt or poly(ADP-ribosyl)ation-

deficient fl MeCP2. In that regard, also clustering-deficient RTT mutants before and after PARP inhibition should get analyzed.

The crystal structure as well as CD of a DNA-bound domain, comprising wt or RTT mutant MBD and modified or unmodified ID and TRD, should disclose how poly(ADP-ribosyl)ation affects DNA binding. In addition, structure composition and the degree of disordered residues within these domains could get examined.

iii) Gene expression profiles of MeCP2 mutant cells rescued with wt or poly(ADP-ribosyl)ation-deficient MeCP2 and / or *in vivo* reporter gene assays would reveal to which extent poly(ADP-ribosyl)ation of MeCP2 impacts on transcriptional regulation. The effect of poly(ADP-ribosyl)ation on MeCP2-mediated regulation of already identified candidate genes (Chen et al., 2003; Martinowich et al., 2003; McGill et al., 2006; Nuber et al., 2005) should also be examined. It would be interesting to evaluate whether besides phosphorylation, poly(ADP-ribosyl)ation influences MeCP2 activity-dependent transcriptional regulation (Chen et al., 2003; Martinowich et al., 2003; Tao et al., 2009).

iv) Apart from MeCP2 poly(ADP-ribosyl)ation identified in this study, phosphorylation of MeCP2 has also been described. It would therefore be logical to check for interconnections between these different modifications and analyze whether they occur simultaneously, sequentially or whether they are mutually exclusive. Does phosphorylation also impact on MeCP2 large-scale heterochromatin reorganization or does this modification exclusively regulate MeCP2 chromatin binding at specific limited regions? Repeating the battery of assays described above with regard to MeCP2 i) chromatin binding and remodeling, ii) secondary structure as well as iii) transcriptional regulation using either phosphorylation- or poly(ADP-ribosyl)ation-deficient MeCP2 constructs – or both at the same time - would answer how and to which extent these modifications modulate MeCP2 function.

v) In line with the finding that reduced poly(ADP-ribosyl)ation level restores the capacity of the RTT mutant P101H to reorganize heterochromatin, the effect of PARP inhibition on other clustering-impaired mutants such as P152R or P101R should also be analyzed. Can modulation of poly(ADP-ribosyl)ation further rescue the binding deficit of the strongly affected mutants R111G and / or R133L, carrying RTT-inducing mutations of aa that directly interact with DNA (Ho et al., 2008; 5.1)? This would further answer whether poly(ADP-ribosyl)ation exclusively impacts on RTT-mediating mutations located on the MBD subdomain responsible for chromatin clustering or whether both subregions can be modulated (5.1). Furthermore, it would be interesting to address how RTT mutations affect MeCP2 ability to be modified. A detailed analysis of the poly(ADP-ribosyl)ation and / or phosphorylation levels of the RTT mutants examined in this study would further

reveal if and how those levels correlate with the degree of functional derogation of these mutants.

vi) The fact that MeCP2 poly(ADP-ribosyl)ated residues reside within the CoRID of MeCP2 (2.2.5 and 5.1) together with the finding that MeCP2 does not interact with Sin3A and other proteins in a stable manner (Klose and Bird, 2004) underline the possibility that these interactions may be regulated through MeCP2 modifications. In that regard, numerous MeCP2 protein interactions mediated through the poly(ADP-ribosyl)ation sites bearing ID and TRD (Fig. 4 and 2.3.4) should get examined using wt or poly(ADP-ribosyl)ation-deficient fl MeCP2. Also MeCP2 binding to itself and MBD2 (5.2) should be included in these analyses.

In addition, the question arises whether specific level of MeCP2 covalently bound poly(ADP-ribose) chains or whether non-covalently MeCP2 associated poly(ADP-ribose) regulates its homodimerization and hetero-association with other MBDs. Incubation of, e.g., two different tagged poly(ADP-ribosyl)ation-deficient fl MeCP2 constructs with increasing amounts of poly(ADP-ribose) could decipher whether poly(ADP-ribose) itself cross-links MeCP2 to form (stable) associations.

vii) In order to determine the magnitude of homo- and hetero-complexes between MeCP2 and MBD2, gel filtration analysis of cell extracts could be performed. PARP inhibition of the cells, followed by extraction and gel-filtration could further reveal the effect of poly(ADP-ribose) on the association between the MBD proteins.

viii) Based on the finding that the hinge domain of HP1 α gets poly(ADP-ribosyl)ated and also recognizes poly(ADP-ribose) (Quenet et al., 2008), it would be interesting to analyze the interaction between MeCP2 and HP1 α with regard to a potential regulation either through covalent modification or non-covalent poly(ADP-ribose) binding. Chemical inhibition of PARP activity could further be used to estimate the impact of MeCP2 poly(ADP-ribosyl)ation on HP1 α and HP1 γ -increased heterochromatin association upon myogenic differentiation (Agarwal et al., 2007; Appendix).

7 Appendix

7.1 References

- Adams, V.H., McBryant, S.J., Wade, P.A., Woodcock, C.L., and Hansen, J.C. (2007). Intrinsic disorder and autonomous domain function in the multifunctional nuclear protein, MeCP2. *J Biol Chem* **282**, 15057-15064.
- Agarwal, N., Hardt, T., Brero, A., Nowak, D., Rothbauer, U., Becker, A., Leonhardt, H., and Cardoso, M.C. (2007). MeCP2 interacts with HP1 and modulates its heterochromatin association during myogenic differentiation. *Nucleic Acids Res* **35**, 5402-5408.
- Ahringer, J. (2000). NuRD and SIN3 histone deacetylase complexes in development. *Trends Genet* **16**, 351-356.
- Allan, J., Rau, D.C., Harborne, N., and Gould, H. (1984). Higher order structure in a short repeat length chromatin. *J Cell Biol* **98**, 1320-1327.
- Altmeyer, M., Messner, S., Hassa, P.O., Fey, M., and Hottiger, M.O. (2009). Molecular mechanism of poly(ADP-ribosylation) by PARP1 and identification of lysine residues as ADP-ribose acceptor sites. *Nucleic Acids Res* **37**, 3723-3738.
- Alvarez-Gonzalez, R., and Althaus, F.R. (1989). Poly(ADP-ribose) catabolism in mammalian cells exposed to DNA-damaging agents. *Mutat Res* **218**, 67-74.
- Ame, J.C., Spelshauer, C., and de Murcia, G. (2004). The PARP superfamily. *Bioessays* **26**, 882-893.
- Amir, R.E., Van den Veyver, I.B., Wan, M., Tran, C.Q., Francke, U., and Zoghbi, H.Y. (1999). Rett syndrome is caused by mutations in X-linked MECP2, encoding methyl-CpG-binding protein 2. *Nat Genet* **23**, 185-188.
- Amir, R.E., and Zoghbi, H.Y. (2000). Rett syndrome: methyl-CpG-binding protein 2 mutations and phenotype-genotype correlations. *Am J Med Genet* **97**, 147-152.
- Armstrong, D., Dunn, J.K., Antalffy, B., and Trivedi, R. (1995). Selective dendritic alterations in the cortex of Rett syndrome. *J Neuropathol Exp Neurol* **54**, 195-201.
- Bader, S., Walker, M., and Harrison, D. (2000). Most microsatellite unstable sporadic colorectal carcinomas carry MBD4 mutations. *Br J Cancer* **83**, 1646-1649.
- Bannister, A.J., Zegerman, P., Partridge, J.F., Miska, E.A., Thomas, J.O., Allshire, R.C., and Kouzarides, T. (2001). Selective recognition of methylated lysine 9 on histone H3 by the HP1 chromo domain. *Nature* **410**, 120-124.
- Bedford, M.T., Chan, D.C., and Leder, P. (1997). FBP WW domains and the Abl SH3 domain bind to a specific class of proline-rich ligands. *EMBO J* **16**, 2376-2383.

- Bednar, J., Horowitz, R.A., Grigoryev, S.A., Carruthers, L.M., Hansen, J.C., Koster, A.J., and Woodcock, C.L. (1998). Nucleosomes, linker DNA, and linker histone form a unique structural motif that directs the higher-order folding and compaction of chromatin. *Proc Natl Acad Sci U S A* 95, 14173-14178.
- Bellacosa, A., Cicchillitti, L., Schepis, F., Riccio, A., Yeung, A.T., Matsumoto, Y., Golemis, E.A., Genuardi, M., and Neri, G. (1999). MED1, a novel human methyl-CpG-binding endonuclease, interacts with DNA mismatch repair protein MLH1. *Proc Natl Acad Sci U S A* 96, 3969-3974.
- Bhattacharya, S.K., Ramchandani, S., Cervoni, N., and Szyf, M. (1999). A mammalian protein with specific demethylase activity for mCpG DNA. *Nature* 397, 579-583.
- Bird, A. (2002). DNA methylation patterns and epigenetic memory. *Genes Dev* 16, 6-21.
- Bird, A.P. (1986). CpG-rich islands and the function of DNA methylation. *Nature* 321, 209-213.
- Bird, A.P., and Wolffe, A.P. (1999). Methylation-induced repression--belts, braces, and chromatin. *Cell* 99, 451-454.
- Birnboim, H. C., and Doly, J. (1979). A rapid alkaline extraction procedure for screening recombinant plasmid DANN. *Nucleic Acids Res* 7, 1513-1523.
- Bodnar, A.G., Ouellette, M., Frolkis, M., Holt, S.E., Chiu, C.P., Morin, G.B., Harley, C.B., Shay, J.W., Lichtsteiner, S., and Wright, W.E. (1998). Extension of life-span by introduction of telomerase into normal human cells. *Science* 279, 349-352.
- Boeke, J., Ammerpohl, O., Kegel, S., Moehren, U., and Renkawitz, R. (2000). The minimal repression domain of MBD2b overlaps with the methyl-CpG-binding domain and binds directly to Sin3A. *J Biol Chem* 275, 34963-34967.
- Bracaglia, G., Conca, B., Bergo, A., Rusconi, L., Zhou, Z., Greenberg, M.E., Landsberger, N., Soddu, S., and Kilstrup-Nielsen, C. (2009). Methyl-CpG-binding protein 2 is phosphorylated by homeodomain-interacting protein kinase 2 and contributes to apoptosis. *EMBO Rep* 10, 1327-1333.
- Brero, A., Easwaran, H.P., Nowak, D., Grunewald, I., Cremer, T., Leonhardt, H., and Cardoso, M.C. (2005). Methyl CpG-binding proteins induce large-scale chromatin reorganization during terminal differentiation. *J Cell Biol* 169, 733-743.
- Buki, K.G., and Kun, E. (1988). Polypeptide domains of ADP-ribosyltransferase obtained by digestion with plasmin. *Biochemistry* 27, 5990-5995.
- Buschdorf, J.P., and Stratling, W.H. (2004). A WW domain binding region in methyl-CpG-binding protein MeCP2: impact on Rett syndrome. *J Mol Med* 82, 135-143.
- Calzado, M.A., Renner, F., Roscic, A., and Schmitz, M.L. (2007). HIPK2: a versatile switchboard regulating the transcription machinery and cell death. *Cell Cycle* 6, 139-143.

- Campanero, M.R., Armstrong, M.I., and Flemington, E.K. (2000). CpG methylation as a mechanism for the regulation of E2F activity. *Proc Natl Acad Sci U S A* 97, 6481-6486.
- Cervantes-Laurean, D., Jacobson, E.L., and Jacobson, M.K. (1996). Glycation and glycooxidation of histones by ADP-ribose. *J Biol Chem* 271, 10461-10469.
- Chahrour, M., Jung, S.Y., Shaw, C., Zhou, X., Wong, S.T., Qin, J., and Zoghbi, H.Y. (2008). MeCP2, a key contributor to neurological disease, activates and represses transcription. *Science* 320, 1224-1229.
- Chahrour, M., and Zoghbi, H.Y. (2007). The story of Rett syndrome: from clinic to neurobiology. *Neuron* 56, 422-437.
- Chandler, S.P., Guschin, D., Landsberger, N., and Wolffe, A.P. (1999). The methyl-CpG binding transcriptional repressor MeCP2 stably associates with nucleosomal DNA. *Biochemistry* 38, 7008-7018.
- Chang, Q., Khare, G., Dani, V., Nelson, S., and Jaenisch, R. (2006). The disease progression of *Mecp2* mutant mice is affected by the level of BDNF expression. *Neuron* 49, 341-348.
- Chen, R.Z., Akbarian, S., Tudor, M., and Jaenisch, R. (2001). Deficiency of methyl-CpG binding protein-2 in CNS neurons results in a Rett-like phenotype in mice. *Nat Genet* 27, 327-331.
- Chen, W.G., Chang, Q., Lin, Y., Meissner, A., West, A.E., Griffith, E.C., Jaenisch, R., and Greenberg, M.E. (2003). Derepression of BDNF transcription involves calcium-dependent phosphorylation of MeCP2. *Science* 302, 885-889.
- Chiarugi, A., and Moskowitz, M.A. (2003). Poly(ADP-ribose) polymerase-1 activity promotes NF-kappaB-driven transcription and microglial activation: implication for neurodegenerative disorders. *J Neurochem* 85, 306-317.
- Chuang, L.S., Ian, H.I., Koh, T.W., Ng, H.H., Xu, G., and Li, B.F. (1997). Human DNA-(cytosine-5) methyltransferase-PCNA complex as a target for p21WAF1. *Science* 277, 1996-2000.
- Collins, A.L., Levenson, J.M., Vilaythong, A.P., Richman, R., Armstrong, D.L., Noebels, J.L., David Sweatt, J., and Zoghbi, H.Y. (2004). Mild overexpression of MeCP2 causes a progressive neurological disorder in mice. *Hum Mol Genet* 13, 2679-2689.
- Cooke, H.J., and Hindley, J. (1979). Cloning of human satellite III DNA: different components are on different chromosomes. *Nucleic Acids Res* 6, 3177-3197.
- Dantzer, F., Giraud-Panis, M.J., Jaco, I., Ame, J.C., Schultz, I., Blasco, M., Koering, C.E., Gilson, E., Menissier-de Murcia, J., de Murcia, G., *et al.* (2004). Functional

- interaction between poly(ADP-Ribose) polymerase 2 (PARP-2) and TRF2: PARP activity negatively regulates TRF2. *Mol Cell Biol* 24, 1595-1607.
- de Murcia, G., and Menissier de Murcia, J. (1994). Poly(ADP-ribose) polymerase: a molecular nick-sensor. *Trends Biochem Sci* 19, 172-176.
- de Murcia, J.M., Niedergang, C., Trucco, C., Ricoul, M., Dutrillaux, B., Mark, M., Oliver, F.J., Masson, M., Dierich, A., LeMeur, M., *et al.* (1997). Requirement of poly(ADP-ribose) polymerase in recovery from DNA damage in mice and in cells. *Proc Natl Acad Sci U S A* 94, 7303-7307.
- Duriez, P.J., Desnoyers, S., Hoflack, J.C., Shah, G.M., Morelle, B., Bourassa, S., Poirier, G.G., and Talbot, B. (1997). Characterization of anti-peptide antibodies directed towards the automodification domain and apoptotic fragment of poly (ADP-ribose) polymerase. *Biochim Biophys Acta* 1334, 65-72.
- Fraga, M.F., Ballestar, E., Montoya, G., Taysavang, P., Wade, P.A., and Esteller, M. (2003). The affinity of different MBD proteins for a specific methylated locus depends on their intrinsic binding properties. *Nucleic Acids Res* 31, 1765-1774.
- Fujita, N., Takebayashi, S., Okumura, K., Kudo, S., Chiba, T., Saya, H., and Nakao, M. (1999). Methylation-mediated transcriptional silencing in euchromatin by methyl-CpG binding protein MBD1 isoforms. *Mol Cell Biol* 19, 6415-6426.
- Fujita, N., Watanabe, S., Ichimura, T., Ohkuma, Y., Chiba, T., Saya, H., and Nakao, M. (2003a). MCAF mediates MBD1-dependent transcriptional repression. *Mol Cell Biol* 23, 2834-2843.
- Fujita, N., Watanabe, S., Ichimura, T., Tsuruzoe, S., Shinkai, Y., Tachibana, M., Chiba, T., and Nakao, M. (2003b). Methyl-CpG binding domain 1 (MBD1) interacts with the Suv39h1-HP1 heterochromatic complex for DNA methylation-based transcriptional repression. *J Biol Chem* 278, 24132-24138.
- Fuks, F., Hurd, P.J., Wolf, D., Nan, X., Bird, A.P., and Kouzarides, T. (2003). The methyl-CpG-binding protein MeCP2 links DNA methylation to histone methylation. *J Biol Chem* 278, 4035-4040.
- Georgel, P.T., Horowitz-Scherer, R.A., Adkins, N., Woodcock, C.L., Wade, P.A., and Hansen, J.C. (2003). Chromatin compaction by human MeCP2. Assembly of novel secondary chromatin structures in the absence of DNA methylation. *J Biol Chem* 278, 32181-32188.
- Ghosh, R.P., Horowitz-Scherer, R.A., Nikitina, T., Gierasch, L.M., and Woodcock, C.L. (2008). Rett syndrome-causing mutations in human MeCP2 result in diverse structural changes that impact folding and DNA interactions. *J Biol Chem* 283, 20523-20534.

- Ghosh, R.P., Nikitina, T., Horowitz-Scherer, R.A., Gierasch, L.M., Uversky, V.N., Hite, K., Hansen, J.C., and Woodcock, C.L. (2010). Unique physical properties and interactions of the domains of methylated DNA binding protein 2. *Biochemistry* *49*, 4395-4410.
- Giacometti, E., Luikenhuis, S., Beard, C., and Jaenisch, R. (2007). Partial rescue of MeCP2 deficiency by postnatal activation of MeCP2. *Proc Natl Acad Sci U S A* *104*, 1931-1936.
- Guy, J., Gan, J., Selfridge, J., Cobb, S., and Bird, A. (2007). Reversal of neurological defects in a mouse model of Rett syndrome. *Science* *315*, 1143-1147.
- Guy, J., Hendrich, B., Holmes, M., Martin, J.E., and Bird, A. (2001). A mouse *Mecp2*-null mutation causes neurological symptoms that mimic Rett syndrome. *Nat Genet* *27*, 322-326.
- Hagberg, B. (1985). Rett's syndrome: prevalence and impact on progressive severe mental retardation in girls. *Acta Paediatr Scand* *74*, 405-408.
- Hagberg, B., Aicardi, J., Dias, K., and Ramos, O. (1983). A progressive syndrome of autism, dementia, ataxia, and loss of purposeful hand use in girls: Rett's syndrome: report of 35 cases. *Ann Neurol* *14*, 471-479.
- Hansen, J.C., Lu, X., Ross, E.D., and Woody, R.W. (2006). Intrinsic protein disorder, amino acid composition, and histone terminal domains. *J Biol Chem* *281*, 1853-1856.
- Harikrishnan, K.N., Chow, M.Z., Baker, E.K., Pal, S., Bassal, S., Brasacchio, D., Wang, L., Craig, J.M., Jones, P.L., Sif, S., *et al.* (2005). Brahma links the SWI/SNF chromatin-remodeling complex with MeCP2-dependent transcriptional silencing. *Nat Genet* *37*, 254-264.
- Harmon, B., and Sedat, J. (2005). Cell-by-cell dissection of gene expression and chromosomal interactions reveals consequences of nuclear reorganization. *PLoS Biol* *3*, e67.
- Hassa, P.O., Haenni, S.S., Elser, M., and Hottiger, M.O. (2006). Nuclear ADP-ribosylation reactions in mammalian cells: where are we today and where are we going? *Microbiol Mol Biol Rev* *70*, 789-829.
- Hendrich, B., and Bird, A. (1998). Identification and characterization of a family of mammalian methyl-CpG binding proteins. *Mol Cell Biol* *18*, 6538-6547.
- Hendrich, B., Guy, J., Ramsahoye, B., Wilson, V.A., and Bird, A. (2001). Closely related proteins MBD2 and MBD3 play distinctive but interacting roles in mouse development. *Genes Dev* *15*, 710-723.

- Hendrich, B., Hardeland, U., Ng, H.H., Jiricny, J., and Bird, A. (1999). The thymine glycosylase MBD4 can bind to the product of deamination at methylated CpG sites. *Nature* 401, 301-304.
- Ho, K.L., McNae, I.W., Schmiedeberg, L., Klose, R.J., Bird, A.P., and Walkinshaw, M.D. (2008). MeCP2 binding to DNA depends upon hydration at methyl-CpG. *Mol Cell* 29, 525-531.
- Hsu, T.C., Cooper, J.E., Mace, M.L., Jr., and Brinkley, B.R. (1971). Arrangement of centromeres in mouse cells. *Chromosoma* 34, 73-87.
- Hutchins, A.S., Mullen, A.C., Lee, H.W., Sykes, K.J., High, F.A., Hendrich, B.D., Bird, A.P., and Reiner, S.L. (2002). Gene silencing quantitatively controls the function of a developmental trans-activator. *Mol Cell* 10, 81-91.
- Iguchi-Ariga, S.M., and Schaffner, W. (1989). CpG methylation of the cAMP-responsive enhancer/promoter sequence TGACGTCA abolishes specific factor binding as well as transcriptional activation. *Genes Dev* 3, 612-619.
- Ikejima, M., Noguchi, S., Yamashita, R., Ogura, T., Sugimura, T., Gill, D.M., and Miwa, M. (1990). The zinc fingers of human poly(ADP-ribose) polymerase are differentially required for the recognition of DNA breaks and nicks and the consequent enzyme activation. Other structures recognize intact DNA. *J Biol Chem* 265, 21907-21913.
- Ishibashi, T., Thambirajah, A.A., and Ausio, J. (2008). MeCP2 preferentially binds to methylated linker DNA in the absence of the terminal tail of histone H3 and independently of histone acetylation. *FEBS Lett* 582, 1157-1162.
- Jeffery, L., and Nakielny, S. (2004). Components of the DNA methylation system of chromatin control are RNA-binding proteins. *J Biol Chem* 279, 49479-49487.
- Jones, K.W. (1970). Chromosomal and nuclear location of mouse satellite DNA in individual cells. *Nature* 225, 912-915.
- Jones, P.L., Veenstra, G.J., Wade, P.A., Vermaak, D., Kass, S.U., Landsberger, N., Strouboulis, J., and Wolffe, A.P. (1998). Methylated DNA and MeCP2 recruit histone deacetylase to repress transcription. *Nat Genet* 19, 187-191.
- Jorgensen, H.F., Ben-Porath, I., and Bird, A.P. (2004). Mbd1 is recruited to both methylated and nonmethylated CpGs via distinct DNA binding domains. *Mol Cell Biol* 24, 3387-3395.
- Kaneda, M., Okano, M., Hata, K., Sado, T., Tsujimoto, N., Li, E., and Sasaki, H. (2004). Essential role for de novo DNA methyltransferase Dnmt3a in paternal and maternal imprinting. *Nature* 429, 900-903.

- Kaufmann, U., Kirsch, J., Irintchev, A., Wernig, A., and Starzinski-Powitz, A. (1999). The M-cadherin catenin complex interacts with microtubules in skeletal muscle cells: implications for the fusion of myoblasts. *J Cell Sci* 112 (Pt 1), 55-68.
- Kauppinen, T.M., and Swanson, R.A. (2007). The role of poly(ADP-ribose)polymerase-1 in CNS disease. *Neuroscience* 145, 1267-1272.
- Kernohan, K.D., Jiang, Y., Tremblay, D.C., Bonvissuto, A.C., Eubanks, J.H., Mann, M.R., and Berube, N.G. (2010). ATRX partners with cohesin and MeCP2 and contributes to developmental silencing of imprinted genes in the brain. *Dev Cell* 18, 191-202.
- Kim, M.Y., Mauro, S., Gevry, N., Lis, J.T., and Kraus, W.L. (2004). NAD⁺-dependent modulation of chromatin structure and transcription by nucleosome binding properties of PARP-1. *Cell* 119, 803-814.
- Kimura, H., and Shiota, K. (2003). Methyl-CpG-binding protein, MeCP2, is a target molecule for maintenance DNA methyltransferase, Dnmt1. *J Biol Chem* 278, 4806-4812.
- Klose, R.J., and Bird, A.P. (2004). MeCP2 behaves as an elongated monomer that does not stably associate with the Sin3a chromatin remodeling complex. *J Biol Chem* 279, 46490-46496.
- Klose, R.J., Sarraf, S.A., Schmiedeberg, L., McDermott, S.M., Stancheva, I., and Bird, A.P. (2005). DNA binding selectivity of MeCP2 due to a requirement for A/T sequences adjacent to methyl-CpG. *Mol Cell* 19, 667-678.
- Kokura, K., Kaul, S.C., Wadhwa, R., Nomura, T., Khan, M.M., Shinagawa, T., Yasukawa, T., Colmenares, C., and Ishii, S. (2001). The Ski protein family is required for MeCP2-mediated transcriptional repression. *J Biol Chem* 276, 34115-34121.
- Kondo, E., Gu, Z., Horii, A., and Fukushige, S. (2005). The thymine DNA glycosylase MBD4 represses transcription and is associated with methylated p16(INK4a) and hMLH1 genes. *Mol Cell Biol* 25, 4388-4396.
- Kraus, W.L., and Lis, J.T. (2003). PARP goes transcription. *Cell* 113, 677-683.
- Kriaucionis, S., and Bird, A. (2004). The major form of MeCP2 has a novel N-terminus generated by alternative splicing. *Nucleic Acids Res* 32, 1818-1823.
- Kudo, S., Nomura, Y., Segawa, M., Fujita, N., Nakao, M., Schanen, C., and Tamura, M. (2003). Heterogeneity in residual function of MeCP2 carrying missense mutations in the methyl CpG binding domain. *J Med Genet* 40, 487-493.
- Kumar, A., Kamboj, S., Malone, B.M., Kudo, S., Twiss, J.L., Czymmek, K.J., LaSalle, J.M., and Schanen, N.C. (2008). Analysis of protein domains and Rett syndrome mutations indicate that multiple regions influence chromatin-binding dynamics of the chromatin-associated protein MECP2 *in vivo*. *J Cell Sci* 121, 1128-1137.

- Lachner, M., O'Carroll, D., Rea, S., Mechtler, K., and Jenuwein, T. (2001). Methylation of histone H3 lysine 9 creates a binding site for HP1 proteins. *Nature* *410*, 116-120.
- Lawson-Yuen, A., Liu, D., Han, L., Jiang, Z.I., Tsai, G.E., Basu, A.C., Picker, J., Feng, J., and Coyle, J.T. (2007). Ube3a mRNA and protein expression are not decreased in Mecp2R168X mutant mice. *Brain Res* *1180*, 1-6.
- Leonhardt, H., Page, A.W., Weier, H.U., and Bestor, T.H. (1992). A targeting sequence directs DNA methyltransferase to sites of DNA replication in mammalian nuclei. *Cell* *71*, 865-873.
- Leonhardt, H., and Cardoso, M.C. (2000). DNA methylation, nuclear structure, gene expression and cancer. *J Cell Biochem Suppl*, 78-83.
- Lewis, J.D., Meehan, R.R., Henzel, W.J., Maurer-Fogy, I., Jeppesen, P., Klein, F., and Bird, A. (1992). Purification, sequence, and cellular localization of a novel chromosomal protein that binds to methylated DNA. *Cell* *69*, 905-914.
- Lin, C., Franco, B., and Rosner, M.R. (2005). CDKL5/Stk9 kinase inactivation is associated with neuronal developmental disorders. *Hum Mol Genet* *14*, 3775-3786.
- Luikenhuis, S., Giacometti, E., Beard, C.F., and Jaenisch, R. (2004). Expression of MeCP2 in postmitotic neurons rescues Rett syndrome in mice. *Proc Natl Acad Sci U S A* *101*, 6033-6038.
- Lunyak, V.V., Burgess, R., Prefontaine, G.G., Nelson, C., Sze, S.H., Chenoweth, J., Schwartz, P., Pevzner, P.A., Glass, C., Mandel, G., *et al.* (2002). Corepressor-dependent silencing of chromosomal regions encoding neuronal genes. *Science* *298*, 1747-1752.
- Lyst, M.J., Nan, X., and Stancheva, I. (2006). Regulation of MBD1-mediated transcriptional repression by SUMO and PIAS proteins. *EMBO J* *25*, 5317-5328.
- Makarova, O., Kamberov, E., and Margolis, B. (2000). Generation of deletion and point mutations with one primer in a single cloning step. *Biotechniques* *29*, 970-972.
- Marchi, M., Guarda, A., Bergo, A., Landsberger, N., Kilstrup-Nielsen, C., Ratto, G.M., and Costa, M. (2007). Spatio-temporal dynamics and localization of MeCP2 and pathological mutants in living cells. *Epigenetics* *2*, 187-197.
- Mari, F., Azimonti, S., Bertani, I., Bolognese, F., Colombo, E., Caselli, R., Scala, E., Longo, I., Grosso, S., Pescucci, C., *et al.* (2005). CDKL5 belongs to the same molecular pathway of MeCP2 and it is responsible for the early-onset seizure variant of Rett syndrome. *Hum Mol Genet* *14*, 1935-1946.
- Martinowich, K., Hattori, D., Wu, H., Fouse, S., He, F., Hu, Y., Fan, G., and Sun, Y.E. (2003). DNA methylation-related chromatin remodeling in activity-dependent BDNF gene regulation. *Science* *302*, 890-893.

- Masutani, M., Suzuki, H., Kamada, N., Watanabe, M., Ueda, O., Nozaki, T., Jishage, K., Watanabe, T., Sugimoto, T., Nakagama, H., *et al.* (1999). Poly(ADP-ribose) polymerase gene disruption conferred mice resistant to streptozotocin-induced diabetes. *Proc Natl Acad Sci U S A* **96**, 2301-2304.
- McGill, B.E., Bundle, S.F., Yaylaoglu, M.B., Carson, J.P., Thaller, C., and Zoghbi, H.Y. (2006). Enhanced anxiety and stress-induced corticosterone release are associated with increased *Crh* expression in a mouse model of Rett syndrome. *Proc Natl Acad Sci U S A* **103**, 18267-18272.
- Meehan, R.R., Lewis, J.D., and Bird, A.P. (1992). Characterization of MeCP2, a vertebrate DNA binding protein with affinity for methylated DNA. *Nucleic Acids Res* **20**, 5085-5092.
- Meehan, R.R., Lewis, J.D., McKay, S., Kleiner, E.L., and Bird, A.P. (1989). Identification of a mammalian protein that binds specifically to DNA containing methylated CpGs. *Cell* **58**, 499-507.
- Michaels, M.L., Pham, L., Nghiem, Y., Cruz, C., and Miller, J.H. (1990). MutY, an adenine glycosylase active on G-A mispairs, has homology to endonuclease III. *Nucleic Acids Res* **18**, 3841-3845.
- Millar, C.B., Guy, J., Sansom, O.J., Selfridge, J., MacDougall, E., Hendrich, B., Keightley, P.D., Bishop, S.M., Clarke, A.R., and Bird, A. (2002). Enhanced CpG mutability and tumorigenesis in MBD4-deficient mice. *Science* **297**, 403-405.
- Miyake, K., and Nagai, K. (2007). Phosphorylation of methyl-CpG binding protein 2 (MeCP2) regulates the intracellular localization during neuronal cell differentiation. *Neurochem Int* **50**, 264-270.
- Mnatzakanian, G.N., Lohi, H., Munteanu, I., Alfred, S.E., Yamada, T., MacLeod, P.J., Jones, J.R., Scherer, S.W., Schanen, N.C., Friez, M.J., *et al.* (2004). A previously unidentified MECP2 open reading frame defines a new protein isoform relevant to Rett syndrome. *Nat Genet* **36**, 339-341.
- Modrich, P., and Lahue, R. (1996). Mismatch repair in replication fidelity, genetic recombination, and cancer biology. *Annu Rev Biochem* **65**, 101-133.
- Moretti, P., Bouwknecht, J.A., Teague, R., Paylor, R., and Zoghbi, H.Y. (2005). Abnormalities of social interactions and home-cage behavior in a mouse model of Rett syndrome. *Hum Mol Genet* **14**, 205-220.
- Morgan, H.D., Dean, W., Coker, H.A., Reik, W., and Petersen-Mahrt, S.K. (2004). Activation-induced cytidine deaminase deaminates 5-methylcytosine in DNA and is expressed in pluripotent tissues: implications for epigenetic reprogramming. *J Biol Chem* **279**, 52353-52360.

- Mortusewicz, O., Rothbauer, U., Cardoso, M.C., and Leonhardt, H. (2006). Differential recruitment of DNA Ligase I and III to DNA repair sites. *Nucleic Acids Res* 34, 3523-3532.
- Mullen, A.C., Hutchins, A.S., Villarino, A.V., Lee, H.W., High, F.A., Cereb, N., Yang, S.Y., Hua, X., and Reiner, S.L. (2001). Cell cycle controlling the silencing and functioning of mammalian activators. *Curr Biol* 11, 1695-1699.
- Nan, X., Campoy, F.J., and Bird, A. (1997). MeCP2 is a transcriptional repressor with abundant binding sites in genomic chromatin. *Cell* 88, 471-481.
- Nan, X., Hou, J., Maclean, A., Nasir, J., Lafuente, M.J., Shu, X., Kriaucionis, S., and Bird, A. (2007). Interaction between chromatin proteins MECP2 and ATRX is disrupted by mutations that cause inherited mental retardation. *Proc Natl Acad Sci U S A* 104, 2709-2714.
- Nan, X., Meehan, R.R., and Bird, A. (1993). Dissection of the methyl-CpG binding domain from the chromosomal protein MeCP2. *Nucleic Acids Res* 21, 4886-4892.
- Nan, X., Ng, H.H., Johnson, C.A., Laherty, C.D., Turner, B.M., Eisenman, R.N., and Bird, A. (1998). Transcriptional repression by the methyl-CpG-binding protein MeCP2 involves a histone deacetylase complex. *Nature* 393, 386-389.
- Nan, X., Tate, P., Li, E., and Bird, A. (1996). DNA methylation specifies chromosomal localization of MeCP2. *Mol Cell Biol* 16, 414-421.
- Neddermann, P., Gallinari, P., Lettieri, T., Schmid, D., Truong, O., Hsuan, J.J., Wiebauer, K., and Jiricny, J. (1996). Cloning and expression of human G/T mismatch-specific thymine-DNA glycosylase. *J Biol Chem* 271, 12767-12774.
- Ng, H.H., Jeppesen, P., and Bird, A. (2000). Active repression of methylated genes by the chromosomal protein MBD1. *Mol Cell Biol* 20, 1394-1406.
- Ng, H.H., Zhang, Y., Hendrich, B., Johnson, C.A., Turner, B.M., Erdjument-Bromage, H., Tempst, P., Reinberg, D., and Bird, A. (1999). MBD2 is a transcriptional repressor belonging to the MeCP1 histone deacetylase complex. *Nat Genet* 23, 58-61.
- Nikitina, T., Ghosh, R.P., Horowitz-Scherer, R.A., Hansen, J.C., Grigoryev, S.A., and Woodcock, C.L. (2007a). MeCP2-chromatin interactions include the formation of chromatosome-like structures and are altered in mutations causing Rett syndrome. *J Biol Chem* 282, 28237-28245.
- Nikitina, T., Shi, X., Ghosh, R.P., Horowitz-Scherer, R.A., Hansen, J.C., and Woodcock, C.L. (2007b). Multiple modes of interaction between the methylated DNA binding protein MeCP2 and chromatin. *Mol Cell Biol* 27, 864-877.
- Nuber, U.A., Kriaucionis, S., Roloff, T.C., Guy, J., Selfridge, J., Steinhoff, C., Schulz, R., Lipkowitz, B., Ropers, H.H., Holmes, M.C., *et al.* (2005). Up-regulation of

- glucocorticoid-regulated genes in a mouse model of Rett syndrome. *Hum Mol Genet* **14**, 2247-2256.
- Ogata, N., Ueda, K., and Hayaishi, O. (1980a). ADP-ribosylation of histone H2B. Identification of glutamic acid residue 2 as the modification site. *J Biol Chem* **255**, 7610-7615.
- Ogata, N., Ueda, K., Kagamiyama, H., and Hayaishi, O. (1980b). ADP-ribosylation of histone H1. Identification of glutamic acid residues 2, 14, and the COOH-terminal lysine residue as modification sites. *J Biol Chem* **255**, 7616-7620.
- Okano, M., Bell, D.W., Haber, D.A., and Li, E. (1999). DNA methyltransferases Dnmt3a and Dnmt3b are essential for de novo methylation and mammalian development. *Cell* **99**, 247-257.
- Orrico, A., Lam, C., Galli, L., Dotti, M.T., Hayek, G., Tong, S.F., Poon, P.M., Zappella, M., Federico, A., and Sorrentino, V. (2000). MECP2 mutation in male patients with non-specific X-linked mental retardation. *FEBS Lett* **481**, 285-288.
- Pardue, M.L., and Gall, J.G. (1970). Chromosomal localization of mouse satellite DNA. *Science* **168**, 1356-1358.
- Petronzelli, F., Riccio, A., Markham, G.D., Seeholzer, S.H., Stoerker, J., Genuardi, M., Yeung, A.T., Matsumoto, Y., and Bellacosa, A. (2000). Biphasic kinetics of the human DNA repair protein MED1 (MBD4), a mismatch-specific DNA N-glycosylase. *J Biol Chem* **275**, 32422-32429.
- Pleschke, J.M., Kleczkowska, H.E., Strohm, M., and Althaus, F.R. (2000). Poly(ADP-ribose) binds to specific domains in DNA damage checkpoint proteins. *J Biol Chem* **275**, 40974-40980.
- Poirier, G.G., de Murcia, G., Jongstra-Bilen, J., Niedergang, C., and Mandel, P. (1982). Poly(ADP-ribosyl)ation of polynucleosomes causes relaxation of chromatin structure. *Proc Natl Acad Sci U S A* **79**, 3423-3427.
- Prilusky, J., Felder, C.E., Zeev-Ben-Mordehai, T., Rydberg, E.H., Man, O., Beckmann, J.S., Silman, I., and Sussman, J.L. (2005). FoldIndex: a simple tool to predict whether a given protein sequence is intrinsically unfolded. *Bioinformatics* **21**, 3435-3438.
- Prusov, A.N., and Zatsepina, O.V. (2002). Isolation of the Chromocenter Fraction from Mouse Liver Nuclei. *Biochemistry (Moscow)* **67**, 423-431.
- Quenet, D., El Ramy, R., Schreiber, V., and Dantzer, F. (2009). The role of poly(ADP-ribose) in epigenetic events. *Int J Biochem Cell Biol* **41**, 60-65.
- Quenet, D., Gasser, V., Fouillen, L., Cammas, F., Sanglier-Cianferani, S., Losson, R., and Dantzer, F. (2008). The histone subcode: poly(ADP-ribose) polymerase-1 (Parp-1) and Parp-2 control cell differentiation by regulating the transcriptional

- intermediary factor TIF1beta and the heterochromatin protein HP1alpha. *FASEB J* 22, 3853-3865.
- Rai, K., Huggins, I.J., James, S.R., Karpf, A.R., Jones, D.A., and Cairns, B.R. (2008). DNA demethylation in zebrafish involves the coupling of a deaminase, a glycosylase, and gadd45. *Cell* 135, 1201-1212.
- Ricceri, L., De Filippis, B., and Laviola, G. (2008). Mouse models of Rett syndrome: from behavioural phenotyping to preclinical evaluation of new therapeutic approaches. *Behav Pharmacol* 19, 501-517.
- Riccio, A., Aaltonen, L.A., Godwin, A.K., Loukola, A., Percesepe, A., Salovaara, R., Masciullo, V., Genuardi, M., Paravatou-Petsotas, M., Bassi, D.E., *et al.* (1999). The DNA repair gene MBD4 (MED1) is mutated in human carcinomas with microsatellite instability. *Nat Genet* 23, 266-268.
- Rinaldo, C., Prodosmo, A., Siepi, F., and Soddu, S. (2007). HIPK2: a multitasking partner for transcription factors in DNA damage response and development. *Biochem Cell Biol* 85, 411-418.
- Rothbauer, U., Zolghadr, K., Muyldermans, S., Schepers, A., Cardoso, M.C., and Leonhardt, H. (2008). A versatile nanotrap for biochemical and functional studies with fluorescent fusion proteins. *Mol Cell Proteomics* 7, 282-289.
- Rouleau, M., Aubin, R.A., and Poirier, G.G. (2004). Poly(ADP-ribosyl)ated chromatin domains: access granted. *J Cell Sci* 117, 815-825.
- Ruf, A., de Murcia, G., and Schulz, G.E. (1998). Inhibitor and NAD⁺ binding to poly(ADP-ribose) polymerase as derived from crystal structures and homology modeling. *Biochemistry* 37, 3893-3900.
- Ruf, A., Mennissier de Murcia, J., de Murcia, G., and Schulz, G.E. (1996). Structure of the catalytic fragment of poly(AD-ribose) polymerase from chicken. *Proc Natl Acad Sci U S A* 93, 7481-7485.
- Saito, M., and Ishikawa, F. (2002). The mCpG-binding domain of human MBD3 does not bind to mCpG but interacts with NuRD/Mi2 components HDAC1 and MTA2. *J Biol Chem* 277, 35434-35439.
- Sambrook, J., and Russel, D.W. (2001). *Molecular Cloning, A Laboratory Manual* (Third Edition). Cold Spring Harbor Laboratory Press.
- Sarraf, S.A., and Stancheva, I. (2004). Methyl-CpG binding protein MBD1 couples histone H3 methylation at lysine 9 by SETDB1 to DNA replication and chromatin assembly. *Mol Cell* 15, 595-605.
- Sastry, S.S., Buki, K.G., and Kun, E. (1989). Binding of adenosine diphosphoribosyltransferase to the termini and internal regions of linear DNAs. *Biochemistry* 28, 5670-5680.

- Scala, E., Ariani, F., Mari, F., Caselli, R., Pescucci, C., Longo, I., Meloni, I., Giachino, D., Bruttini, M., Hayek, G., *et al.* (2005). CDKL5/STK9 is mutated in Rett syndrome variant with infantile spasms. *J Med Genet* 42, 103-107.
- Schermelleh, L., Carlton, P.M., Haase, S., Shao, L., Winoto, L., Kner, P., Burke, B., Cardoso, M.C., Agard, D.A., Gustafsson, M.G., *et al.* (2008). Subdiffraction multicolor imaging of the nuclear periphery with 3D structured illumination microscopy. *Science* 320, 1332-1336.
- Schreiber, V., Ame, J.C., Dolle, P., Schultz, I., Rinaldi, B., Fraulob, V., Menissier-de Murcia, J., and de Murcia, G. (2002). Poly(ADP-ribose) polymerase-2 (PARP-2) is required for efficient base excision DNA repair in association with PARP-1 and XRCC1. *J Biol Chem* 277, 23028-23036.
- Schreiber, V., Dantzer, F., Ame, J.C., and de Murcia, G. (2006). Poly(ADP-ribose): novel functions for an old molecule. *Nat Rev Mol Cell Biol* 7, 517-528.
- Shahbazian, M., Young, J., Yuva-Paylor, L., Spencer, C., Antalffy, B., Noebels, J., Armstrong, D., Paylor, R., and Zoghbi, H. (2002). Mice with truncated MeCP2 recapitulate many Rett syndrome features and display hyperacetylation of histone H3. *Neuron* 35, 243-254.
- Shall, S., and de Murcia, G. (2000). Poly(ADP-ribose) polymerase-1: what have we learned from the deficient mouse model? *Mutat Res* 460, 1-15.
- Simonin, F., Poch, O., Delarue, M., and de Murcia, G. (1993). Identification of potential active-site residues in the human poly(ADP-ribose) polymerase. *J Biol Chem* 268, 8529-8535.
- Skene, P.J., Illingworth, R.S., Webb, S., Kerr, A.R., James, K.D., Turner, D.J., Andrews, R., and Bird, A.P. (2010). Neuronal MeCP2 Is Expressed at Near Histone-Octamer Levels and Globally Alters the Chromatin State. *Mol Cell* 37, 457-468.
- Suzuki, M., Yamada, T., Kihara-Negishi, F., Sakurai, T., Oikawa, T. (2003). Direct association between PU.1 and MeCP2 that recruits mSin3A-HDAC complex for PU.1-mediated transcriptional repression. *Oncogene* 22, 8688-98.
- Tao, J., Hu, K., Chang, Q., Wu, H., Sherman, N.E., Martinowich, K., Klose, R.J., Schanen, C., Jaenisch, R., Wang, W., *et al.* (2009). Phosphorylation of MeCP2 at Serine 80 regulates its chromatin association and neurological function. *Proc Natl Acad Sci U S A* 106, 4882-4887.
- Tong, J.K., Hassig, C.A., Schnitzler, G.R., Kingston, R.E., and Schreiber, S.L. (1998). Chromatin deacetylation by an ATP-dependent nucleosome remodelling complex. *Nature* 395, 917-921.

- Tudor, M., Akbarian, S., Chen, R.Z., and Jaenisch, R. (2002). Transcriptional profiling of a mouse model for Rett syndrome reveals subtle transcriptional changes in the brain. *Proc Natl Acad Sci U S A* 99, 15536-15541.
- Tulin, A., Stewart, D., and Spradling, A.C. (2002). The *Drosophila* heterochromatic gene encoding poly(ADP-ribose) polymerase (PARP) is required to modulate chromatin structure during development. *Genes Dev* 16, 2108-2119.
- Uchimura, Y., Ichimura, T., Uwada, J., Tachibana, T., Sugahara, S., Nakao, M., and Saitoh, H. (2006). Involvement of SUMO modification in MBD1- and MCAF1-mediated heterochromatin formation. *J Biol Chem* 281, 23180-23190.
- Wacker, D.A., Ruhl, D.D., Balagamwala, E.H., Hope, K.M., Zhang, T., and Kraus, W.L. (2007). The DNA binding and catalytic domains of poly(ADP-ribose) polymerase 1 cooperate in the regulation of chromatin structure and transcription. *Mol Cell Biol* 27, 7475-7485.
- Wade, P.A. (2001). Methyl CpG binding proteins: coupling chromatin architecture to gene regulation. *Oncogene* 20, 3166-3173.
- Wade, P.A., Geggion, A., Jones, P.L., Ballestar, E., Aubry, F., and Wolffe, A.P. (1999). Mi-2 complex couples DNA methylation to chromatin remodelling and histone deacetylation. *Nat Genet* 23, 62-66.
- Wakefield, R.I., Smith, B.O., Nan, X., Free, A., Soteriou, A., Uhrin, D., Bird, A.P., and Barlow, P.N. (1999). The solution structure of the domain from MeCP2 that binds to methylated DNA. *J Mol Biol* 291, 1055-1065.
- Wang, H., An, W., Cao, R., Xia, L., Erdjument-Bromage, H., Chatton, B., Tempst, P., Roeder, R.G., and Zhang, Y. (2003). mAM facilitates conversion by ESET of dimethyl to trimethyl lysine 9 of histone H3 to cause transcriptional repression. *Mol Cell* 12, 475-487.
- Wang, W., and Malcolm, B.A. (1999). Two-stage PCR protocol allowing introduction of multiple mutations, deletions and insertions using QuikChange Site-Directed Mutagenesis. *Biotechniques* 26, 680-682.
- Wang, Z.Q., Stingl, L., Morrison, C., Jantsch, M., Los, M., Schulze-Osthoff, K., and Wagner, E.F. (1997). PARP is important for genomic stability but dispensable in apoptosis. *Genes Dev* 11, 2347-2358.
- Wiebauer, K., and Jiricny, J. (1989). *In vitro* correction of G.T mispairs to G.C pairs in nuclear extracts from human cells. *Nature* 339, 234-236.
- Wong, E., Yang, K., Kuraguchi, M., Werling, U., Avdievich, E., Fan, K., Fazzari, M., Jin, B., Brown, A.M., Lipkin, M., *et al.* (2002). Mbd4 inactivation increases Cright-arrowT transition mutations and promotes gastrointestinal tumor formation. *Proc Natl Acad Sci U S A* 99, 14937-14942.

- Woodcock, C.L., Skoultchi, A.I., and Fan, Y. (2006). Role of linker histone in chromatin structure and function: H1 stoichiometry and nucleosome repeat length. *Chromosome Res* 14, 17-25.
- Xue, Y., Wong, J., Moreno, G.T., Young, M.K., Cote, J., and Wang, W. (1998). NURD, a novel complex with both ATP-dependent chromatin-remodeling and histone deacetylase activities. *Mol Cell* 2, 851-861.
- Yasui, D.H., Peddada, S., Bieda, M.C., Vallero, R.O., Hogart, A., Nagarajan, R.P., Thatcher, K.N., Farnham, P.J., and Lasalle, J.M. (2007). Integrated epigenomic analyses of neuronal MeCP2 reveal a role for long-range interaction with active genes. *Proc Natl Acad Sci U S A* 104, 19416-19421.
- You, A., Tong, J.K., Grozinger, C.M., and Schreiber, S.L. (2001). CoREST is an integral component of the CoREST- human histone deacetylase complex. *Proc Natl Acad Sci U S A* 98, 1454-1458.
- Young, J.I., Hong, E.P., Castle, J.C., Crespo-Barreto, J., Bowman, A.B., Rose, M.F., Kang, D., Richman, R., Johnson, J.M., Berget, S., *et al.* (2005). Regulation of RNA splicing by the methylation-dependent transcriptional repressor methyl-CpG binding protein 2. *Proc Natl Acad Sci U S A* 102, 17551-17558.
- Zhang, Y., LeRoy, G., Seelig, H.P., Lane, W.S., and Reinberg, D. (1998). The dermatomyositis-specific autoantigen Mi2 is a component of a complex containing histone deacetylase and nucleosome remodeling activities. *Cell* 95, 279-289.
- Zhang, Y., Ng, H.H., Erdjument-Bromage, H., Tempst, P., Bird, A., and Reinberg, D. (1999). Analysis of the NuRD subunits reveals a histone deacetylase core complex and a connection with DNA methylation. *Genes Dev* 13, 1924-1935.
- Zhao, X., Ueba, T., Christie, B.R., Barkho, B., McConnell, M.J., Nakashima, K., Lein, E.S., Eadie, B.D., Willhoite, A.R., Muotri, A.R., *et al.* (2003). Mice lacking methyl-CpG binding protein 1 have deficits in adult neurogenesis and hippocampal function. *Proc Natl Acad Sci U S A* 100, 6777-6782.
- Zhou, Z., Hong, E.J., Cohen, S., Zhao, W.N., Ho, H.Y., Schmidt, L., Chen, W.G., Lin, Y., Savner, E., Griffith, E.C., *et al.* (2006). Brain-specific phosphorylation of MeCP2 regulates activity-dependent Bdnf transcription, dendritic growth, and spine maturation. *Neuron* 52, 255-269.

7.2 Abbreviations

A

A/T	Adenine/Thymine
3AB	3-amino-benzamide
AID	Activated Induced Deaminase
APC	Adenomatous polyposis coli

B

Bdnf	Brain derived neutrophilic factor
BER	Base excision repair
BRCT	BRCA1 C-terminus

C

CaMK	Calcium/calmodulin-dependent protein kinase
CBB	Coomassie Brilliant Blue
CD	Circular dichroism
CDKL5	Cyclin-dependent kinase-like 5
cDNA	Complementary DNA
ChIP	Chromatin immunoprecipitation
CoRID	Co-Repressor Interacting Domain
CTD	COOH-terminal domain

D

DAPI	4' -6'-Diamidino-2-Phenylindol
DBD	DNA binding domain
DMEM	Dulbecco's modified Eagle's medium
DMSO	Dimethyl sulfoxide
DNA	Deoxyribonucleic acid
Dnmt	DNA methyltransferase

E

E.coli	Escherichia coli
EtBr	Ethidium bromide

F

FISH	Fluorescent in situ hybridization
FL	Full Length
FRAP	Fluorescence recovery after photobleaching

G

GFP	Green fluorescent protein
-----	---------------------------

H

H3K9	Histone H3 lysine 9
HDAC	Histone deacetylase
HEK CBB	Human Embryonic Kidney
HIPK2	Homeodomain-interacting protein kinase 2
HP1	Heterochromatin protein 1

I

IAP	Intracisternal A particle
ID	Interdomain
IgG	Immunoglobulin G
IL-4	Interleukin-4

M	
5mC	5-methylcytosine
MBD	Methyl-CpG binding domain
MBDs	Methyl-CpG binding domain proteins
MBP	Methyl-CpG binding proteins
MCAF	MBD1-containing chromatin-associated factor
mCpGs	Methylated CpGs
MeCP1	Methyl-CpG Binding Protein 1
MED1	Methyl-CpG binding endonuclease 1
MEF	Mouse embryonic fibroblast
MMR	Mismatch repair
Mnase	Micrococcal nuclease
mRNP	Messenger ribonucleoprotein particle
MSI	Microsatellite instability
MT	Methyltransferase
N	
NAD+	Nicotinamide adenine dinucleotide
NMR	Nuclear magnetic resonance
NP40	Nonidet P-40 (octyl phenoxy)polyethoxyethanol)
NTD	NH2 – terminus
P	
PAGE	Polyacrylamide gel electrophoresis
PAR	Poly(ADP-ribose)
PARG	Poly(ADP-ribose)glycohydrolase
PARP-1	Poly(ADP-ribose)polymerase-1
PBS	Phosphate buffered saline
PIAS	Protein Inhibitors of activated STAT
PTM	Post translational modification
R	
RNA	Ribonucleic acid
RT	Room temperature
RTT	Rett Syndrome
S	
siRNA	Small interfering RNA
st	Strep
T	
TDG	Thymine DNA glycosylase
TRD	Transcriptional repression domain
TSA	Trichostatin A
Tween-20	Polyoxyethylene (20) sorbitan monolaurate
W	
WDR	WW domain binding region
WT	Wild type
X	
XCI	X chromosome inactivation
Y	
YB-1	Y box binding protein 1
YFP	Yellow Fluorescent Protein

7.3 Declaration

Declaration according to the “Promotionsordnung der LMU München für die Fakultät Biologie”

Betreuung:

Hiermit erkläre ich, dass die vorgelegte Arbeit an der LMU von Herrn Prof. Dr. Leonhardt betreut wurde.

Anfertigung:

Hiermit versichere ich ehrenwörtlich, dass die Dissertation selbstständig und ohne unerlaubte Hilfsmittel angefertigt wurde.

Prüfung:

Hiermit erkläre ich, dass die Dissertation weder als Ganzes noch in Teilen an einem anderen Ort einer Prüfungskommission vorgelegt wurde. Weiterhin habe ich weder an einem anderen Ort eine Promotion angestrebt oder angemeldet oder versucht eine Doktorprüfung abzulegen.

München, den 20. Juli 2010

(Annette Becker)

7.4 Publications

5402–5408 *Nucleic Acids Research*, 2007, Vol. 35, No. 16
doi:10.1093/nar/gkm599

Published online 13 August 2007

MeCP2 interacts with HP1 and modulates its heterochromatin association during myogenic differentiation

Noopur Agarwal¹, Tanja Hardt¹, Alessandro Brero¹, Danny Nowak¹,
Ulrich Rothbauer², Annette Becker¹, Heinrich Leonhardt² and M. Cristina Cardoso^{1,*}

¹Max Delbrück Center for Molecular Medicine, 13125 Berlin and ²Ludwig Maximilians University Munich, Biocenter, Department of Biology, 82152 Planegg-Martinsried, Germany

Received March 7, 2007; Revised and Accepted July 20, 2007

ABSTRACT

There is increasing evidence of crosstalk between epigenetic modifications such as histone and DNA methylation, recognized by HP1 and methyl CpG-binding proteins, respectively. We have previously shown that the level of methyl CpG-binding proteins increased dramatically during myogenesis leading to large-scale heterochromatin reorganization. In this work, we show that the level of HP1 isoforms did not change significantly throughout myogenic differentiation but their localization did. In particular, HP1 γ relocalization to heterochromatin correlated with MeCP2 presence. Using co-immunoprecipitation assays, we found that these heterochromatic factors interact *in vivo* via the chromo shadow domain of HP1 and the first 55 amino acids of MeCP2. We propose that this dynamic interaction of HP1 and MeCP2 increases their concentration at heterochromatin linking two major gene silencing pathways to stabilize transcriptional repression during differentiation.

INTRODUCTION

Post-translational modifications of chromatin such as histone and DNA methylation are recognized by epigenetic regulators HP1 (heterochromatin protein 1) and MeCP2 (methyl CpG-binding protein 2) respectively and play an important role in transcriptional regulation. These non-histone chromatin factors read the epigenetic marks and translate them into inactive chromatin states.

MeCP2 is a member of a family of proteins, which share a conserved methyl cytosine-binding domain (MBD) that recognizes methylated CpG dinucleotides (1).

Moreover, MeCP2 contains a nuclear localization signal [NLS; (2)] and a transcriptional repression domain (TRD), which binds a corepressor complex containing mSin3a and histone deacetylases [HDACs; (3)].

HP1 proteins are conserved from yeast to humans (4) and recognize histone H3 trimethylated at the lysine 9 position [H3K9Me₃; (5,6)]. In mammals, three isoforms viz α , β , γ have been identified (7,8). Functionally, three domains have been defined in HP1(s). The chromodomain [CD; (9)] and the chromo shadow domain [CSD; (10)] are highly conserved and are linked by the poorly conserved hinge domain. The CD has been shown to be important for binding methylated histones, while the CSD is known to interact with several proteins (11) as well as mediate homo (12) and heterodimerization of HP1 isoforms (13). The hinge domain interacts with DNA (14) and RNA (15).

In mouse cells, both HP1 and MeCP2 accumulate at pericentric regions of chromosomes organized into chromocenters, which play an important role in epigenetic gene regulation possibly by creating silencing compartments within the nucleus. Recently, we have shown that the level of MeCP2 as well as of MBD proteins starkly increased during myogenic differentiation concomitant with large-scale chromatin reorganization (16). To investigate a potential crosstalk between both epigenetic regulators, we analyzed the amount and localization of HP1 with respect to MBD proteins during cellular differentiation. We found that although the level of HP1 proteins does not change dramatically, there is spatial relocalization of HP1 (especially HP1 γ) during myogenesis from a more diffused distribution to a focal enrichment at pericentric heterochromatin. Furthermore, this redistribution to heterochromatin correlates with MeCP2 and MBD1 protein presence. We also demonstrate that HP1 and MeCP2 interact physically with each other,

*To whom Correspondence should be addressed: Tel: +49 30 94062109; Fax: +49 30 94063343; Email: cardoso@mdc-berlin.de
Present address:

Tanja Hardt, Medical Proteomics Center, Ruhr University, 44801, Germany
Alessandro Brero, Ludwig Maximilians University, Gene Center, 81377 Munich, Germany

© 2007 The Author(s)

This is an Open Access article distributed under the terms of the Creative Commons Attribution Non-Commercial License (<http://creativecommons.org/licenses/by-nc/2.0/uk/>) which permits unrestricted non-commercial use, distribution, and reproduction in any medium, provided the original work is properly cited.

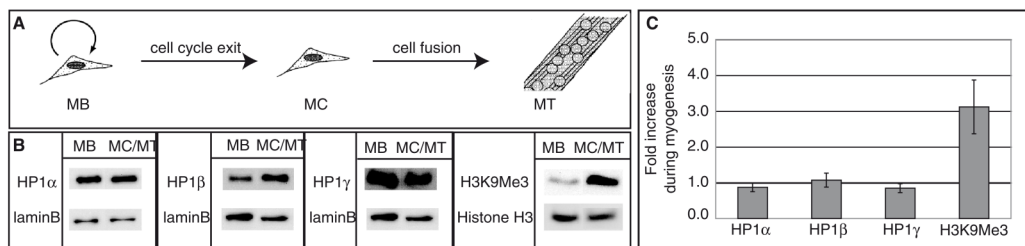


Figure 1. Level of HP1 proteins during differentiation. (A) Schematic representation of myogenesis. (B) Western blot analysis of the level of HP1 isoforms and of HP1-binding site on chromatin (H3K9Me3) in MB versus MC/MT. Lamin B and histone H3 are taken as controls for equal nuclear protein amounts and for total histone H3, respectively. (C) Quantitative analysis of western blots. Error bars indicate SDs.

strengthening the argument that they cooperate in the formation of repressive subnuclear compartments involved in epigenetic gene silencing.

MATERIALS AND METHODS

Expression plasmids

The following HP1 plasmids were used: GFP-tagged full-length human HP1 α /HP1 β /HP1 γ (17); YFP-tagged deletion mutants of human HP1 α /HP1 β /HP1 γ and full-length human HP1 α /HP1 β tagged with DsRed2 (18). To construct a DsRed2 fusion of HP1 γ , the BamHI–HindIII fragment of GFP-HP1 γ containing HP1 γ was subcloned into BglIII–HindIII site of pDsRed2-C1 (Clontech). MeCP2 constructs used were GFP/YFP/mRFP1-tagged full-length and deletion mutants of rat MeCP2 (16). MeCP2Y.6 and MeCP2G.7 were constructed by subcloning XhoI–HindIII and XhoI–PstI fragments of MeCP2 from MeCP2Y into pEYFP-N1 and pEGFP-N1 (Clontech) cut with the same restriction enzymes, respectively. pEGFP-N1 (Clontech) was used as a control.

Cell culture and transfection

Pmi28 mouse myoblast cells (MB) were cultured as described in (19), transfected using Transfectin (Biorad) and differentiated as described before (16). Differentiated cultures include syncytial myotubes (MT) and unfused myocytes (MC).

HEK293-EBNA human cells (Invitrogen) were maintained in Dulbecco's modified Eagle's medium (DMEM) supplemented with 10% fetal bovine serum at 37°C with 5% CO₂. 4 × 10⁵ HEK293-EBNA cells plated onto 100 mm diameter culture dishes were transfected using PEI (poly-ethyleneimine 25 kDa from Polysciences 1 mg/ml in ddH₂O, neutralized with HCl). For transfection 500 μ l of DMEM without serum, 12 μ g of DNA and 50 μ l of PEI were mixed well, incubated for 10 min at room temperature, vortexed and added to the cells dropwise. The culture was incubated at 37°C overnight, next day cells were washed in PBS, pelleted and used for co-immunoprecipitation assays.

Immunofluorescence analysis and microscopy

Proliferating and differentiated Pmi28 cultures were fixed in 3.7% formaldehyde/PBS and permeabilized with 0.5% TritonX-100/1XPBS and immunostained as described in (20). Primary antibodies used were: mouse monoclonal anti-HP1 isoform-specific antibodies (Chemicon), rabbit polyclonal anti-MeCP2 (Upstate) and anti-MBD1 (Santa Cruz) antibodies. Secondary antibodies used were: anti-mouse IgG-Cy5, anti-rabbit IgG-FITC (Jackson Immuno Research). Samples were counterstained with DAPI and examined on a Zeiss Axiocvert 200 using 40 \times and 63 \times objectives. Images were acquired with a PCO Sencicam QE cooled CCD camera using Zeiss Axiovision V.3 software and processed with Adobe Photoshop. To quantify the correlation between HP1 γ localization at chromocenters and presence of MeCP2 or MBD1, we analyzed 375 MB cells; 71 cells with positive staining for MeCP2; 99 cells with positive staining for MBD1; 125 cells transfected with MeCP2-GFP and 345 MT nuclei from two independent experiments done in triplicate. The mean and SDs were plotted using Microsoft Excel software (Figure 2).

Immunoprecipitation and western blot analysis

Differentiated and non-differentiated Pmi28 cells were grown on p100 culture dishes, boiled in Laemmli sample buffer and analyzed on western blots (Figure 1). Immunoprecipitations (Figures 3 and 4) were done as described before (21). The following primary antibodies were used: rabbit polyclonal anti-lamin B [kind gift of R.Bastos; (22)], rabbit polyclonal anti-H3K9Me3 (Upstate), rabbit polyclonal anti-MeCP2 (Upstate), chromatographically purified rabbit IgG (Organon Teknika), mouse monoclonal anti-HP1 α /HP1 β /HP1 γ (Chemicon), rabbit polyclonal anti-histone H3 (Upstate), mouse monoclonal anti-GFP (Roche), GFP binder (23), anti-mRFP1 rabbit polyclonal antiserum. Secondary antibodies used were: anti-mouse IgG HRP (Amersham) and anti-rabbit IgG HRP (Sigma). Immunoreactive signals were visualized using an ECL plus Detection kit (Amersham) and recorded using a luminescence imager (Luminescent Image Analyzer LAS-1000, Fuji). To compare the amounts of the different proteins in proliferating and differentiated myogenic cultures,

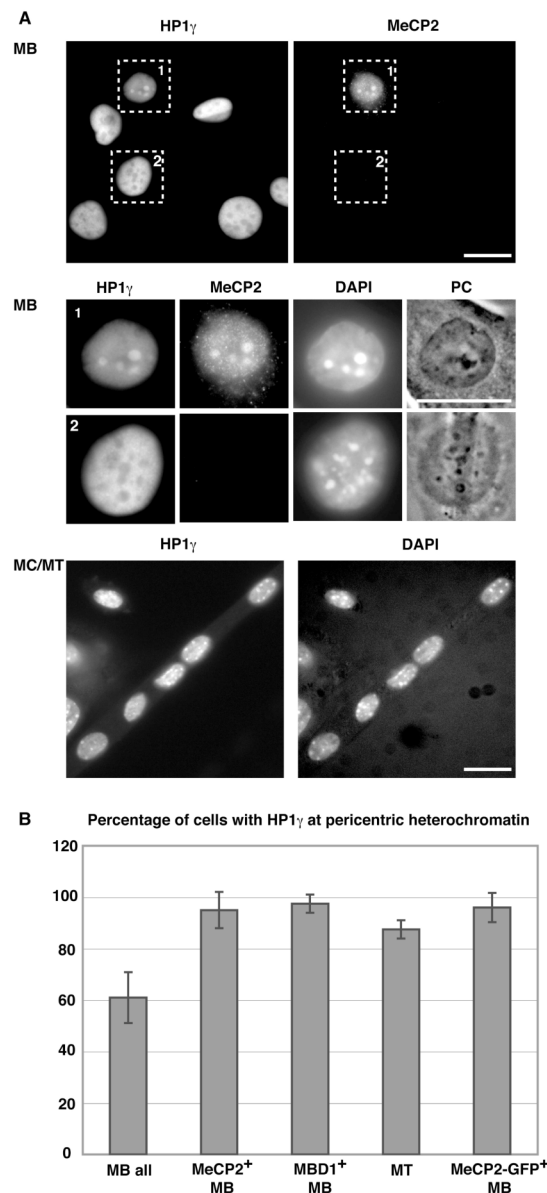


Figure 2. Pericentric heterochromatin association of HP1 γ increases during differentiation and correlates with the presence of MeCP2 and MBD1 proteins. (A) Cells were stained with HP1 γ and MeCP2-specific antibodies and DNA counterstained with DAPI, highlighting the chromocenters. In the upper panels, overview images and below them representative magnified MB cells are shown, of which only the MeCP2 positive cell has HP1 γ accumulated at chromocenters. The lower panels show an overview of a differentiated culture, with most nuclei having HP1 γ at chromocenters. Scale bar: 20 μ m. (B) Percentage of cells with HP1 γ at pericentric heterochromatin and correlation with MeCP2 and MBD1 proteins. Error bars indicate SD.

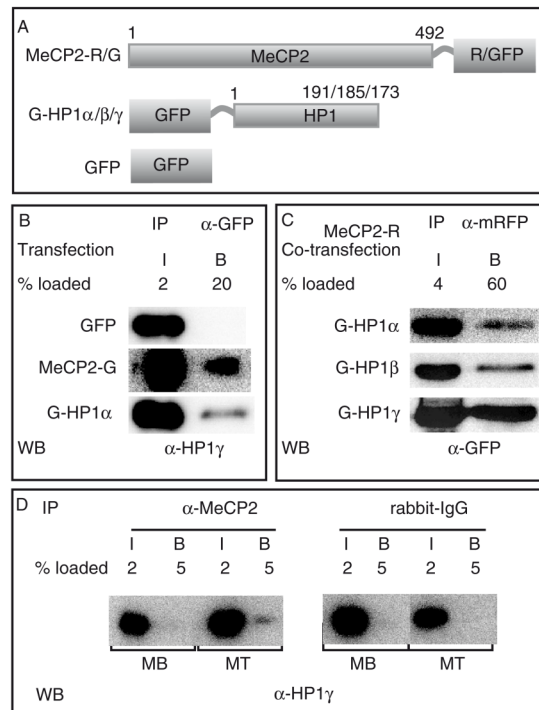


Figure 3. MeCP2 interacts with HP1 *in vivo*. (A) Schematic representation of the fusion proteins. Numbers represent amino acid coordinates. (B and C) HEK293-EBNA cells were transfected with the plasmids indicated and extracts prepared the next day. Immunoprecipitations were done using either anti-GFP (B) or anti-mRFP (C) antibody. (D) Extracts from MB and MT were subjected to immunoprecipitation using the antibodies, as indicated. Input (I) and bound (B) fractions were loaded in the percentages mentioned and analyzed by western blotting using anti-HP1 γ (B, D) or anti-GFP (C).

quantification of the recorded signals was done with the Image Gauge Ver.3.0 software (Fuji). Equal sized boxes were made around the recorded signals and for calculating the background. Integrated pixel intensity was measured for each band and the respective background signal was subtracted. Signals were normalized to the loading control (lamin B or histone H3) and the fold difference between the normalized signals in differentiated versus proliferating cultures was calculated. The mean and SDs were calculated from three independent experiments and plotted using Microsoft Excel software (Figure 1).

RESULTS AND DISCUSSION

Level of HP1 isoforms remains mostly constant during myogenesis

During cellular differentiation progressive inactivation of the genome occurs in parallel with the activation of tissue-specific gene expression patterns (24). We have shown that the level of methyl CpG-binding protein

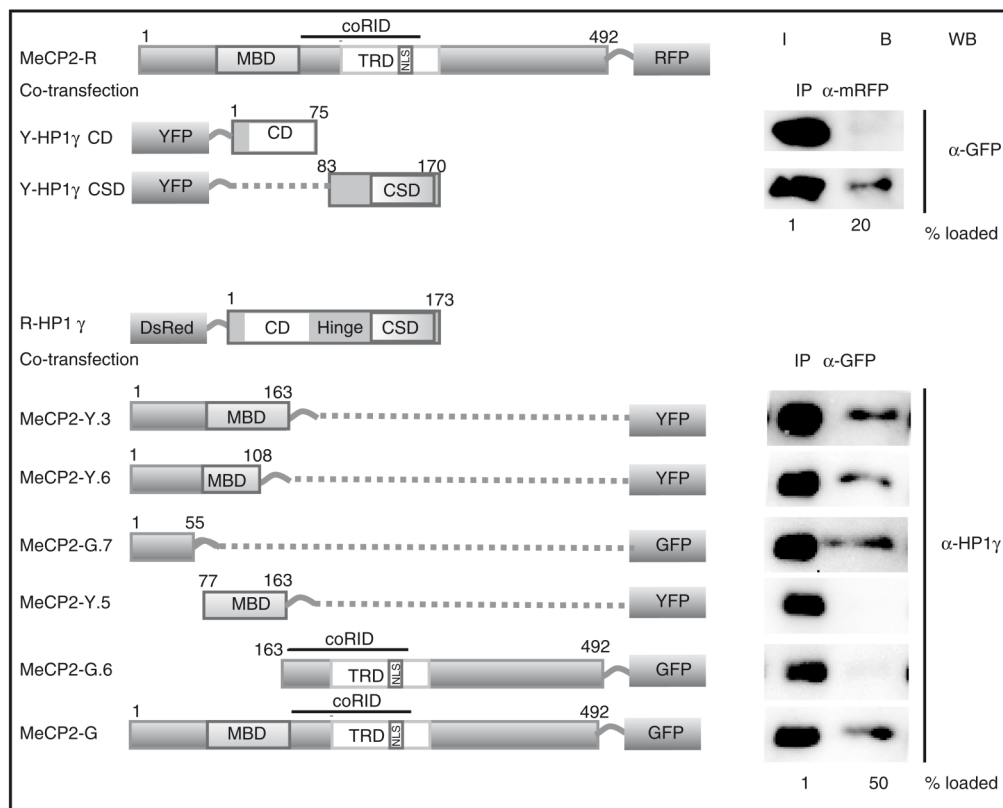


Figure 4. MeCP2 interacts via its N-terminal domain with the CSD domain of HP1. Schematic representation of the fusion proteins. Numbers represent amino acid coordinates. HEK293-EBNA cells were transfected with the plasmids indicated. Immunoprecipitations were done using either anti-mRFP or anti-GFP antibody. Input (I) and bound (B) fractions were loaded in the percentages mentioned and analyzed by western blotting using anti-GFP or anti-HP1 γ (shown here is the endogenous HP1 γ).

dramatically increased during muscle differentiation and induced large-scale aggregation of pericentric heterochromatin (16). A second major pathway associated with transcriptional silencing is mediated by HP1 binding of histone H3K9Me3. We therefore investigated whether the level of the different HP1 isoforms varied during cellular differentiation using a well-established *in vitro* culture system for myogenesis (Figure 1A). Pmi28 mouse myoblasts (MB) were induced to differentiate by incubation in horse-serum-containing medium. After three to four days, cells fused to form post-mitotic multinucleated myotubes (MT). These cultures still contained mononucleated not fully differentiated cells termed myocytes (MC). We quantified the level of HP1 in proliferating versus differentiated cell extracts by western blot analysis and normalized it to lamin B level as a loading control for nuclear proteins. The level of HP1 α , β , γ remained almost constant during differentiation (Figure 1B and C). However, the fraction of histone H3 that was trimethylated at lysine 9 position (H3K9Me3) increased about 3-fold in differentiated cells.

Association of HP1 γ with heterochromatin increases during differentiation and correlates with methyl CpG-binding protein presence

Previous studies have reported a cell cycle stage and isoform-specific localization of HP1 (18). To address this possibility, we examined the *in situ* localization of the HP1 isoforms as well as H3K9Me3 by immunofluorescence staining during myogenic differentiation. Pericentric heterochromatin organized in chromocenters was highlighted by counterstaining with the DNA dye 4',6-diamidino-2-phenylindole (DAPI). We found that the level of association of HP1 with pericentric heterochromatin differed between isoforms and changed during differentiation. While HP1 α protein could be found accumulated at pericentric heterochromatin in most of the MBs (89%; Supplementary Figure 1), HP1 β did not show such an accumulation (data not shown) and HP1 γ showed only a weak heterochromatin accumulation in about half of the MBs (61%; Figure 2). This weak accumulation was not due to the absence of H3K9Me3, since chromocenters of all MBs stained clearly positive for

this histone modification (Supplementary Figure 2) and is consistent with earlier reports showing HP1 γ mostly excluded from constitutive heterochromatin (25). We can also rule out epitope masking (26), as in the same population of MBs, there were cells where HP1 γ staining was detected at chromocenters (Figure 2A magnified nucleus). The fraction of MT nuclei with HP1 α and γ accumulated at heterochromatin increased to 100 and 90%, respectively (Supplementary Figure 1 and Figure 2). In contrast, upon differentiation there was no major change in the distribution of HP1 β (data not shown) even though there was an increase in the level of its binding site H3K9Me3 (Figure 1). We reasoned therefore, that this increase in heterochromatin association could depend on differentiation-specific factors other than the histone methylation mark *per se*. Since MeCP2 and other MBDs are present in a few MB only but increase during differentiation and label almost all chromocenters in MT (16), we tested whether the change in heterochromatin association of HP1 γ was correlated to MBD protein. Indeed we found a clear correlation of HP1 heterochromatin association in MB and the presence of either MeCP2 or MBD1. Almost all MeCP2 or MBD1 positive MB contained HP1 α (100%) and HP1 γ (95%) at chromocenters (Figure 2 and Supplementary Figure 1). Furthermore, 96 and 94% of MB cells ectopically expressing MeCP2-GFP fusion had HP1 γ and HP1 α accumulation at pericentric heterochromatin (Figure 2B and Supplementary Figure 1B). Altogether, these data showed that the chromocenter association of HP1 with particular emphasis for HP1 γ clearly increased upon myogenic differentiation and was positively correlated with the presence of MeCP2 and MBD1.

MeCP2 interacts via its N-terminal domain with the chromo shadow domain of HP1

Since the accumulation of HP1 at chromocenters correlated with the presence of MBD proteins at these sites, we tested whether they could physically interact. HEK293-EBNA cells, which express HP1 proteins, were transfected with plasmids coding for GFP, GFP-tagged MeCP2 or GFP-tagged HP1 (Figure 3A). Twelve hours later, cells were lysed and immunoprecipitations performed with an anti-GFP-specific antibody fragment [GFP binder; (23)]. Input and bound fractions were analyzed on western blots for precipitated GFP-tagged protein (data not shown) and for co-precipitated endogenous HP1 γ protein. HP1 γ did not bind to GFP alone but was co-precipitated with MeCP2-GFP (Figure 3B) and the same was true for HP1 α and β (data not shown). Since HP1 α , β and γ have been shown to form homodimers (12,13) as well as heterodimers [HP1 α - γ ; (12)], [HP1 α - β ; (27)], we reproduced this data as a positive control for our co-immunoprecipitation conditions. Moreover, the fraction of HP1 γ bound to HP1 α was comparable with the amount bound to MeCP2 (Figure 3B). Using a mRFP-tagged MeCP2, we co-immunoprecipitated GFP-tagged HP1 α , β and γ (Figure 3C). MeCP2-GFP proteins could likewise immunoprecipitate DsRed2-tagged HP1s (Figure 4 and data not shown) showing that the interaction of HP1 with MeCP2

was independent of the tags. Further, we tested whether endogenous HP1 and MeCP2 could interact. We performed immunoprecipitations using anti-MeCP2 antibody on Pmi28 MBs (expressing low level of MeCP2) and MTs (expressing higher level of MeCP2) (16). Indeed, the rabbit anti-MeCP2 antibody but not the control rabbit IgG could co-precipitate HP1 γ from MT extracts. Finally, to test whether MeCP2 could directly interact with HP1, we used GST pull down assays. Recombinant MeCP2 purified from bacteria was incubated with glutathione agarose coupled GST or GST-HP1 γ (Supplementary Figure 3). While no MeCP2 protein was detected in the GST-bound fraction, GST-HP1 γ was able to specifically pull down MeCP2. In summary, these results showed that MeCP2 and HP1 interact *in vivo* and at a level comparable to the dimerization of HP1 proteins.

The N terminus of HP1 contains the H3K9Me3-binding site (5) while the C terminus mediates dimerization of HP1 as well as interaction with other proteins (11,28). To test which domain would be involved in the interaction with MeCP2, we co-transfected HEK293-EBNA cells with plasmids coding for MeCP2-mRFP and with different YFP-tagged deletion constructs of HP1 isoforms coding either for the CD or the CSD. Co-immunoprecipitation assays demonstrated that the CSD of HP1s was necessary and sufficient for binding to MeCP2 *in vivo* (Figure 4 and data not shown). The CSD of HP1 has previously been shown to be important for the interaction of HP1 with other nuclear proteins (11). We then investigated which domain of MeCP2 binds to HP1 by using a series of fluorescently tagged deletion constructs of MeCP2. The results indicate that amino acids 1-55 of MeCP2 are primarily involved in binding HP1 (Figure 4), though weaker binding could be detected with other regions of MeCP2 as well (Supplementary Figure 4). We conclude that MeCP2 and HP1 interact via the CSD of HP1 and the N-terminal domain of MeCP2.

The domains of MeCP2 that have been better functionally characterized are the MBD, the transcriptional repressor domain (TRD) and the overlapping Sin3a co-repressor domain (coRID), all of which are in the central part of MeCP2 (29). Our data now implicate the N-terminal region before the MBD in binding to HP1, suggesting a direct physical link between the factors translating DNA and histone methylation. On the one hand, MeCP2 recognizes methyl CpGs and interacts with DNA methyltransferase 1 (30). On the other hand, HP1 binds to H3K9Me3 and associates with the histone H3K9 methyltransferase [Suv39h1; (31)]. Our data showing that HP1 and MeCP2 interact with each other interconnects these two major epigenetic pathways. Most recently, HP1 was also reported to interact with Dnmt1 (32). It is noteworthy that another MBD protein, MBD1 has been reported to interact with HP1 α via the MBD (33). Since other MBDs (Figure 2 and Supplementary Figure 1) were also able to enhance the accumulation of HP1 at heterochromatin, any single MBD knockout would not be expected to disrupt it. In line with this, we have previously shown that other MBDs have overlapping functions and knockout of MeCP2 alone did not affect heterochromatin reorganization during myogenic differentiation (16).

Significantly, we found that the heterochromatin association of HP1 γ increased during differentiation and that this was correlated with either MeCP2 or MBD1 presence. The differentiation-specific increase of the MBD proteins could enhance HP1 γ binding to constitutive heterochromatin, which would then recruit histone H3K9 methyltransferases leading to higher levels of H3K9 methylation. In Suv39h1/2 double knockout cells where H3K9 methylation at chromocenters is abrogated, MeCP2 still induced clustering (16), indicating that its interaction with HP1 is not required for its function in large-scale chromatin organization. We further propose that the multiple interactions of these factors with chromatin and with each other generate subnuclear silencing compartments, which stabilize the differentiated phenotype by reducing transcriptional noise. Individually these interactions are transient but their cumulative effect at heterochromatin increases the local concentration of repressing factors and thereby the efficiency of gene silencing.

SUPPLEMENTARY DATA

Supplementary Data are available at NAR Online.

ACKNOWLEDGEMENTS

We are indebted to R. Bastos, T. Misteli, Y. Hiraoka, P. Chambon and C.L. Woodcock for providing antibodies and plasmids. We thank Ingrid Grunewald for technical support and Jeffrey H. Stear for comments on the manuscript. T.H. was supported by the European Union (ESF Program). This work was funded by grants of the Deutsche Forschungsgemeinschaft to M.C.C. Funding to pay the Open Access publication charges for this article was provided by Deutsche Forschungsgemeinschaft (DFG).

Conflict of interest statement. None declared.

REFERENCES

- Nan, X., Meehan, R.R. and Bird, A. (1993) Dissection of the methyl-CpG binding domain from the chromosomal protein MeCP2. *Nucleic Acids Res.*, **21**, 4886–4892.
- Nan, X., Tate, P., Li, E. and Bird, A. (1996) DNA methylation specifies chromosomal localization of MeCP2. *Mol. Cell Biol.*, **16**, 414–421.
- Nan, X., Ng, H.H., Johnson, C.A., Laherty, C.D., Turner, B.M., Eisenman, R.N. and Bird, A. (1998) Transcriptional repression by the methyl-CpG-binding protein MeCP2 involves a histone deacetylase complex. *Nature*, **393**, 386–389.
- Eissenberg, J.C. and Elgin, S.C. (2000) The HP1 protein family: getting a grip on chromatin. *Curr. Opin. Genet. Dev.*, **10**, 204–210.
- Bannister, A.J., Zegerman, P., Partridge, J.F., Miska, E.A., Thomas, J.O., Allshire, R.C. and Kouzarides, T. (2001) Selective recognition of methylated lysine 9 on histone H3 by the HP1 chromo domain. *Nature*, **410**, 120–124.
- Lachner, M., O'Carroll, D., Rea, S., Mechtler, K. and Jenuwein, T. (2001) Methylation of histone H3 lysine 9 creates a binding site for HP1 proteins. *Nature*, **410**, 116–120.
- Saunders, W.S., Chue, C., Goebel, M., Craig, C., Clark, R.F., Powers, J.A., Eissenberg, J.C., Elgin, S.C., Rothfield, N.F. et al. (1993) Molecular cloning of a human homologue of Drosophila heterochromatin protein HP1 using anti-centromere autoantibodies with anti-chromo specificity. *J. Cell Sci.*, **104**, 573–582.
- Singh, P.B., Miller, J.R., Pearce, J., Kothary, R., Burton, R.D., Paro, R., James, T.C. and Gaunt, S.J. (1991) A sequence motif found in a Drosophila heterochromatin protein is conserved in animals and plants. *Nucleic Acids Res.*, **19**, 789–794.
- Paro, R. and Hogness, D.S. (1991) The Polycomb protein shares a homologous domain with a heterochromatin-associated protein of Drosophila. *Proc. Natl Acad. Sci. USA*, **88**, 263–267.
- Aasland, R. and Stewart, A.F. (1995) The chromo shadow domain, a distinct chromo domain in heterochromatin-binding protein 1, HP1. *Nucleic Acids Res.*, **23**, 3168–3173.
- Lechner, M.S., Schultz, D.C., Negorev, D., Maul, G.G. and Rauscher, F.J.III (2005) The mammalian heterochromatin protein 1 binds diverse nuclear proteins through a common motif that targets the chromo shadow domain. *Biochem. Biophys. Res. Commun.*, **331**, 929–937.
- Ye, Q., Callebaut, I., Pezhman, A., Courvalin, J.C. and Worman, H.J. (1997) Domain-specific interactions of human HP1-type chromodomain proteins and inner nuclear membrane protein LBR. *J. Biol. Chem.*, **272**, 14983–14989.
- Brasher, S.V., Smith, B.O., Fogh, R.H., Nietlispach, D., Thiru, A., Nielsen, P.R., Broadhurst, R.W., Ball, L.J., Murzina, N.V. et al. (2000) The structure of mouse HP1 suggests a unique mode of single peptide recognition by the shadow chromo domain dimer. *EMBO J.*, **19**, 1587–1597.
- Sugimoto, K., Yamada, T., Muro, Y. and Himeno, M. (1996) Human homolog of Drosophila heterochromatin-associated protein 1 (HP1) is a DNA-binding protein which possesses a DNA-binding motif with weak similarity to that of human centromere protein C (CENP-C). *J. Biochem.*, **120**, 153–159.
- Muchardt, C., Guilleme, M., Seeler, J.S., Trouche, D., Dejean, A. and Yaniv, M. (2002) Coordinated methyl and RNA binding is required for heterochromatin localization of mammalian HP1alpha. *EMBO Rep.*, **3**, 975–981.
- Brero, A., Easwaran, H.P., Nowak, D., Grunewald, I., Cremer, T., Leonhardt, H. and Cardoso, M.C. (2005) Methyl CpG-binding proteins induce large-scale chromatin reorganization during terminal differentiation. *J. Cell Biol.*, **169**, 733–743.
- Cheutin, T., McNairn, A.J., Jenuwein, T., Gilbert, D.M., Singh, P.B. and Misteli, T. (2003) Maintenance of stable heterochromatin domains by dynamic HP1 binding. *Science*, **299**, 721–725.
- Hayakawa, T., Haraguchi, T., Masumoto, H. and Hiraoka, Y. (2003) Cell cycle behavior of human HP1 subtypes: distinct molecular domains of HP1 are required for their centromeric localization during interphase and metaphase. *J. Cell Sci.*, **116**, 3327–3338.
- Kaufmann, U., Kirsch, J., Irintchev, A., Wernig, A. and Starzinski-Powitz, A. (1999) The M-cadherin catenin complex interacts with microtubules in skeletal muscle cells: implications for the fusion of myoblasts. *J. Cell Sci.*, **112**, 55–68.
- Sporbert, A., Gahl, A., Ankerhold, R., Leonhardt, H. and Cardoso, M.C. (2002) DNA polymerase clamp shows little turnover at established replication sites but sequential de novo assembly at adjacent origin clusters. *Mol. Cell*, **10**, 1355–1365.
- Mortusewicz, O., Rothbauer, U., Cardoso, M.C. and Leonhardt, H. (2006) Differential recruitment of DNA Ligase I and III to DNA repair sites. *Nucleic Acids Res.*, **34**, 3523–3532.
- Chaudhary, N. and Courvalin, J.C. (1993) Stepwise reassembly of the nuclear envelope at the end of mitosis. *J. Cell Biol.*, **122**, 295–306.
- Rothbauer, U., Zolghadr, K., Tillib, S., Nowak, D., Schermelleh, L., Gahl, A., Backmann, N., Conrath, K., Muyldermans, S. et al. (2006) Targeting and tracing antigens in live cells with fluorescent nanobodies. *Nat. Methods*, **3**, 887–889.
- Fisher, A.G. and Merkenschlager, M. (2002) Gene silencing, cell fate and nuclear organisation. *Curr. Opin. Genet. Dev.*, **12**, 193–197.
- Horsley, D., Hutchings, A., Butcher, G.W. and Singh, P.B. (1996) M32, a murine homologue of Drosophila heterochromatin protein 1 (HP1), localises to euchromatin within interphase nuclei and is largely excluded from constitutive heterochromatin. *Cytogenet. Cell Genet.*, **73**, 308–311.
- Minc, E., Courvalin, J.C. and Buendia, B. (2000) HP1gamma associates with euchromatin and heterochromatin in mammalian nuclei and chromosomes. *Cytogenet. Cell Genet.*, **90**, 279–284.
- Nielsen, A.L., Oulad-Abdelghani, M., Ortiz, J.A., Remboutsika, E., Chambon, P. and Losson, R. (2001) Heterochromatin formation in

5408 *Nucleic Acids Research*, 2007, Vol. 35, No. 16

- mammalian cells: interaction between histones and HP1 proteins. *Mol. Cell*, **7**, 729–739.
28. Cowieson, N.P., Partridge, J.F., Allshire, R.C. and McLaughlin, P.J. (2000) Dimerisation of a chromo shadow domain and distinctions from the chromodomain as revealed by structural analysis. *Curr. Biol.*, **10**, 517–525.
29. Brero, A., Leonhardt, H. and Cardoso, M.C. (2006) Replication and translation of epigenetic information. *Curr. Top. Microbiol. Immunol.*, **301**, 21–44.
30. Kimura, H. and Shiota, K. (2003) Methyl-CpG-binding protein, MeCP2, is a target molecule for maintenance DNA methyltransferase, Dnmt1. *J. Biol. Chem.*, **278**, 4806–4812.
31. Yamamoto, K. and Sonoda, M. (2003) Self-interaction of heterochromatin protein 1 is required for direct binding to histone methyltransferase, SUV39H1. *Biochem. Biophys. Res. Commun.*, **301**, 287–292.
32. Smallwood, A., Esteve, P.O., Pradhan, S. and Carey, M. (2007) Functional cooperation between HP1 and DNMT1 mediates gene silencing. *Genes Dev.*, **21**, 1169–1178.
33. Fujita, N., Watanabe, S., Ichimura, T., Tsuruzoe, S., Shinkai, Y., Tachibana, M., Chiba, T. and Nakao, M. (2003) Methyl-CpG binding domain 1 (MBD1) interacts with the Suv39h1-HP1 heterochromatic complex for DNA methylation-based transcriptional repression. *J. Biol. Chem.*, **278**, 24132–24138.

SUPPLEMENTARY INFORMATION**Figure S1**

Pericentric heterochromatin association of HP1 α increases during differentiation and correlates with the presence of MBD proteins. (A) Cells were stained with HP1 α and MeCP2 specific antibodies and DNA counterstained with DAPI, highlighting the chromocenters. The upper panel shows representative MB cells and the lower panel an overview of a differentiated culture. Scale bar: 20 μ m. (B) Percentage of cells with HP1 α at pericentric heterochromatin and correlation with MBD protein presence.

HP1 α protein could be found accumulated in chromocenters of 89% of MB (N= 131 cells). In contrast, the fraction of MT nuclei with HP1 α accumulated at heterochromatin increased to 100% (N= 100 cells). Indeed we found a correlation of HP1 heterochromatin association in MB and the presence of either MeCP2 or MBD1 with all MeCP2 or MBD1 positive MB (N=42 and 28 cells, respectively) containing HP1 α (100%) at chromocenters. Furthermore, 94% of MB cells ectopically expressing MeCP2-GFP fusion (N= 35 cells) had HP1 α accumulation at pericentric heterochromatin. Altogether, these data showed that the chromocenter association of HP1 α clearly increased upon myogenic differentiation and was positively correlated with the presence of MeCP2 and MBD1.

Figure S2

H3K9Me3 is present at chromocenters in MB and shows slight increase during differentiation. Cells were stained with H3K9Me3 specific antibody and DNA counterstained with DAPI. Scale bar: 20 μ m.

Figure S3

MeCP2 physically interacts with HP1 γ . Schematic representation of the constructs used in the experiment. GST and GST-HP1 γ were immobilized and incubated with purified MeCP2 (see supplemental method). Input (1%) and bound (15%) MeCP2 is shown. Whereas GST alone did not pull down MeCP2, an equivalent amount of GST-HP1 γ was able to specifically pull down MeCP2.

Figure S4

MeCP2 interacts preferentially via its N-terminal domain with the CSD domain of HP1. Schematic representation of the fusion proteins. Numbers represent amino acid coordinates. HEK293-EBNA cells were transfected with the plasmids indicated. Immunoprecipitations were done using anti-GFP antibody. Input (I) and bound (B) fractions were loaded in the percentages mentioned and analyzed by western blotting using anti-HP1 γ antibody. The ectopically expressed R-HP1 γ binds to low and high affinity sites creating a competitive situation that reveals the preferential binding of the endogenous HP1 γ protein to the N-terminus of MeCP2.

Figure S2

H3K9Me3 is present at chromocenters in MB and shows slight increase during differentiation. Cells were stained with H3K9Me3 specific antibody and DNA counterstained with DAPI. Scale bar: 20 μ m.

Figure S3

MeCP2 physically interacts with HP1 γ . Schematic representation of the constructs used in the experiment. GST and GST-HP1 γ were immobilized and incubated with purified MeCP2 (see supplemental method). Input (1%) and bound (15%) MeCP2 is shown. Whereas GST alone did not pull down MeCP2, an equivalent amount of GST-HP1 γ was able to specifically pull down MeCP2.

Figure S4

MeCP2 interacts preferentially via its N-terminal domain with the CSD domain of HP1. Schematic representation of the fusion proteins. Numbers represent amino acid coordinates. HEK293-EBNA cells were transfected with the plasmids indicated. Immunoprecipitations were done using anti-GFP antibody. Input (I) and bound (B) fractions were loaded in the percentages mentioned and analyzed by western blotting using anti-HP1 γ antibody. The ectopically expressed R-HP1 γ binds to low and high affinity sites creating a competitive situation that reveals the preferential binding of the endogenous HP1 γ protein to the N-terminus of MeCP2.

Supplemental Method

GST pull down assay

BL21 competent cells were transformed with Glutathione S Transferase (GST) expressing plasmid pGex2T1 (Pharmacia) and pGST-HP1 γ (1). Single colonies from each were inoculated in 4ml of LB-Amp separately and incubated with overnight shaking at 37°C. 2ml of this culture was used to inoculate 200ml of LB-Amp media and further incubated till O.D₆₀₀ reached to 0.6. 200 μ l of 1M IPTG (1mM final concentration) was added to each flask. After 3 hours of incubation, the culture was pelleted at 4000 rpm for 30 min 4°C. All the further steps were done at 4°C unless otherwise stated. Cells were lysed using a high pressure homogenizer (EmulsiFlex-C5, Avestin) and extracts loaded on pre-equilibrated Glutathione Superflow Resin (Clontech) for 2 hours with shaking. Bound GST and GST-HP1 γ were checked on a gradient NuPAGE 4-12% Bis-Tris gel using MOPS SDS running buffer, and stained with Simply Blue Safe Stain (Invitrogen) along with purified MeCP2. MeCP2 (pTYB1) was produced and purified as described (2). Equal amounts of GST and GST-HP1 γ were then incubated with purified MeCP2 overnight. Bound and flow through fractions were boiled in Laemmli sample buffer and analyzed on a gradient gel.

1. Nielsen, A.L., Oulad-Abdelghani, M., Ortiz, J.A., Remboutsika, E., Chambon, P. and Losson, R. (2001) Heterochromatin formation in mammalian cells: interaction between histones and HP1 proteins. *Mol Cell*, **7**, 729-739.
2. Georgel, P.T., Horowitz-Scherer, R.A., Adkins, N., Woodcock, C.L., Wade, P.A. and Hansen, J.C. (2003) Chromatin compaction by human MeCP2. Assembly of

novel secondary chromatin structures in the absence of DNA methylation. *J Biol Chem*, **278**, 32181-32188.

Figure S1

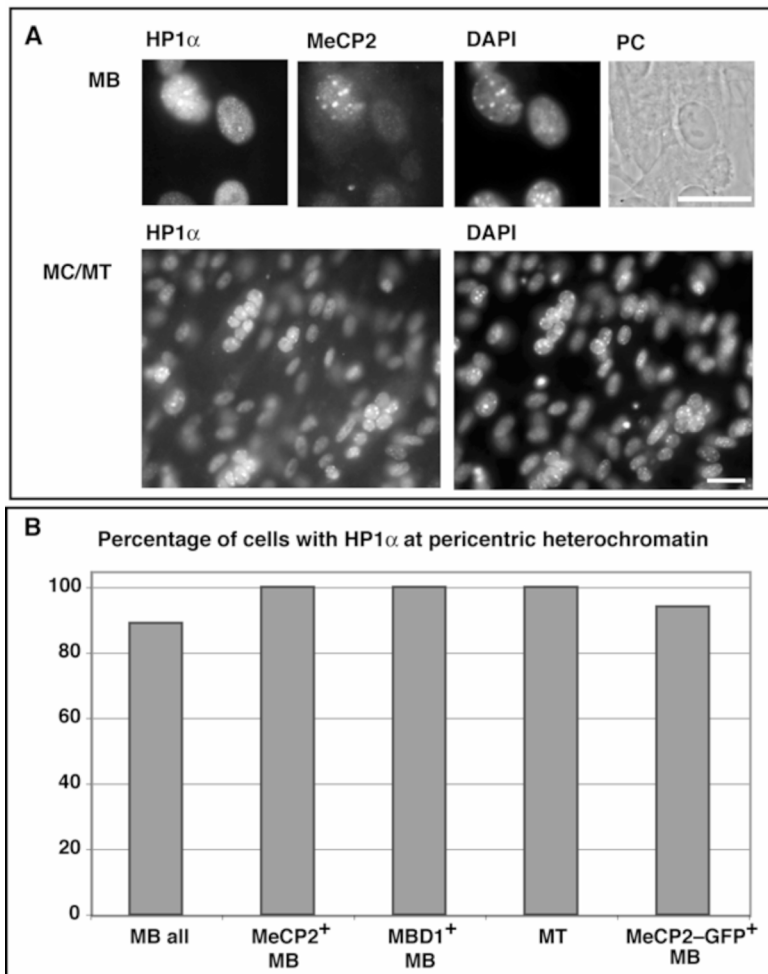


Figure S2

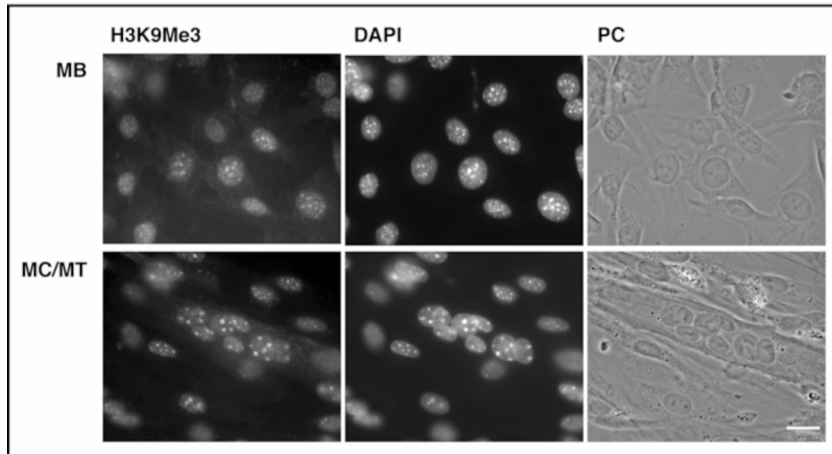


Figure S3

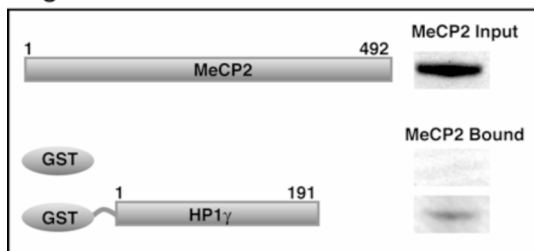
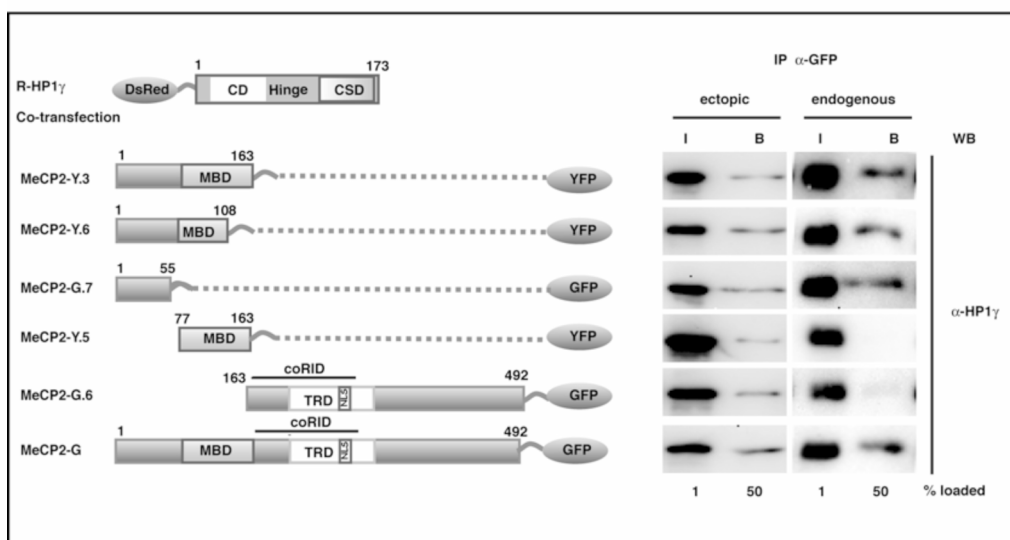


Figure S4



7.5 Acknowledgements

First of all I want to thank Cristina Cardoso for the opportunity to perform my PhD thesis in her lab as well as for the very interesting and exciting topic. Without her constant and fruitful scientific contributions and discussions the outcome of this thesis and my opinion about science would not be the same. Furthermore, I want to deeply thank her for maintaining a great and friendly atmosphere in the lab throughout the years.

Huge thanks go to Heinrich Leonhardt for supporting this thesis and for his numerous and excellent scientific ideas, advice and contributions.

I further want to thank Prof. Dr. Ruth Brack-Werner for evaluating my PhD thesis.

Also I want to thank all the members of Heinrichs lab for their help regarding scientific and bureaucratic questions and support. Particular thanks goes to Anja Gahl, Daniela Meilinger, Sebastian Bultmann and Ulrich Rothbauer. I also want to acknowledge Oliver Mortusewicz for supervising me during my stay in Munich and for the friendly atmosphere throughout. Many thanks also to Andrea Rottach, for her great help regarding antibodies, PyMol and scientific tasks, especially for her personal support during my stay in Munich and the last weeks of my PhD thesis.

Special thanks goes to those who have actively contributed to my projects and ongoing publications. Noopur Agarwal, Alessandro Brero and Tanja Hardt for their contributions regarding accumulation at chromocenters and clustering of chromocenters of MeCP2 RTT mutants, Laurence Jost for her FISH analysis to study chromatin clustering of MeCP2 RTT mutants in human cells, Sebastian Haase for generating the chromocenter counting program, Danny Nowak for performing the IP to detect poly(ADP-ribosyl)ation of MeCP2 in mouse brain, Jenny Völger for generating a significant amount of MeCP2 point mutations for identification of the poly(ADP-ribosyl)ated sites and Shinichi Kudo for his scientific input.

For the interaction project among the MBDs, I greatly appreciate the help from Maria Hofstätter who cloned the Sf9 expression constructs of MBD1, MBD2, MBD3 and MBD4 and generated recombinant proteins of the latter using the Baculovirus Expression System. Maria Hofstätter as well as Valentina Casa also performed the *in vitro* pull down experiments of MeCP2 with itself and MBD2.

Special thanks goes to Valérie Schreiber for her scientific input throughout the years and her contributions regarding noncovalent PAR binding of the MBDs.

I also want to thank Anne Lehmkuhl, Ingrid Grunewald and Petra Domaing for their great help and support regarding cultivation of cells and protein expression.

I further want to thank all the members of the MDC lab for the nice and friendly atmosphere, especially Gilla Tünnemann, Petra Domaing, Danny Nowak, Joke van

Bemmel and Sabine Görisch especially for helping me personally and scientifically during the beginning of my PhD.

For his help with urgent problems I want to thank Alexander Rapp as well as all the other lab members for their constant help, advice, the fruitful scientific and hospitable atmosphere.

For proof reading and correcting of this thesis I thank Corella Casas Delucchi and Laurence Jost.

My special thanks goes to Corella Casas Delucchi for having been such a great colleague and friend, for introducing me to microscopy and for our refreshing lunch breaks.

I also want to mention Annette Schledz and Anne Lehmkuhl for their friendly and emotional support throughout.

I am greatly indebted to my family. I want to express my deepest thanks to my mom, my sister Birgit and my father. You have always been there for me and your overall belief in my capabilities and my personality strengthened me throughout the years.

I am very thankful for our great relationship.

Most of all I want to thank Basi for his ongoing support and his ability to bring happiness and fun into my life even in the most difficult and frustrating moments.

I am deeply grateful for having you in my life.

8 Curriculum vitae

Personal information

Name: Annette Becker
Date of birth: 16/10/1980
Place of birth: Köln
Nationality: German
Current work address: Technische Universität Darmstadt
Schnittspahnstr.10
64287 Darmstadt, Germany

Education

2000 Allgemeine Hochschulreife
Werner-Heisenberg Gymnasium
Leverkusen, Germany
10/2000-11/2005 Diploma in Biochemistry
Universität Hannover
Hannover, Germany
03/2006 – present PhD in biology (LMU, München, Germany)
Max Delbrück Center for Molecular Medicine
Berlin, Germany
Technische Universität Darmstadt
Darmstadt, Germany

Positions and teaching

2009 – present supervision of basic and advanced practical courses
2009 - present student assistant in the group of Cristina Cardoso

List of publications

Becker, A., Agarwal, N., Jost, L., Haase, S., Nowak, D., Brero, A., Hardt, T., Kudo, S., Schreiber, V., Leonhardt, H., Cardoso, M.C. MeCP2 Rett mutations affect chromatin organization and inhibition of MeCP2 poly(ADP-ribosyl)ation rescues this defect.

Under revision.

Agarwal, N., Hardt, T., Brero, A., Nowak, D., Rothbauer, U., **Becker, A.**, Leonhardt, H., and Cardoso, M.C. (2007). MeCP2 interacts with HP1 and modulates its heterochromatin association during myogenic differentiation. *Nucleic Acids Res* 35, 5402-5408.

Conference contributions

XX International Congress of Genetics

Poster: "Post-translational modification and interaction of MeCP2 with PARP-1."

Berlin, Germany; July 12 - 17, 2008

3rd MC-GARD Meeting on Higher Order Genome Architecture

Poster: "Post-translational modification and interaction of MeCP2 with PARP-1."

Edinburgh, Scotland, 1-5 April, 2009

17th school in life sciences on Nuclear Organization and Dynamics

Poster: "MeCP2 Rett mutations affect chromatin organization and inhibition of MeCP2 poly(ADP-ribosyl)ation rescues this defect."

Jerusalem, Israel; September 13 – 17, 2009

SPP1356 Internal Progress Meeting

Oral presentation: "Poly(ADP-ribosyl)ation of MeCP2 regulates chromatin structure."

Wurzburg, Germany; November 9 – 11, 2009

3rd International Congress on Stem Cells and Tissue Formation

Poster: "Regulation of MeCP2 induced heterochromatin remodelling."

Dresden, Germany; July 11 – 14, 2010